

**LOCAL AND SUSTAINED DELIVERY OF HYDROPHOBIC DRUGS
TO THE SPINAL CORD WITH POLYKETAL MICROPARTICLES**

A Dissertation
Presented to
The Academic Faculty

by

Chen-Yu Kao

In Partial Fulfillment
of the Requirements for the Degree
Doctor of Philosophy in the
Department of Biomedical Engineering

Georgia Institute of Technology
December, 2009

**LOCAL AND SUSTAINED DELIVERY OF HYDROPHOBIC DRUGS
TO THE SPINAL CORD BT USING POLYKETAL
MICROPARTICLES**

Approved by:

Dr. Niren Murthy, Advisor
School of Biomedical Engineering
Georgia Institute of Technology

Dr. Michael E. Davis
School of Biomedical Engineering
Georgia Institute of Technology

Dr. Thomas H. Barker
School of Biomedical Engineering
Georgia Institute of Technology

Dr. Valeria T. Milam
School of Material Science and
Engineering
Georgia Institute of Technology

Dr. Jonathan D. Glass
School of Medicine
Emory University

Date Approved: 07/10/2009

To my beautiful wife and best friend, Yih-Tsu, for her love, support, and prayers
throughout this journey

ACKNOWLEDGEMENTS

I wish to thank my advisor, Dr. Niren Murthy, for giving me the opportunity to pursue my Ph.D. study in his laboratory. Niren has been a great source of knowledge and ingenuity in the fields of chemistry, bioengineering, and drug delivery, and his enthusiasm has helped me to accomplish what I may not have thought was possible. He has also provided me with opportunities to collaborate with other researchers, with whom I was able to pursue various clinical applications using the materials we developed in our laboratory.

I also wish to thank all members of my research lab, past and present. Dr. Michael Heffernan, Dr. Stephen Yang, D. Scott Wilson, Dr. Sungmun Lee, Dr. Madhuri Dasari, Dr. Dongwon Lee, Dr. Venkata Reddy Erigala, Dr. Kousik Kundu, Dr. Seungjun Lee, Dr. Dongin Kim, Dr. Xinghai Ning, Jay Sy, John Perng, Guillermo Alas, Ben Solomon, and Sydney Shaffer. Michael and Stephen are the pioneers in the polyketal studies; they gave me a lot of advice in both science and daily life. Scott always cheers me up when I were sad and give me suggestion on the polymer synthesis. Their support and friendship have made my journey much more pleasant and enjoyable. Sungmun and Madhuri have provided me with much help in my research both the forms of discussions and collaborative research. They have served as my mentors from whom I have learned a great deal about how to become a successful scientist. I am particularly grateful to my undergraduate student Sydney whom I mentored. She gave me an opportunity to develop as a mentor, and at the same time, greatly helped me make progress in my research projects.

I would also like to thank our collaborators for their contributions to my thesis project. Particularly, I would like to thank Dr. Nick Boulis and his laboratory members; Dr. Michele Kleim, Dr. Bethwel Raore, Dr. Colin Franz, Christina Krudy, Jing Ma, Brenten Heeke for their contributions for the delivery of calpain inhibitors with polyketal microparticles to treat amyotrophic lateral sclerosis. I would also like to thank Dr. Sheldon May and his laboratory for their contributions for the delivery of anti-inflammatory drug AOPHA-Me with polyketal microparticles to treat arthritis. Special thanks to Jacob Lucrezi helped me to set up the HPLC system and we also have a lot of discuss in polyketal microparticle formulation. I also want to thank the other GT students who contribute to my research. Dr. Christina Hampton has helped me to analyze the AK295 polyketal using LC0MS. Dr. Asli Ovat provided me the AK295 and give me suggestions in the calpain assay, Dr. Matthew Di Prima helps me to measure the thermal properties of polyketal using DSC.

I would like to thank Dr. Michael Davis, Dr. Thomas Barker, Dr. Valeria Milam, and Dr. Jonathan Glass for serving on my thesis committee. Their advice and guidance have helped me greatly in going forward with my thesis research.

I would like to thank all of our fellow parishioners at Atlanta Taiwanese Presbyterian Church, their cares and prayers have helped me to overcome the difficult time during my Ph.D. study. I also like to thanks all my friends at Anlo Presbyterian Church in Taiwan, they always keep me and my family in their prayers in the past eight years.

I thank my Dad Sheng-Tsai Kao, step Mom Shu-Ching Chan , my two sisters Ying-Ying Kao and Jing-Jing Kao for their love and support during this time, for all the

times they have taken my daughter into their care, and for their many prayers, which have helped bring me many blessings throughout the years. I also thank my mother-in-law Man-hui Chen and father-in-law Liang-Junn Hahn, for their support and reassurance; and all of our family members, relatives, and friends for all their support and encouragement during my Ph.D. studies.

I also want to thank my daughter Wensing Kao, who always cheers me up and gives me her full support. She spends a lot of times in front of the webcam and told me everything in Taiwan. She have been told me how she love me every day since she went back to Taiwan two years ago. She is one of the driving force to help me overcome the fatigue and moving forward.

I am truly grateful to my wife, Yih-Tsu, for her tireless support and efforts during these past eight years, for all the encouragement she has given me in switching lab and throughout the Ph.D. program. She continued to do all house works and take care of Wensing at home while taking on a full-time job as an assistant professor in social welfare in the last two years as well. Yih-tsu has stood by me every step of the way, through all the challenges we faced during this period, and I could not have done any of this without her. She is my best friend and my soulmate, and she has consoled me on many occasions during the difficult times. Yih-tsu has so many talents and wonderful qualities, and I love her with all of my heart. I thank God for bringing Yih-tsu into my life, for the love that we share, and for guiding us on our spiritual journey together.

Finally, I give thanks to God the Father, Son, and Holy Spirit, my creator, savior, and counselor; who makes all things possible. This work is offered for His glory.

TABLE OF CONTENTS

	Page
Acknowledgements	iv
LIST OF TABLES	ix
LIST OF FIGURES	x
LIST OF SYMBOLS AND ABBREVIATIONS	xiii
SUMMARY	xvii
<u>CHAPTER</u>	
1 INTRODUCTION	1
1.1 Background and Motivation	1
1.2 Research Objectives and Specific Aims	4
1.3 Review of Relevant Literature	8
2 DEVELOPMENT OF HIGH MOLECULAR WEIGHT POLYKETALS THAT PROVIDE SUSTAINED RELEASE PROPERTIES FOR HYDROPHOBIC MOLECULES	20
2.1 Introduction	20
2.2 Experimental Methods	25
2.3 Results	35
2.4 Discussion	52
3 PCADKe MICROPARTICLES AS A SUSTAINED RELEASE SYSTEM FOR HYDROPHOBIC CALPAIN INHIBITORS	63
3.1 Introduction	63
3.2 Experimental Methods	65
3.3 Results	71
3.4 Discussion	81

4	<i>IN VIVO</i> EVALUATION OF CALPAIN INHIBITORS-ENCAPSULATED PCADK ϵ MICROPARTICLES	86
4.1	Introduction	86
4.2	Experimental Methods	88
4.3	Results	94
4.4	Discussion	104
5	CONCLUSIONS AND FUTURE DIRECTIONS	111
5.1	Conclusions	111
5.2	Future direction	112
	REFERENCES	118

LIST OF TABLES

	Page
Table 2.1: Optimization of PK8	36
Table 2.2: Composition and molecular weights of polyketal copolymers and PCADK synthesized from DEP/DMP mixtures	38
Table 2.3: Optimization of PCADKe	41
Table 2.4: The DSC results of polyketal polymers	47
Table 3.1: Encapsulation efficiency, and particle sizes of various AK295 encapsulated polyketal microparticles	72
Table 3.2: Encapsulation efficiency and particle size of MDL-PKMs	76
Table 3.3: Calpain inhibitors loading, encapsulation efficiency and inhibitory activity in PCADKe microparticles form AK295-PKMs and MDL-28170-PKMs	80

LIST OF FIGURES

	Page
Scheme 1.1: Polyketal-based drug delivery system for ALS treatment	4
Scheme 2.1: A novel methodology to synthesize high molecular weight polyketal using DEP formulation	23
Figure 2.1: Comparison between calpain inhibitors and hydrophobic fluorescent dyes	24
Figure 2.2: Optimization of reaction temperature for PK8	36
Figure 2.3: (A) ¹ H-NMR and (B) GPC spectra of PK8	37
Figure 2.4: (A) ¹ H-NMR and (B) GPC spectra of PK9	39
Figure 2.5: (A) ¹ H-NMR and (B) GPC spectra of PK10	40
Figure 2.6: Optimization of reaction temperature for PCADKe using (A) PTSA, (B) PPTSA as catalyst	42
Figure 2.5: (A) ¹ H-NMR and (B) GPC spectra of PCADKe	43
Figure 2.8: Hydrolysis of PK3, PK8 and PK10 at (A) pH 5.0 and (B) pH7.4 environment	44
Figure 2.9: SEM images of AOPHA-Me PKMs prepared from (A) high molecular weight PCADKe (Mw=9,623), (B) medium molecular weight PCADK (Mw=6,317)	45
Figure 2.10: SEM images of PCADKe nanoparticles prepared from (A) high molecular weight PCADKe (Mw/Mn =12,234/6,623) and (B) low molecular weight PCADK (Mw/Mn = 2,849/1,981)	46
Figure 2.11: DSC of polyketal. (A) high molecular weight PCADKe, (B) medium molecular weight PCADK,, (C) low molecular weight PCADK, (D) PK3, (E) PK8, and (F) PK10	46
Figure 2.12: Uptake of fl-siRNA PKN in HUVEC cells. (A) A SEM image of fl-siRNA PKNs. (B) Mean fluorescent intensity of HUVECs after treated with free fl-siRNA, DOTAP-fl-siRNA complex and fl-siRNA PKNs. (C) HUVECs, (D) HUVECs after uptaking of fl-siRNA PKN.	48

- Figure 2.13: SEM images of Nile Red PCADKe microparticles prepared at different homogenization speeds (A) 24,000 rpm, the particle size ranges from 1 to 2 μm (6,000X magnification), (B) 17,500 rpm, the particle size ranges from 1 to 5 μm (1,000X magnification), and (C) 9,500 rpm, the particle size ranges from 2 to 10 μm (1,000X magnification). 49
- Figure 2.14: Calibration curve of DiI in (A) PBS (pH 7.4), (B) 0.1 % SDS in PBS (pH 7.4). 50
- Figure 2.15: SEM images of DiI-encapsulated PCADKe microparticles prepared at different homogenization speeds (A) 21,500 rpm, the particle size is $1.96 \pm 0.64 \mu\text{m}$ (encapsulation efficiency: 67.79 %), (B) 13,500 rpm, the particle size is $2.90 \pm 1.17 \mu\text{m}$ (encapsulation efficiency: 82.87 %), and (C) 9,500 rpm, the particle size is $5.49 \pm 3.21 \mu\text{m}$ (encapsulation efficiency: 82.16 %). 50
- Figure 2.16: Effects of particle size on the *in vitro* release of DiI from polyketal microparticles: $1.96 \pm 0.64 \mu\text{m}$ (◆), $2.90 \pm 1.17 \mu\text{m}$ (■) and $5.49 \pm 3.21 \mu\text{m}$ (▲), n=5 for each time point. Polyketal microparticles have drug contents of 0.68 % (◆), 0.83 % (■) and 0.82 % (▲) 51
- Figure 3.1: (Representative chromatogram of (A) AK295 standard solution, (B) blank PCADKe microparticles, and (C) AK295-encapsulated PCADKe particles from LC-MS 71
- Figure 3.2: SEM images of AK-PKMs. (A) AK-PKM1, (B) AK-PKM2, (C) AK-PKM3, (D) AK-PKM 4, (E) AK-PKM5, (F) AK-PKM6, (G) AK-PKM7 and (H) AK-PKM8 73
- Figure 3.3: Representative chromatogram of (A) MDL-28170-encapsulated PCADKe particles (B) MDL-28170 standard solution, and (C) blank PCADK microparticles from reverse phase HPLC 75
- Figure 3.4: SEM images of (A) MDL-PKM1, (B) MDL-PKM2, and (C) MDL-PKM3 75
- Figure 3.5: Release kinetics of MDL-28170 encapsulated in PCADKe microparticles (n=4 for each time point) 77
- Figure 3.6: SEM images of MDL-PKMs at (A) Day 0, and (B) Day 60 in PBS (pH 7.4) 77
- Figure 3.7: inhibitory activities of AK295 were determined by establishing a calibration curve. The inhibitory effect of AK295 was determined by measuring the fluorescent intensity of AMC released from calpain substrate 79
- Figure 3.8: Inhibitory activities of MDL-28170 were determined by establishing a calibration curve. The inhibitory effect of MDL-28170 was determined by measuring the fluorescent intensity of AMC released from calpain substrate 80

Figure 3.9: Representative chromatogram of (A) AK295, (B) Blank PCADKe microparticles and (C) AK295-encapsulated PCADKe microparticles from reverse phase HPLC.	82
Figure 4.1: Distribution of the (A) DiI-PKMs, (B) coumarin-6-PKMs in the spinal cord.	94
Figure 4.2: Distribution of DiI loaded PCADKe microparticles in the spinal cord. (A) the nuclei were stained with DAPI to visualize the structure of spinal cord section (B) DiI-PKMs distribution in the L1/L2 spinal cord, (c) merged images of DAPI and DiI-PKMs (10 X) (D) merged images of DAPI and DiI-PKMs (2 X)	95
Figure 4.3: Comparison of disease progression by (A) ALS motor score (B) BBB score (A) ¹ H-NMR and (B) GPC spectra of PK8	97
Figure 4.4: (A) Hindlimb grip strength and (B) Rotarod treadmill performance	99
Figure 4.5: (A) Weight loss (B) Survival Study	100
Figure 4.6: Nissl stain of spinal cord	102
Figure 4.7: (A) motor neuron density and (B) motor neuron soma area in the spinal cord at L1-L2	103

LIST OF ABBREVIATIONS

AK295	Cbz-Leu-aminobuturate-CONH(CH ₂) ₃ morpholine
AK-PKM	AK295 encapsulated PCADKe microparticle
ALF	Acute liver failure
ALS	Amyotrophic lateral sclerosis
ALT	Alanine aminotransferase
AMC	7-amino-4-methylcoumarin
AOPHA-Me	5-(Acetylamino)-4-oxo-6-phenyl-2-hexenoic Acid Methyl Ester
AOPHA-Me-	AOPHA-Me-encapsulated PCADKe microparticle
PKM	
BBB	Blood brain barrier
BBB scale	The Basso, Beattie, Bresnahan Locomotor Rating Scale
BSCB	Blood spinal cord barrier
BSA	Bovine serum albumin
CDM	1,4-Cyclohexanedimethanol
CNS	Central nervous system
Coumarin-6-PKM	Coumarin-6-encapsulated PCADKe microparticle
CSF	Cerebral spinal fluid
Da	Dalton
DAPI	4',6-diamidino-2-phenylindole
DCM	Dichloromethane
DEP	2,2-diethoxypropane

DiI	1,1'-Dioctadecyl-3,3,3',3'-tetramethylindocarbocyanine perchlorate
DiI-PKM	DiI-encapsulated PCADKe microparticle
DLS	Dynamic light scattering
DMF	Dimethylformamide
DMP	2,2-Dimethoxypropane
DMSO	Dimethylsulfoxide
DNA	Deoxyribonucleic acid
DOTAP	1,2-Dioleoyl-3-Trimethylammonium-Propane
FBS	Fetal bovine serum
Fl-siRNA	Fluorescein-labeled siRNA
Fl-siRNA	Fluorescein-labeled siRNA-encapsulated microparticles
GPC	Gel permeation chromatography
HPLC	high performance liquid chromatography
HUVECs	Human umbilical vein endothelial cells
LC-MS	Liquid chromatography-mass spectrometry
K _i	The inhibitory constant
MDL-PKM	MDL-28170 encapsulated PCADKe microparticle
M _n	Number-average molecular weight
M _w	Weight-average molecular weight
NADPH oxidase	Nicotinamide adenine dinucleotide phosphate-oxidase
NMR	Nuclear magnetic resonance
NR-PKM	Nile Red-encapsulated PCADKe microparticle

OCT	Optimal cutting temperature
PBS	Phosphate-buffered saline
PCADKe	Poly(cyclohexane-1,4-diyl acetone dimethylene ketal), which is synthesized using DEP/DMP method
PCADKi	Poly(cyclohexane-1,4-diyl acetone dimethylene ketal), which has low solubility in DCM and THF
PCADK	Poly(cyclohexane-1,4-diyl acetone dimethylene ketal)
PCR	Polymerase chain reaction
PDE4	Phosphodiesterase IV
PK3	Poly(cyclohexane-1,4-diyl acetone dimethylene ketal -co-1,5-pentane-acetone dimethylene ketal) (87:13 mol %)
PK8	Poly(cyclohexane-1,4-diyl acetone dimethylene ketal -co-1,5-pentane-acetone dimethylene ketal) (83:17 mol %)
PK9	Poly(cyclohexane-1,4-diyl acetone dimethylene ketal -co-1,5-pentane-acetone dimethylene ketal) (81:19 mol %)
PK10	Poly(cyclohexane-1,4-diyl acetone dimethylene ketal-co-1,4-butane-acetone dimethylene ketal) (70:30 mol %)
PKM	polyketal microparticles
PLGA	Poly(lactic acid), poly(lactic- <i>co</i> -glycolic acid)
PPADK	poly(1,4-phenylene-acetonedimethylene ketal)
PTSA	p-Toluenesulfonic acid
PPTSA	pyridinium <i>p</i> -toluenesulfonate
PVA	Poly(vinyl alcohol)

RFU	Relative-fluorescence-units
RNA	Ribonucleic acid
RPM	Revolutions per minute
SCI	Spinal cord injury
SEM	Scanning electron microscopy/microscope
SEM	Scanning electron microscopy/microscope
EM	Standard error of the mean
SDS	sodium dodecyl sulfate
SOD	Superoxide dismutase
TBI	Traumatic brain injury
TFA	Trifluoroacetic acid
TNF- α	Tumor necrosis factor-alpha

SUMMARY

Amyotrophic lateral sclerosis (ALS) is a devastating disease. Currently, there is no cure for this disease, and effective treatment strategies are greatly needed. Calpain activation plays a major role in the motor neuron degeneration that causes ALS. Therefore, therapeutic strategies can inhibit calpain activity in the central nervous system (CNS) have great clinical potential. The calpain inhibitors AK295 and MDL-28170 have been demonstrated to be neuroprotective in animal models of neurological injury, and should have great potential to treat ALS; however delivery problems have hindered their clinical success. Although many delivery strategies have been developed for overcoming CNS barriers, none of them have the properties needed for treating ALS with AK295. Therefore, development of a new strategy that can locally deliver the calpain inhibitors to the central nervous system could significantly improve the treatment of ALS. The objectives of my thesis research were (1) to develop high molecular weight polyketals that provide sustained release properties for hydrophobic molecules, (2) to formulate calpain inhibitor-encapsulated polyketal microparticles which have a release half life of one month *in vitro*, (3) and to evaluate the performance of polyketal microparticles for delivering calpain inhibitors to the spinal cord *in vivo*.

The first two specific aims focused on developing a biodegradable polymeric delivery system which has the sustained release properties needed for calpain inhibitor delivery. In the first specific aim, we developed a polyketal microparticle delivery system which has a sustained release profile of one month for hydrophobic dye, as a model delivery system for calpain inhibitors. Using a new methodology, we synthesized

a series of high molecular weight polyketal polymers, which can enhance the encapsulation efficiency of calpain inhibitors and improve their structural stability of polyketal microparticles. The goal of the second specific aim was to develop a polyketal microparticle delivery system for the calpain inhibitors, AK295 and MDL-28170, and evaluate their *in vitro* release profiles and bioactivities. AK295- and MDL-28170-loaded polyketal microparticles (AK-PKMs and MDL-PKMs) were prepared by a single emulsion solvent evaporation procedure. The results of calpain assay showed that both AK-PKMs and MDL-PKMs maintain most of their inhibitory activities even after the robust emulsion process. The *in vitro* release profile of MDL-28170 in MDL-PKMs showed 50% of the drug was released in the first 30 days.

In the third specific aim, we demonstrated that polyketal microparticles can be safely delivered to the spinal cord. Experiments using dye-encapsulated microparticles showed that polyketal microparticles (1-2 μm diameter) are not easily cleared in the neutral physiological environment and can have potential to continuously release drug from the injection sites in the spinal cord. The efficacy of calpain inhibitor-encapsulated PKMs were studied by evaluation the behavior and survival of SOD1^{G93A} rats, a genetic rat model for ALS. We observed the trend toward improvements in grip strength and rotarod performance in the first two months from the AK-PKMs treated group, however, there was no statistical differences between calpain inhibitor treated group with saline control. In summary, our data show that polyketal microparticles have considerable potential as delivery system for calpain inhibitor for the treatment of ALS, however, further improvements are needed to enhance the *in vivo* efficacy.

CHAPTER 1

INTRODUCTION

1.1. Background and Motivation

Amyotrophic lateral sclerosis (ALS) is a progressive neurodegenerative disease that causes rapid loss of motor neurons and leads to muscular atrophy, respiratory failure and eventually death (Sejvar, Holman et al. 2005). In the United States alone, approximately 5,600 new cases of ALS are expected to be diagnosed each year, and the life expectancy of an ALS patient averages two to five years from the time of diagnosis. Although the disease was first identified 140 years ago, the exact cause of motor neuron loss in ALS remains unknown. Currently, riluzole (Rilutek[®]) is the only drug treatment for ALS approved by the Food and Drug Administration (FDA). However, the drug only slows progression of ALS rather than curing the disease (Bruijn, Miller et al. 2004; Nirmalanathan and Greensmith 2005). Therefore, new treatment options are greatly needed for this devastating disease.

Calpain activation is a known important mechanism of motor neuron degeneration in ALS (Fischer, Culver et al. 2004), and therefore therapeutic strategies that can inhibit calpain activity specifically in the CNS have clinical potential. Calpain inhibitors have been demonstrated to be neuroprotective in animal models of neurological injury, and should have great potential to treat ALS; however delivery problems have hindered their clinical success. For example, AK295 is a hydrophobic calpain inhibitor, which shows great drug properties but has low efficacy *in vivo*, due to issues with crossing the CNS barriers. Thus, there is a great need to find a safe and effective CNS drug delivery system that can translate these experimental strategies into clinical therapies.

Drug delivery to the CNS has been particularly inefficient, largely due to the barriers in the CNS. Only some small hydrophobic agents (< 500 Daltons) can penetrate these barriers (Lesniak and Brem 2004). To achieve therapeutic levels of drug in the CNS, the drug must be administered systemically at high dosage, which leads to serious side effects. One possible way to minimize systemic side effects is to administer the drug directly into the CNS.

Many strategies have been developed to improve the safety and efficiency of local drug delivery, such as implantable catheter pump systems and implantable polymeric drug delivery systems (Gill, Patel et al. 2003). Direct drug infusion by minipumps can precisely control the dosage at the site of interest; however, there are still some flaws limiting the success of this type of drug delivery systems, such as infection, catheter obstruction and patient discomfort. Implantation of drug-containing biodegradable devices such as microparticles can deliver the highest local drug concentration (Kirik, Georgievska et al. 2004; Clavreul, Sindji et al. 2006), however, despite their attractive features; microparticles have not been used extensively for the treatment of ALS or other neurodegenerative diseases. This is primarily because currently used biomaterials for microparticle-based drug delivery are predominantly based on polyesters such as poly(lactic-co-glycolic acid) (PLGA), which degrade into acidic products that may destroy the encapsulated therapeutic agents and cause an inflammatory response (Shenderova, Burke et al. 1999; Fu, Pack et al. 2000; Tamber, Johansen et al. 2005).

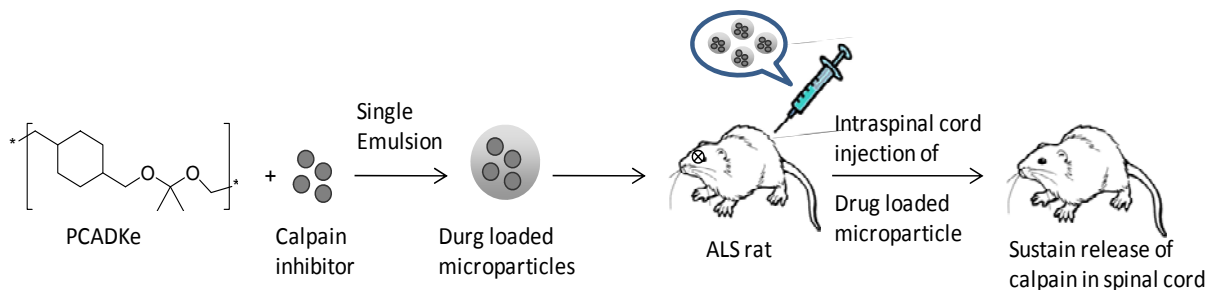
Polyketals are new biodegradable polymers which degrade into the neutral products, acetone and diols (Heffernan and Murthy 2005; Lee, Yang et al. 2007; Yang, Bhide et al. 2008). Microparticles formulated from polyketals have shown promise as

drug delivery vehicles for the treatment of ALS because they have excellent biocompatibility and do not generate inflammatory acid degradation products as do polyester-based biomaterials (Sy, Seshadri et al. 2008). In addition, polyketals provide a wide range of degradation rates, ranging from weeks to months at pH 7.4, depending on their compositions. Drug release rates from polyketal microparticles can be controlled by manipulation of the hydrophobicity of the polymers. Due to these advantages, microparticles formulated from polyketals show promise to enhance the treatment of inflammatory diseases (Sy, Seshadri et al. 2008; Yang, Bhide et al. 2008).

However, polyketal-based delivery systems have lower drug loading efficiency than the delivery systems based on other biodegradable polymers, such as PLGA and polyanhydride. This is possibly due to the low molecular weight of current polyketals. Also, particles formulated from low molecular weight polyketals have less structure stability and tend to collapse under high speed centrifugation. Given these limitations of current polyketal polymers, a new synthetic methodology which can increase the molecular weight of polyketals and expand their applications is needed.

1.2 Research Objectives and Specific Aims

Calpain activation is an important mechanism of motor neuron degeneration in ALS, and therapeutic strategies that can inhibit calpain activity in the central nervous system (CNS) have great clinical potential. Calpain inhibitors have been demonstrated to be neuroprotective in animal models of neurological injury, and have great potential to treat ALS; however delivery problems have hindered their clinical success. AK295 is a hydrophobic calpain inhibitor, which shows great drug properties for treating ALS but has low efficacy *in vivo*, due to the barriers in the CNS. Although many delivery strategies have been developed for overcoming CNS barriers, none of them have properties needed for treating ALS with AK295. Therefore, development of a new strategy that can locally deliver calpain inhibitor to the central nervous system could significantly improve the treatment of ALS.



Scheme 1.1 Polyketal-based drug delivery system for ALS treatment. Calpain inhibitors (AK295 and MDL-28170) were encapsulated within polyketal microparticles and injected into the spinal cord of rats. The microparticles are designed to release AK295 slowly into the spinal cord over a period of weeks to months.

The goal of this research was to develop an injectable polyketal microparticle delivery system which can generate a several micromolar concentration of calpain inhibitor in the spinal cord for two months after a single injection (Scheme 1.1).

The **objectives** of my thesis research were (1) to develop high molecular weight polyketal microparticles that provide sustained release properties for hydrophobic

molecules, (2) to formulate calpain inhibitor-encapsulated polyketal microparticles which have a release half life of 1 month *in vitro*, (3) to evaluate the performance of polyketal microparticles for delivering calpain inhibitors to the spinal cord *in vivo*. The central hypothesis of this research is that: *a direct injection of calpain inhibitor-polyketal microparticles into the spinal cord will generate several micromolar concentration of calpain inhibitor in a two month period.* The central hypothesis of this thesis was tested by completing the following aims.

Specific Aim 1: Formulate hydrophobic dye-encapsulated PKMs which have a release half-life of 1 month *in vitro*.

Hypothesis 1: We hypothesize that (1) high molecular weight polyketals can enhance drug loading efficiency, (2) that the drug release rate from PKMs can be controlled by manipulating their sizes.

In this aim, high molecular weight polyketals were synthesized via a new methodology using 2,2-diethoxypropane (DEP), a ketal with a high boiling point. The reactions were optimized with regards to the reaction temperature, duration and fine-tuned by an extra volume of ketals. The resulting high molecular weight polyketals were characterized by gel permeation chromatography (GPC) and nuclear magnetic resonance (NMR) spectroscopy, and their pH-sensitive degradation were demonstrated by NMR. One of the high molecular weight polyketals, PCADKe, had lowest hydrolysis rate of the polyketals, thus microparticles formulated from PCADKe have the potential for sustained delivery of hydrophobic compounds at pH 7.4. The release kinetics of polyketal microparticles (PKMs) were optimized by using a fluorescent dye, DiI as a model compound for calpain inhibitors, due to a similar hydrophobicity between DiI and calpain

inhibitors (AK295 and MDL-28170), and can be measured by fluorescence spectrometry. Various formulations and sizes of polyketal microparticles (PKMs) were prepared and characterized to optimize their release rates.

Specific Aim 2: Formulate calpain inhibitor-encapsulated PKMs which have a release half-life of 1 month *in vitro*.

Hypothesis 2: We hypothesize that calpain inhibitor-encapsulated microparticles (AK-PKMs and MDL-PKMs) can preserve the activity of calpain inhibitors and have a release half-life of 1 month.

In this aim, PKMs which contain the calpain inhibitors (AK295 or MDL-28170) were fabricated, using formulation procedures developed in Aim 1. The size of AK295 encapsulated PCADKe microparticles (AK-PKMs) and MDL-28170 encapsulated PCADKe microparticles (MDL-PKMs) were characterized by scanning electron microscopy (SEM). The encapsulation efficiency of AK295 in AK-PKMs was measured by liquid chromatography-mass spectrometry (LC-MS). The encapsulation efficiency and *in vitro* release profile of MDL-28170 in MDL-PKMs were measured by reverse phase high performance liquid chromatography (HPLC). The inhibitory activity of AK295 and MDL-28170 released from microparticles were measured by a modified *in vitro* calpain assay.

Specific Aim 3: Deliver calpain inhibitor-encapsulated microparticles to the spinal cord and evaluate their *in vivo* efficacy.

Hypothesis 3: We hypothesize that polyketal microparticles will deliver several micromolar concentration of calpain inhibitor to the spinal cord for two months after an intraspinal cord injection.

In Specific Aim 3, we investigated the *in vivo* performance of PCADKe microparticles. The dye encapsulated PKMs (Nile Red PKMs, DiI-PKMs and coumarin 6 PKMs) formulated in Aim 1 were used to study the fate of the polyketal microparticles after intraspinal cord injection. The distribution of the microparticles was measured by fluorescence microscopy. The AK-PKMs and MDL-PKMs formulated in Aim 2 were used to investigate the *in vivo* activity of calpain inhibitors in the spinal cord tissue. In this specific aim, either AK-PKMs (n = 8), MDL-PKMs (n = 8), or PBS (n = 6) were injected into the lumbar enlargement, L1-L2, of SOD1^{G93A} rats, a genetic rat model for ALS. For each SOD1^{G93A} rats, 5 μ L of 50 mg/mL AK-PKMs, 50 mg/mL MDL-PKMs, or PBS was injected into both hemispheres of the spinal cord at 70 days, which precedes symptom onset. Disease progression was monitored by weekly assessment of weight loss, grip strength, rotarod performance, and ALS motor score. A survival curve of the ALS animals was generated using Kaplan-Meier method.

1.3 Review of Relevant Literature

Calpain inhibitors have great potential to treat ALS

Calpains are a family of calcium-dependent cysteine proteases that play a major role in the process of axonal and neuronal degradation in ALS and other neurodegenerative diseases (Bartus 1997; Ray and Banik 2003). Although the cause of ALS is still unknown, studies have shown that excessive interstitial glutamate, cytosolic calcium and oxidative stress upregulate calpain activation. Activation of intracellular calpain leads to proteolysis of calpain-specific substrates such as cytoskeletal proteins, microtubule-associated proteins and neurofilament proteins and consequently induces the death of neurons (Huang and Wang 2001). Therapeutic strategies that can inhibit calpain activity in the CNS have been shown to be neuroprotective in animal models of many neurological disorders.

Kupina *et al.* have studied the effect of the calpain inhibitor SJA6017 in the treatment of mice suffering from diffuse brain injury. They measured the 24-hour postinjury functional outcome after treating the animals with SJA6017 at different time points, and have indicated a potential therapeutic window of 4 hours for diffuse brain injury (Kupina, Nath *et al.* 2001). *Ai et al.* also showed that early administration of MDL-28170 could protect the brain from focal ischemic brain damage in a rat fluid percussion model for up to 3 days (Ai, Liu *et al.* 2007). In addition to these promising results, calpain inhibitors have also provided several advantages over glutamate receptor antagonists and calcium ion channel blockers, such as reduced detrimental side-effects outside the central nervous system (Wang, Larner *et al.* 2006).

Among all of the calpain inhibitors, the dipeptide α -ketoamide calpain inhibitors have shown the greatest inhibitory potency and specificity for calpains, and thus they have the potential to treat ALS (Li, Patil et al. 1993; Harbeson, Abelleira et al. 1994; Li, Ortega-Vilain et al. 1996). However, the solubility of these inhibitors in aqueous solution is extremely low and this has limited their clinical applications. AK295 (Cbz-Leu-aminobuturate-CONH(CH₂)₃morpholine), a modified dipeptide α -ketoamide calpain inhibitor, was developed to increase the solubility while preserving the effectiveness of the drug. The inhibitory constant (K_i) of AK295 to calpain I and calpain II are 140 and 41 nM, respectively (Li, Ortega-Vilain et al. 1996). This low K_i value indicates that AK295 has great potency in the inhibition of calpain. James *et al.* showed that AK295 can inhibit 53-63 % of calpain activity at a 1 μ M concentration; however, it almost had no inhibitory effects on the degradation of calpain proteolysis substrates such as, neurofilament protein (NFP) and myelin basic protein (MBP). At least a 10 μ M concentration of AK295 is needed to achieve 50% inhibition of NFP and MBP degradation (James, Matzelle et al. 1998). Bartus *et al.* also showed that AK295 has a dose-dependent neuroprotective effect in a rat focal ischemia model (Bartus, Hayward et al. 1994). All these studies suggested that AK295 bioavailability is an important factor for inhibition of calpain related proteolysis. Although the solubility of AK295 has been improved (compared to other dipeptide α -ketoamide calpain inhibitors), its solubility is still relatively low (0.13 mg/mL at pH 7.0 and 0.049 mg/mL at pH 8.0) (data from SciFinder). In order to get an optimal pharmacokinetic profile, AK295 needs to be dissolved in acidic pH before injection (Saatman, Murai et al. 1996), which might cause some unwanted inflammatory effects. The other drawback of the current AK295 delivery

system is that it requires the animals to receive a continuous intra-arterial infusion of AK295 solution up to 54 mL in a 48 hour period. In the treatment of ALS, a larger delivery (volume/dose) may be needed and complications such as, infection, catheter obstruction, and discomfort can arise in patients when using this delivery method.

MDL-28170 is another potent calpain inhibitor used in this thesis. Unlike AK295, MDL-28170 can penetrate the BBB due to its low molecular weight and hydrophobicity. However, like AK295, MDL-28170 needs to be dissolved in acidic buffer or organic solvent to get an optimal pharmacokinetic profile, and also has a dose-dependent neuroprotective effect. Therefore, the same complications described for AK295 might apply to MDL-28170 as well. Currently, there is no literature describing the side effects of MDL-28170 because current applications of MDL-28170 mainly focused on the acute diseases such as spinal cord injury (SCI) and acute liver failure (ALF). Galvez *et al.* (Galvez, Diwan et al. 2007) showed that loss of myocardial calpain I activity potentially cause cardiomyocyte degeneration. Since MDL-28170 is a potent calpain I inhibitor, it might increase the risk for heart failure during the treatment of ALS. Thus, there is a great need to improve current calpain inhibitor delivery systems.

CNS barriers for drug delivery

The goal of my research is to design a drug delivery system which can overcome the CNS barriers and enhance the delivery of AK295 in the spinal cord. An understanding of the CNS barriers will be useful for the design of new therapeutic strategies.

The failure of systemically delivered therapeutic agents to effectively treat CNS diseases is mainly due to the presence of the highly impermeable blood brain barrier

(BBB) (Pardridge 2003) and blood-spinal cord barriers (BSCB). Both BBB and BSCB, which are composed of cerebral capillary endothelial cells and tight junctions, prevent the passive uptake of hydrophilic and large molecules into the CNS (Goldstein and Betz 1986). Only small molecular weight, uncharged, and lipophilic molecules can passively cross this barrier (Habgood, Begley et al. 2000). Moreover, the endothelial cells of brain capillaries have fewer pinocytotic vesicles than those of capillaries elsewhere in the body (Pardridge 2002). The transport of molecules, which depends on the cellular transcytosis, is therefore severely compromised. Finally, a number of transport proteins located in the luminal membranes of cerebro capillary endothelium are known to be involved in the influx and efflux of endogenous and exogenous molecules across the BBB (Kusuhara and Sugiyama 2001). Efflux transport proteins such as P-glycoprotein and multidrug resistance associated protein actively remove a wide range of therapeutic agents before they cross into the brain parenchyma, and thus effectively restrict drugs from entering the CNS (Kusuhara and Sugiyama 2001; Taylor 2002).

The second barrier for therapeutic drug delivery to the CNS is the blood-cerebrospinal fluid barrier (BCB). This barrier is formed by the specialized tight junctions of endothelial cells in the choroids plexus. The BCB closely regulates the exchange of molecules between the blood and cerebrospinal fluid (CSF), thus it also regulates drug entry into the brain parenchyma. However, the BCB is not as major of a barrier as the BBB. The surface area of BCB is approximately 1000 fold less than that of the BBB (Pardridge 1997).

These barriers together compose a very delicate control system to maintain homeostasis of the CNS. However, the same control system that protects the brain from

foreign substances also restricts the entry of many potential therapeutic agents. There is a great need to find an effective drug delivery system that can overcome these barriers.

Local drug delivery systems for overcoming CNS barriers

Drug delivery to the CNS has been particularly inefficient, mainly due to the presence of the highly impermeable BBB and BSCB. The understanding of these barriers has been used in the rational design of new therapeutic strategies. There are a series of techniques that have been applied to improve local drug delivery efficacy to CNS. They are discussed below.

Catheter with pump system

The simplest and most direct strategy to overcome the barriers to CNS is to administer the therapeutic drug directly into the CNS via a catheter system. Currently, implantable catheter pump systems are mainly used for treating brain tumors (Lesniak and Brem 2004; Rautioa and Chikhale 2004). However, researchers have begun to explore the feasibility of using this delivery system for ALS therapy. For example, the Alzet Osmotic Minipump system has been used to deliver therapeutic agents (including cannabitol, hepatocyte growth factor, amino acids, antibodies and siRNA) for treating ALS animals (Nakamura, Kamakura et al. 1997; Weydt, Hong et al. 2005; Ishigaki, Aoki et al. 2007; Locatelli, Corti et al. 2007; Urushitani, Ezzi et al. 2007). This system can provide two to four weeks of continuous infusion of drugs in the intrathecal space, however, they cannot be refilled, and require surgical removals. Recently, a more advanced implantable infusion pump, the Medtronic SynchorMed system was tested in clinical trials for ALS treatment (Nakamura, Kamakura et al. 1997). This system is able to deliver drugs at a constant rate over a prolonged period of time at the intrathecal space

through the outlet catheter, and can be refilled by subcutaneous injection. Despite encouraging results, there are still many flaws limiting the success of this type of drug delivery system, such as infection, catheter obstruction and discomfort to the patient.

Local implantation of sustained controlled release polymer

The objective of implantable polymer-based microparticles for treating CNS disease is to provide continuous drug delivery to the CNS using a matrix that also protects the drug from degradation. The first generation of controlled release polymer system is based on non-biodegradable polymers. Langer and Folkman first reported the sustained and controlled release of macromolecules from an ethylene vinyl acetate copolymer (EVAc) (Langer and Folkman 1976). The encapsulated drug is released by diffusion through the micropore of the polymer matrix. Although EVAcs have found applications in glaucoma, diabetes and asthma therapy, it is not specifically FDA approved for use in the brain (Lesniak and Brem 2004).

A major step for developing controlled release polymers in treating CNS diseases is the development of biodegradable polymer systems. Brem and coworkers have studied the treatment of recurrent malignant glioma with the anticancer drug carmustine via a biodegradable polyanhydride wafer (Brem and Gabikian 2001). This biodegradable polymer, poly[bis(p-carboxyphenoxy) propane-sebacic acid](p(CCP-SA)), releases drug by both hydrophobic degradation and drug diffusion. They demonstrated biocompatibility of this polymer system, and sustained release of carmustine in a preclinical study (Brem, Mahaley et al. 1991). After clinical trials, the FDA approved carmustine loaded p(CCP-SA) wafer (Gliadel[®]) for the treatment of malignant glioma. Although Gliadel has been used clinically, one of the limitations of this p(CCP-SA)

copolymer is that it is designed for delivery of hydrophobic molecules. To overcome this limitation, the fatty acid dimer-sebacic acid (FAD-SA) copolymer, another biodegradable polymer, was developed for delivery of hydrophilic molecules (Domb, Maniar et al. 1991). These two biodegradable polymers share the same mechanism of release and the possibility to vary the release kinetics by varying the ratio of the two monomers. The sizes of these implantable polymeric devices are several centimeters which can provide a large drug depot and sustained release of therapeutic agents for a long period of time. However, the sizes of these polymeric devices are too big for intraparenchymal and intraspinal cord implantation and become the major limitations for these implantable devices.

The use of microparticles for delivering therapeutic agents represents a new evolving technology for treating CNS disease. Microparticles are 1 to 1000 μm particles that are made of different types of polymers and provide certain benefits as drug delivery systems. For example, microparticles can: 1) effectively protect the encapsulated drugs from degradation, 2) provide controlled release of therapeutic agents for long periods of time, and 3) can be easily administrated to the targeted area. With stereotaxic technique, the drug-loaded microparticles can be precisely injected to the site of action which makes them able to deliver therapeutics to the spinal cord and inoperable brain tumor.

The general limitation for the above polymeric implant systems is that drug release cannot be controlled once the system has been implanted; thus an increased risk of local neurotoxicity might occur at higher polymer or therapeutic agent concentrations (Rautioa and Chikhale 2004).

Microparticles for spinal cord delivery

Microparticles offer several advantages as drug delivery systems. With the stereotaxic technique, drug loaded microparticles can be precisely injected to the site of action within the CNS and provide controlled release properties over a long period of time. However, most of the microparticle studies relevant to treating CNS disorders mainly focus on delivery of therapeutic agents to the brain. Even in spinal cord delivery, the microparticles are mainly injected to intrathecal or epidural space and only served as a depot for small molecular weight anesthetic drugs which can pass through the BBB easily. Milligan *et al.* encapsulated pDNA-IL-10 in PLGA microparticles and injected these PLGA-pDNA-IL-10 microparticles to the intrathecal space for treating neuropathic pain. They observed that PLGA microparticles can be evenly distributed in the meninges but not in the deeper parenchymal spinal cord layers (Milligan, Soderquist et al. 2006). For treating ALS disease, the therapeutics need to be able to be delivered into the gray matter in the spinal cord. However, currently no polymeric microparticle formulation has been used for intra-spinal cord delivery of therapeutics inside the parenchyma of the spinal cord. This is potentially due to the inflammatory response of current degradable polymer systems. In our preliminary studies, we have shown the PCADK microparticles generate minimal inflammatory response in animals. We therefore anticipate that injection of calpain inhibitor-encapsulated PKMs into the spinal cord will cause less tissue inflammatory response than other microparticle formulations.

Particle size and hydrophobicity of polymer influence the release of hydrophobic drug

Biodegradable nano- and microparticles have been used as controlled drug delivery systems to release therapeutic agents at a controlled rate for days, weeks or months. Drug loading and release rates are important parameters in particle-mediated drug delivery. In general, hydrophobic drugs can be encapsulated into particles using an oil-in-water emulsion-solvent evaporation method, and usually have a higher encapsulation efficiency than hydrophilic drugs. The release profiles from nano- or microparticles are complex due to different interactions between drugs and polymers. The main mechanisms of controlled release are driven by the following phenomena: 1) drug diffusion to the aqueous solution, 2) drug dissolution from the polymer matrix to the solvent, and 3) polymer erosion due to hydrolysis and water penetration (Saltzman 2001). The erosion of biodegradable polymers is classified into two types: bulk erosion and surface erosion. The erosion mechanism of a polymer depends on the diffusivity of water into the polymer matrix, degradation rate of the polymer due to hydrolysis, and the size of the polymer matrix (von Burkersroda, Schedl et al. 2002). The factors that affect the erosion mechanism will influence the release rate of the drug. Among these factors, most of the research showed that two factors, at least, must be taken into account: the hydrophobicity of the polymer and the size of the biodegradable nano- or microparticles. Thus, a thorough investigation of these two factors affecting drug release profile from these polymeric particle devices is critical to the design of optimal delivery systems.

First, the hydrophobicity of a polymer will influence the water diffusion rate into the microparticle and change its drug release profile. Panyam *et al.* described that the

release rate of dexamethasone, a hydrophobic drug, from PLGA nanoparticles is slower when the hydrophobicity of PLGA increased (Panyam, Williams et al. 2004). In another study, Budhian *et al.* encapsulated haloperidol, a hydrophobic drug, into various PLGA nanoparticles which varied in size, polymer hydrophobicity, and particle coatings. They found that increasing the polymer hydrophobicity can extend the period of release (Budhian, Siegel et al. 2008). PLGA 50:50 microparticles completely release haloperidol in a 30 day period, while the same size PLA microparticles (more hydrophobic polymer) only released 35% of the haloperidol in a 40 day period.

Second, the size of microsphere is another important factor that affects the release rate of hydrophobic drugs. In general, smaller microparticle release drug faster due to an increased surface area to volume ratio. Budhian *et al.* also showed that increasing the particle size can reduce the initial burst effect and extend the period of release within nanoparticle formulations (Budhian, Siegel et al. 2008). Their data showed that 50% of the haloperidol was released in the first day from 220 nm PLGA nanoparticle, while only 10 % was released from 1300 nm PLGA microparticles in the same period. This is because the larger size increases the length of the diffusion pathway for the drug and prevents the initial burst.

The particle size also affects the erosion mechanism of the polymer. According to the research done by von Burkersroda *et al.*, polyketals will undergo bulk erosion when the polymer devices are smaller than 400 μm (von Burkersroda, Schedl et al. 2002).

Polyketal-based delivery systems have potential for treating CNS disease

Polyketals are a new family of biodegradable polymers designed for drug delivery (Heffernan and Murthy 2005; Lee, Yang et al. 2007; Yang, Bhide et al. 2008).

Microparticles formulated from polyketals degrade into neutral compounds and should therefore prevent the inflammatory problems associated with polyester-based and poly-anhydride-based delivery devices. In the last decade, researchers have found increasing evidence demonstrating that inflammation and inflammatory mediators contribute to acute, chronic CNS degenerative diseases (Lucas, Rothwell et al. 2006). For example, Tehranian *et al.* found that inflammatory mediators such as tumor necrosis factor- α (TNF- α), IL-1, and IL-6 were upregulated in closed head injury model (Tehranian, Andell-Jonsson et al. 2002). Yoshihara *et al.* found that the levels of TNF- α are elevated in ALS SOD1 mutant mice, suggesting that inflammation contributes to ALS (Yoshihara, Ishigaki et al. 2002). Therefore, an ideal implantable polymer drug delivery system should produce minimal inflammation, which makes polyketal microparticle a good candidate for CNS delivery.

Currently, a number of polyketals have been synthesized for drug delivery applications, poly(1,4-phenyleneacetone dimethylene ketal) (PPADK), poly(cyclohexane-1,4-diyl acetone dimethylene ketal) (PCADK), and copolymers of PCADK (Heffernan and Murthy 2005; Lee, Yang et al. 2007; Yang, Bhide et al. 2008). PPADK has rapid hydrolysis kinetics, but degrades into benzene dimethanol, a compound with potential toxicity, due to its aromatic ring (Heffernan and Murthy 2005). PCADK and PCADK-copolymers, in contrast, degrade into acetone and 1,4-cyclohexanedimethanol, both of which have excellent biocompatibility. PCADK has a hydrolysis half-life of 24 days at pH 4.5 (Lee, Yang et al. 2007), thus PCADK microparticles can slowly release drugs for a long period of time which makes PCADK microparticles desirable delivery devices for chronic neural degenerative diseases such as

Parkinson's disease, Alzheimer's diseases, and ALS. Copolymers of PCADK have been developed as drug delivery vehicles for the treatment of acute liver failure because of their neutral degradation products and tunable hydrolysis kinetics (Yang, Bhide et al. 2008). In particular, one PCADK copolymer, PK3, has a hydrolysis half-life of 2 days at pH 4.5 and several weeks at pH 7.4. Microparticles formulated from PK3, encapsulated with the kinase inhibitor imatinib, demonstrated improved efficacy in the treatment of acute liver failure caused by the immunotoxin Concanavalin A, *in vivo*. Therefore, microparticles formulated from PK3 should be suitable for treating acute CNS injuries, such as traumatic brain injury (TBI), because they hydrolyze and release therapeutics rapidly in the acidic phagolysosomes of microglia and astrocytes, and also release therapeutics in the neutral extracellular environment in a sustained manner.

Polyketal-based delivery systems have shown to have high encapsulation efficiency in the loading of small hydrophobic drugs; however, a major limitation of current polyketal-based delivery systems is low encapsulation efficiency of large proteins or other hydrophilic compounds. This is possibly due to the low molecular weight of currently used polyketals. For example, the typical M_n of a polyketal used in previous study ranges between 2,000 and 3,000 Daltons, whereas PLGA with a M_n of 10,000 Dalton or larger is used to encapsulate proteins for drug delivery applications. The encapsulation efficiency of lysozyme in PLGA microparticles is typically higher than 39 % (Taluja, Youn et al. 2007). On the other hand, polyketals can only achieve less than 16 % encapsulation efficiency using double emulsion procedures. In this research, we planned to improve the loading efficiency of PKMs by increasing the molecular weight of the polyketals, and the size of the PKMs.

CHAPTER 2

DEVELOP HIGH MOLECULAR WEIGHT POLYKETALS THAT PROVIDE SUSTAINED RELEASE PROPERTIES FOR HYDROPHOBIC MOLECULES

2.1 Introduction

In this chapter, we discuss Specific Aim 1 which is to develop a hydrophobic dye encapsulated polyketal microparticle which has an *in vitro* release half-life of one month at pH 7.4. To reach this goal, we first synthesized a high molecular weight polyketal and used it to encapsulate hydrophobic dyes. The release kinetics of the dye from the microparticles were optimized by altering the particle size. In this section, we also describe the other applications of high molecular weight polyketals. Although the high molecular weight polyketals are originally developed for preparation of calpain inhibitor-loaded microparticles, we also found several new applications of high molecular weight polyketals such as 1) improving the encapsulation of AOPHA-Me, an anti-inflammatory drug for arthritis, and 2) fabricating siRNA loaded nanoparticles that can be delivered to the non-phagocytic cells, such as endothelium cells. We also discuss these new applications in this chapter.

Synthetic biodegradable polymers such as polyesters, polyorthoesters and polyanhydrides have been extensively investigated for controlled drug delivery applications. However, these polymers generate acidic degradation products which are not suitable for treating inflammatory diseases (Fu, Pack et al. 2000; Tamber, Johansen et al. 2005; Sugiyama, Yamashita et al. 2007). Therefore, there is a great need for developing new biodegradable polymers which have tunable hydrolysis profiles and most importantly, can degrade into neutral compounds. Polyketals are novel biodegradable

polymers which have ketal linkages in their backbone that can be rapidly hydrolyzed in an acid environment (Heffernan and Murthy 2005; Lee, Yang et al. 2007; Yang, Bhide et al. 2008). The hydrolysis rates of polyketals can be tailored for a specific application by varying the ratios of hydrophilic copolymers incorporated in the polyketal formulations (Yang, Bhide et al. 2008). Unlike other polyester-based materials, polyketals do not generate inflammatory acidic degradation products, but rather degrade into the neutral products acetone and diols, thus they should have great potential for treating inflammatory diseases (Lee, Yang et al. 2007; Sy, Seshadri et al. 2008; Yang, Bhide et al. 2008).

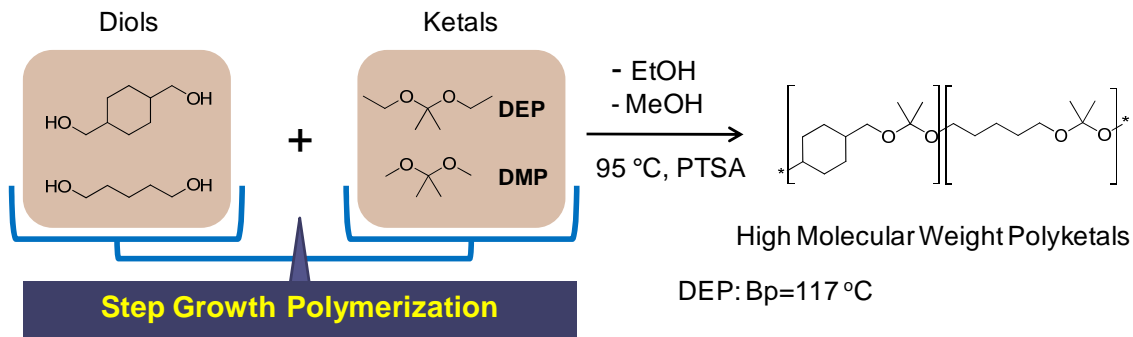
Currently, a number of polyketals have been synthesized, however, only poly(cyclohexane-1,4-diyl acetone dimethylene ketal) (PCADK), and copolymers of PCADK are suitable for drug delivery due to their tunable hydrolysis property and excellent biocompatibility (Lee, Yang et al. 2007; Sy, Seshadri et al. 2008; Yang, Bhide et al. 2008). In our laboratory, we have delivered several therapeutic agents to treat inflammatory diseases using the microparticles formulated from PCADK and its copolymers. For example, Sy *et al.* showed that delivery of p38 inhibitor-loaded PCADK microparticles to the damaged myocardium can improve the treatment of cardiac dysfunction (Sy, Seshadri et al. 2008). Microparticles formulated from PK3, encapsulated with the kinase inhibitor imatinib, demonstrated improved efficacy in the treatment of acute liver failure caused by the immunotoxin Concanavalin A, *in vivo* (Yang, Bhide et al. 2008).

Although polyketal-based delivery systems have shown great potential for treating inflammatory diseases, the loading efficiency of therapeutic agents is lower than

the other commercially available biodegradable polymer such as PLGA (Giovagnoli, Blasi et al. 2004; Lee, Yang et al. 2007). To reach a therapeutic effect, we have to deliver drug loaded polyketal microparticles at higher dosage which limits its clinical application. This is possibly due to the low molecular weight of these current polyketals.

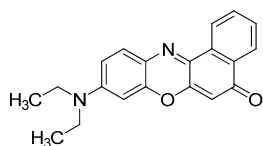
The low molecular weight issue also hindered the development of polyketal polymers with fast hydrolysis kinetics. In our previous report, polyketal copolymers with higher incorporation of 1,5-pentanediol were also generated; however those copolymers have a low molecular weight and were viscous liquids (Yang, Bhide et al. 2008), which are not suitable for formulation into microparticles for drug delivery.

Given these limitations with current polyketal polymers, a new synthetic methodology which can increase the molecular weight of polyketals and expand their applications is needed. The polyketals are synthesized via step-growth polymerization, we therefore speculate that their low molecular weight is due to an imbalance of the reactants during the polymerization process (Stille 1981). Although the diols and ketal are initially mixed at a 1 to 1 ratio (mol/mol), there is a significant loss of the 2,2-dimethoxypropane (DMP) during the polymerization, therefore altering the stoichiometry balance of the reactants. This is because the reaction occurs at 100 °C to remove the byproduct methanol, but also removes the DMP which has a boiling point of 83 °C, which is lower than the reaction temperature.



Scheme 2.1 A novel methodology to synthesize high molecular weight polyketals using DEP formulation.

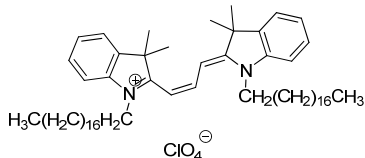
In this section, we used an alternative ketal, 2,2-diethoxypropane (DEP), which has a boiling point of 117 °C, which is above the reaction temperature (100 °C), for this acetal-exchange reaction to alleviate the removal of the reactants. However, in our first few experiments, we could only slightly increase the molecular weight of PK3 by using the DEP method. Thus, we speculate that there was still some DEP being evaporated with benzene and ethanol. Inspired by Tobita and Ohtan's intermediate monomer feed method (Tobita and Ohtani 1991), we added additional ketal (DEP or DMP) two hours after the reaction starts. The primary results showed a dramatic increase in molecular weight by adding additional DMP but not DEP. The optimal result was obtained by starting the reaction with DEP and diol at a 1 to 1 ratio (mol/mol) and adding additional DMP at a later time point to compensate for the loss of DEP during the reaction (Scheme 1). The properties of resulting polyketals were characterized by GPC, NMR, and DSC. The fabrication of drug loaded microparticles was also investigated.



Nile Red

$M_w = 318.37$

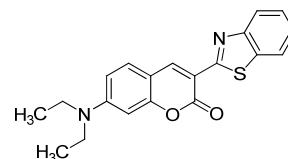
$\text{LogP} = 3.103 \pm 1.187$



DiI

$M_w = 933.87$

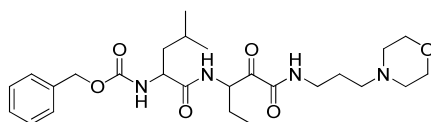
hydrophobic



Coumarin 6

$M_w = 350.43$

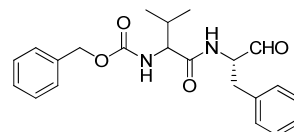
$\text{LogP} = 6.064 \pm 0.75$



AK295

$M_w = 504.66$

$\text{logP} = 2.327 \pm 0.813$



MDL-28170

$M_w = 382.45$

$\text{logP} = 4.156 \pm 0.705$

Figure 2.1 Comparison between calpain inhibitors and hydrophobic fluorescent dyes

The goal of my research is to formulate a polyketal microparticle delivery system which can release calpain inhibitors to the spinal cord in a sustained manner. To reach this goal, three different hydrophobic dyes (Nile Red, DiI and coumarin-6) were chosen as model compounds for the calpain inhibitors because they have similar hydrophobic profiles as calpain inhibitors and should have similar release kinetics (Figure 2.1). The polyketal microparticle formulations were optimized by comparing the release kinetics of the dye from various microparticle formulations. The encapsulation efficiency of DiI-PKMs was analyzed by fluorescence spectrometry. The physical properties of the resulting dye encapsulated microparticles were also investigated.

2.2 Experimental Methods

Material

2,2-diethoxypropane (DEP, acetone diethylacetal) was purchased from TCI (Tokyo, Japan). Double stranded fl-TNF- α siRNA (sense strand: 5'-GAC AAC CAA CUA GUG GUG CUU-3') was synthesized by Dharmacon (Lafayette, CO). 1,2-Dioleoyl-3-Trimethylammonium-Propane (Chloride Salt) (DOTAP) was purchased from Avanti Polar Lipids, Inc. (Alabaster, AL). All other chemicals were purchased from Sigma-Aldrich (St. Louis, MO) and used as received unless otherwise specified. Benzene, 2,2-dimethoxypropane and DEP were purified by distillation. AOPHA-Me was a gift from Dr. May.

Develop a new method for the synthesis of high molecular weight polyketal

Synthesis of PCADK copolymers

Briefly, polyketal copolymer PK8 was synthesized in a 100 mL two-necked flask, connected to a short-path distilling head. The diols, 1,4-cyclohexanedimethanol (CDM) (5 g, 34.86 mmol) and 1,5-pentanediol (0.908 mL, 8.72 mmol) were dissolved in 15 mL of distilled benzene and kept at various temperatures (90, 95, 100 and 110 °C). Recrystallized *p*-toluenesulfonic acid (PTSA) was dissolved in ethyl acetate (1 mg/mL) prior to the reaction, and various amounts of the PTSA ethyl acetate solution were added to the reactions to study the effect of PTSA on the molecular weight of PK8. The added ethyl acetate was distilled off, and distilled 2,2-diethoxypropane (equal molar ratio to the two diols combined) was added to initiate the reaction. The reactions were kept at various temperatures (90, 95, 100 and 100 °C) to optimize the molecular weight of PK8. Additional doses of ketals (1 mL) and benzene (4 mL) were subsequently added to the

reaction 2 hours later, via a pressure equalizing funnel, to compensate for the 2,2-dimethoxypropane and benzene that had been distilled off. Another two doses of 5 mL benzene were added to the reaction at hours 6 and 24 to decrease the viscosity of the reaction mixture. After 48 hours, the reaction was quenched by adding triethylamine (120 μ L). PK 9 and PK10 were synthesized using the optimized reaction conditions from PK8 except using higher ratios of 1,5-pentanediol in the starting materials. The starting 1,5-pentanediol/CDM ratio was 30/70 for PK9 and was 40/60 for PK10. The resulting copolymers were analyzed by $^1\text{H-NMR}$ and GPC.

Synthesis of PCADKe

PCADKe was synthesized by using the DEP/DMP method as described above except that an extra toluene or benzene was added to the reaction to decrease the viscosity of the reaction solution. Briefly, the diol, 1,4-cyclohexanedimethanol, were dissolved in distilled benzene and kept at 95 $^{\circ}\text{C}$. Known amounts of re-crystallized *p*-toluenesulfonic acid (PTSA) or pyridinium *p*-toluenesulfonate (PPTSA) (Acros organic, New Jersey, USA), dissolved in ethyl acetate, were added to the reaction. Distilled 2,2-diethoxypropane (equal molar to the CDM) was then added to initiate the reaction. Additional doses of 2,2-dimethoxypropane (1 mL) and benzene (4 mL) were subsequently added to the reaction 2 hours later, via a metering funnel, to compensate for 2,2-dimethoxypropane and benzene that had been distilled off. The viscosity of the reaction increases with increasing molecular weight and decrease the mixing efficiency, which lower the reaction yield. Two methods were used to decrease the viscosity of the reaction: 1. An extra volume of toluene was added 6 hours later after the start of the

reaction. 2. Small amount of benzene were constantly added by pressure equalizing funnel (1 mL/h). After 48 hours, the reactions were stopped by adding triethylamine (120 μ L). Different reaction times were used to optimize the molecular weight of PCADKe. PCADKe was isolated by precipitation into cold hexanes and analyzed by ^1H -NMR and GPC. ^1H NMR data of PCADK (400 MHz, CDCl_3 , δ): 3.26 – 3.18 (m, 4H, $\text{C}_4\text{H}_8\text{CH}_2\text{O}$), 1.83 – 0.93 (m, 8H, CH_2 from cyclohexane, axial and equatorial), 1.32 (s, 6H, $\text{CH}_2\text{OC}(\text{CH}_3)_2\text{OCH}_2$).

Nuclear magnetic resonance (NMR)

The compositions of the polyketal copolymers were analyzed by ^1H NMR. ^1H NMR spectra were obtained from a Varian Mercury VX 400 MHz NMR spectrometer (Palo Alto, CA) using CDCl_3 as the solvent. ^1H NMR data of PK8 (400 MHz, CDCl_3 , δ): 3.4 – 3.18 (m, 4H, CH_2), 1.66 (s, 2H, CH), 1.85 – 0.93 (m, 8H, CH_2), and 1.32 (s, 6H, CH_3). ^1H NMR data of PK 9 (400 MHz, CDCl_3 , δ): 3.4 – 3.18 (m, 4H, CH_2), 1.66 (s, 2H, CH), 1.85 – 0.93 (m, 8H, CH_2), and 1.32 (s, 6H, CH_3). ^1H NMR data of PK10 (400 MHz, CDCl_3 , δ): 3.4 – 3.18 (m, 4H, CH_2), 1.66 (s, 2H, CH), 1.85 – 0.93 (m, 8H, CH_2), and 1.32 (s, 6H, CH_3).

Gel permeation chromatography (GPC)

The molecular weights of the polyketal copolymers were determined by gel permeation chromatography (GPC) using a Shimadzu system (Kyoto, Japan) equipped with a UV detector. Tetrahydrofuran (THF) was used as the mobile phase at a flow rate of 1 mL/min. Polystyrene standards (Peak Mw = 1,060, 2,970, 10,680 and 19,760) from

Polymer Laboratories (Amherst, MA) were used to establish a molecular weight calibration curve.

Characterization and performance of high molecular weight polyketals

Hydrolysis of PK3, PK8 and PK10 at pH5 and pH7.4

The hydrolysis of polyketal polymers was measured according to the procedures of Lee *et al* (Lee, Yang *et al.* 2007). The hydrolysis of PK3, PK8 and PK10 was measured by ^1H NMR in buffered water at the pH values of 5.0 (100 mM AcOH) and 7.4 (100 mM NaH_2PO_4) at 37°C . For each time point and pH, three samples were analyzed. For each sample, 15 mg of polymer (ground powder) were suspended in 1 mL of aqueous solution, at the appropriate pH, and shaken at 120 rpm and 37°C , using a Labline incubated shaker (Barnstead International, Dubuque, Iowa). At specific time points, the polymer samples were extracted with 1 mL of CDCl_3 , and analyzed by ^1H NMR, to determine the percent of ketal linkages that were hydrolyzed.

Preparation and characterization of AOPHA-ME PCADK microparticle

The anti-inflammatory prodrug 5-(Acetylamino)-4-oxo-6-phenyl-2-hexenoic Acid Methyl Ester (AOPHA-Me) was encapsulated into microparticles using a single oil-in-water emulsion, solvent evaporation method. Briefly, 50 mg of AOPHA-Me and 450 mg of PCADKe were dissolved in 2 mL of dichloromethane. This solution was combined with 16 mL of 5 % poly(vinyl alcohol) (PVA) phosphate buffer solution (pH 7.4) and the mixture was homogenized at 21,500 rpm for 2 minutes. The resulting oil-in-water emulsion was added to 20 mL of 1 % PVA phosphate buffer solution (pH 7.4) and stirred

for 4 hours, evaporating the dichloromethane and forming particles. The resulting particles were washed twice in deionized water (with centrifugation at 10,000 rpm) to remove the PVA, and lyophilized, yielding 400 mg of particles. SEM images of the AOPHA-Me-encapsulated PCADKe microparticles (AOPHA-Me-PKMs) and blank PCADKe microparticles showed their size is between 1-2 μm .

The encapsulation efficiency and loading of AOPHA-Me PKMs was analyzed by reverse phase HPLC. Briefly, 3-6 mg of AOPHA-Me PKMs were dissolved in 1 mL of 40 % acetonitrile, 0.1 % TFA solution. The resulting solution was then injected into a Shimadzu HPLC with a Prevail C18 Column using a 40 % acetonitrile, 0.1% TFA mobile phase at 1.0 mL/min with a PDA detector set from 190-300 nm. A standard curve of AOPHA-Me was generated from 0.053 mg/mL to 0.00053 mg/mL to fit a least square linear regression. Blank PKMs were also analyzed as control.

Formulation of PCADKe nanoparticles

Briefly, 40 mg of PCADK ($M_w=2,849$ Da) or PCADKe ($M_w=12,364$ Da) were dissolved in 1mL dichloromethane containing DOTAP (75 nmole). The solutions were combined with 8 mL of 1 % poly(vinyl alcohol)(PVA) phosphate buffer solution (pH 7.4) and the mixture was sonicated for 2 minute at 20 W (Branson Sonifier 250) to form a fine oil/water emulsion. The resulting oil-in-water emulsion were added to 10 mL of 0.4 % PVA Phosphate buffer solution (pH 7.4) and were stirred for 4 hours, evaporating the dichloromethane to form particles. The resulting particles were washed three times in deionized water (with centrifugation at 15,000 rpm, 20 minutes) to remove PVA, and lyophilized.

Scanning Electron Microscopy (SEM)

SEM images were taken to analyze the morphology of the polyketal microparticles. Briefly, SEM samples were prepared by attaching lyophilized particles onto 12.7 mm diameter aluminum sample mounting stubs (Electron Microscopy Sciences, Hatfield, PA), using conductive double sided carbon discs (SPI Supplies, West Chester, PA). The samples were coated with a gold sputter coater (International Scientific Instruments, Prahran, Australia) for 1 minute under an argon atmosphere. The SEM samples were subsequently analyzed using either a HITACHI S-800 or LEO-1530 scanning electron microscope (Tokyo, Japan).

Dynamic Light Scattering

Particle sizes and distributions were determined by dynamic light scattering (DLS) using a 90plus particle size analyzer (Brookhaven, Holtsville, NY)

Thermal analysis of polyketal polymers

Thermal analyses of the polyketal polymers was carried out on a differential scanning calorimeter (DSC, Thermal Analysis Instruments, Q100) at a temperature ramp from 0 to 300 °C at 10 °C/min with a nitrogen purge rate of 10 mL/min. Glass transition temperature (T_g) was taken as the inflexion of the DSC curve and melting temperature (T_m) was taken as the peak temperature of the endothermic peak using TA Instruments Universal Analysis Software version 3.9A.

In vitro uptake of fl-siRNA encapsulated nanoparticles by HUVEC cells

Ion-pairing of fl-siRNA

Fl-TNF- α siRNA (75 nmole) dissolved in 0.5 mL of RNase-free water was added to an equal volume (0.5 mL) of methylene chloride containing an equal molar cation of DOTAP (3.15 μ mole). Methanol (1.05 mL) was then added to two phase solution to make a single phase solution. The monophasic solution was gently mixed and allowed to stand for 15 min. The mixture was separated by adding 0.5 mL of each of the aqueous phase (RNase free water) and organic phase (methylene chloride). The resulting solutions were gently mixed for 1 min and centrifuged at 600 x g for 5 min. The organic bottom phase (1 mL) was rapidly pipetted out and used for further experiments.

Formulation of fl-siRNA PCADKe nanoparticles

Briefly, 40 mg of PCADKe (Mw=12,234) was dissolved in 1 mL of dichloromethane containing DOTAP fl-siRNA (75 nmole). The solutions were combined with 8 mL of 1% poly (vinyl alcohol) (PVA) phosphate buffer solution (pH 7.4) and the mixture was sonicated for 1 minute at 20 W (Branson Sonifier 250) to form a fine oil/water emulsion. The resulting oil-in-water emulsion was added to 10 mL of a 0.4 % PVA phosphate buffer solution (pH 7.4) and was stirred for 4 hours, evaporating the dichloromethane to form particles. The resulting particles were washed three times in deionized water (with centrifugation at 15,000 rpm, 20 minutes) to remove PVA and salts, and lyophilized.

In vitro uptake of fl-siRNA PKNs by HUVEC cells

Human umbilical vein endothelial cells (HUVECs; Genlantis), (a gift from Dr. Gang Bao), were cultured in endothelial cell growth medium (Genlantis) supplemented with 20 % fetal bovine serum, 13.3 U/ml heparin, 40 µg/ml endothelial mitogen (Biomedical Technologies), 1 % L-glutamine, and penicillin-streptomycin. For flow cytometry, HUVECs (1×10^6 cells/well, 12 well plate) were incubated with fl-siRNA nanoparticles for 4 h. The cells were washed 3 times and then incubated with fresh medium for 24 h. Cells were washed 3 times with ice cold PBS and scraped into tubes for the flow cytometry. Fluorescent cell population was measured by a flow cytometer (BD LSR flow cytometer, BD Bioscience) (San Jose, CA) using a laser for fluorescein ($\lambda_{\text{ex}}/\lambda_{\text{em}} = 494/510$ nm).

In vitro release of hydrophobic dyes from PCADKe microparticles

Preparation of dye encapsulated PCADKe microparticles

The size of the microspheres is another important factor that affects the release rate of hydrophobic drugs (Budhian, Siegel et al. 2008). The speed of homogenization during an oil/water single-emulsion process can affect the size of microparticles (Zhao, Gagnon et al. 2007). Thus, we used various homogenization speeds to prepare dye encapsulated PCADK microparticles (dye-PKMs) to determine the relation between particle size and speed of homogenization. Three different hydrophobic dyes (Nile Red, DiI and coumarin-6) were chosen as model compounds for the calpain inhibitors because they have similar hydrophobic profiles as the calpain inhibitors and should have similar encapsulation efficiencies. Each dye was encapsulated by an oil/water single-emulsion

Briefly, 0.5 mg of dye (Nile Red, DiI or coumarin-6) and 50 mg PCADK were dissolved in 500 μ L of a single-phase solvent (1:3 N,N-dimethylformamide: dichloromethane). This solution was combined with 5 mL of 5 % poly(vinyl alcohol)(PVA) Tris buffer solution (pH 9.0) and the mixture was homogenized at three different speeds (24,000, 17,500 and 9,800 rpm) for 1 minute to generate different particle sizes of dye-PKMs. The resulting oil-in-water emulsion was then added to 20 mL of 1 % PVA Tris buffer solution (pH 9.0) and stirred for 4 hours, evaporating the dichloromethane to form particles. The resulting particles were washed three times in deionized water (with centrifugation at 10,000 rpm) to remove dimethylformamide and PVA, and lyophilized. The sizes and morphologies of dye-PKMs (Nile Red-PKMs, DiI-PKMs and coumarin-PKMs) were visualized on a Hitachi S-800 SEM.

In vitro release of hydrophobic dyes from PCADK microparticles

The release kinetics of the PKMs was optimized by using a fluorescent dye, 1,1'-Dioctadecyl-3,3,3',3'-tetramethylindocarbocyanine perchlorate (DiI), as a model compound for AK295. DiI was chosen as a model compound because it has a similar hydrophobicity profile as AK295 and should therefore have similar release kinetics. The release of DiI was measured by fluorescence spectrometry. PKMs with various sizes ($1.96 \pm 0.64 \mu\text{m}$, $2.90 \pm 1.17 \mu\text{m}$ and $5.49 \pm 3.21 \mu\text{m}$) were prepared and their release rates were characterized and optimized.

Briefly, a 10 mg sample of DiI PKMs (containing 75 μg of DiI dye) were added to a 2 mL microcentrifuge tube and suspended with 1200 μL of PBS (pH 7.4). The microcentrifuge tubes were shaken at 120 rpm, 37°C. At different time intervals (1, 3, 6,

12, 24 hours, 3, 7, 14, 28, and 60 days), the particle suspension were centrifuged at 10,000 rpm for 15 min. An 1100 μL volume of the supernatant was pipetted out and transferred to another micricentrifuge tube. This supernatant was then recentrifuged at 10,000 rpm for 15 min to minimize the particles present in the solution. A 1000 μL volume of the supernatant was pipetted out and the same volume of fresh buffer was added to the tube. The resulting supernatants were then mixed with equal volume of 0.2 % SDS solution to maximize fluorescent signal. The concentrations of DiI released into the supernatant were measured by Fluorescence spectrometry ($\lambda_{\text{ex}}= 550 \text{ nm}$, $\lambda_{\text{em}}= 565 \text{ nm}$). At the last time point (60 days) the remaining particles were hydrolyzed and the amount of unreleased DiI dye the particles were measured and used to calculate the percentage of DiI released at each time point.

2.3 Results

Synthesis of polyketals using DEP/DMP method

Optimization of PK8 copolymer

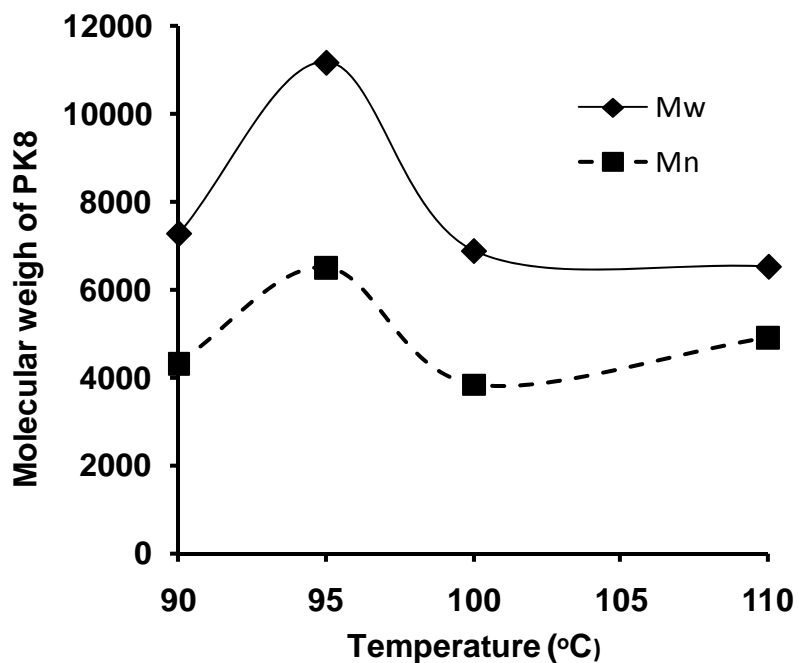
PK8 was synthesized on a multi-gram scale with a yield of 36 %. By different ketal ratios, various molecular weights of PK8 were synthesized, the result was shown in Table 2.1. The reaction was conducted at the various reaction temperatures (90, 95, 100, and 105 °C), to optimize reaction temperature, and the results was shown in Figure 2.2. An ¹H-NMR spectrum and GPC spectrum are shown in Figure 2.3, confirming its chemical structure and molecular weight.

The highest molecular weight of PK8 ($M_w/M_n = 11,171/6,500$) was obtained at the following condition: Initiated the reaction with diols (80 % CDM/ 20 % 1, 5-pentanediol) and equal molar of distilled DEP and three dosage of DMP (1mL) at present of PTSA (1.5 mg) at 95 °C for 48 hours. This optimized condition was used to synthesize the other polyketals.

Table 2.1 Optimization of PK8.

Initial amount of DEP (mL)	Additional ketals	PTSA (mg)	1 st precipitation (Mw/Mn)	2 nd precipitation (Mw/Mn)
7	0	3.5	2,907/1,243	NA
	0	2.0	3,827/1,506	NA
	0	1.5	5,239/2,708	6,037/3,227
	1 mL of DEP	1.5	4,865/2,577	NA
	3 mL of DEP	1.5	3,606/1,208	NA
	1 mL of DMP	1.5	8,035/4,349	9,081/4,619
	2 mL of DMP	1.5	8,408/4,349	9,803/5,540
	3 mL of DMP	1.5	8,241/4,961	11,171/6,500
	5 mL of DMP	1.5	6,977/3,204	82,54/4,805

All polymerizations were conducted at 95 °C for 48 hours and the molecular weight of PK8 were measured by GPC.

**Figure 2.2** Optimization of reaction temperature for PK8.

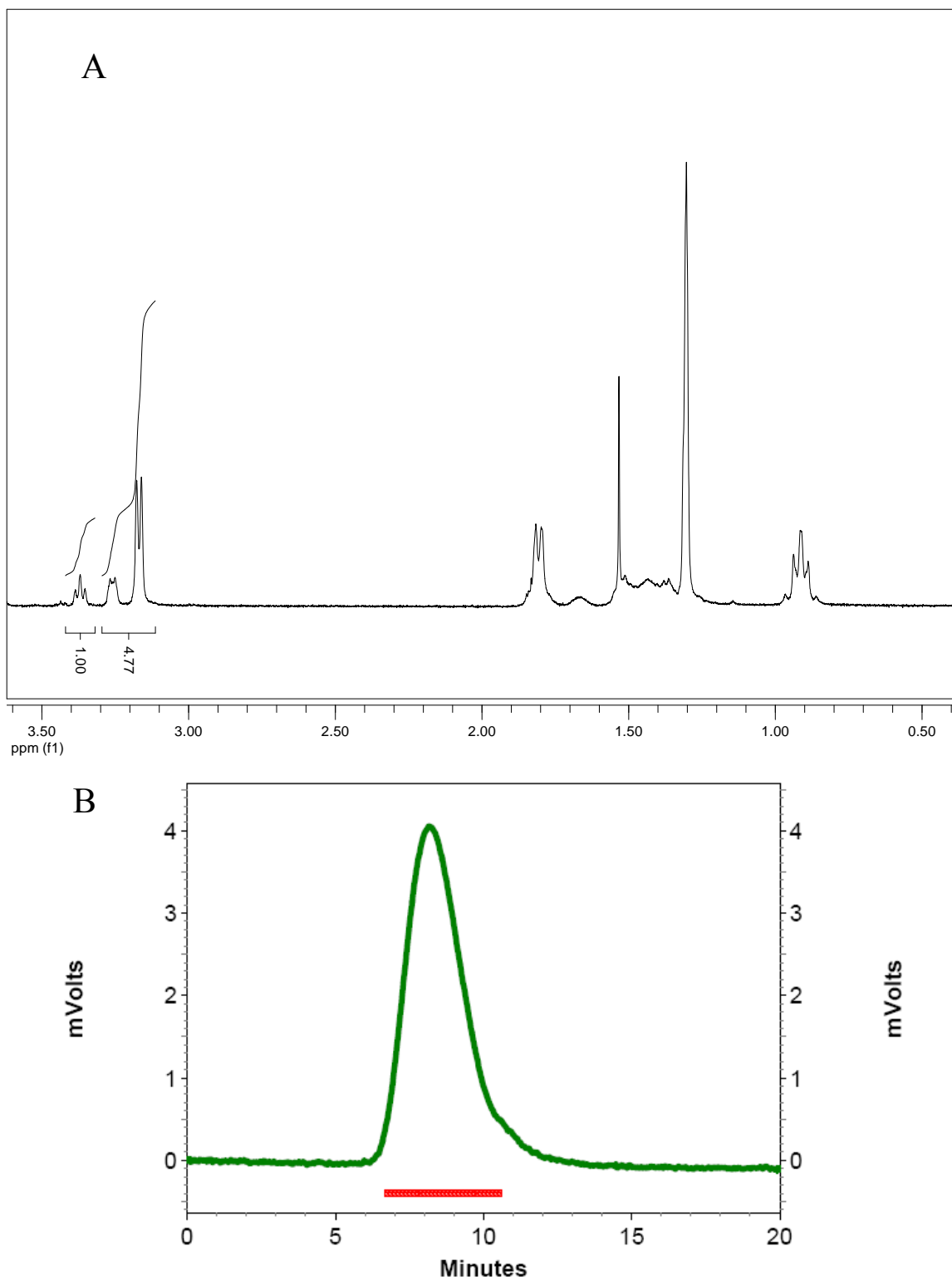


Figure 2.3 (A) $^1\text{H-NMR}$ and (B) GPC spectra of PK8.

By using this DEP/DMP mixture technique, we improved the molecular weights of polyketals and have also developed new polyketal copolymers which can incorporate higher 1,5-pentanediol ratios within the copolymers. The compositions and molecular weights of the polyketal copolymers synthesized from DEP/DMP mixtures are summarized in Table 2-2. The PK10 had the highest 1,5-pentanediol incorporated (30 %) however, the molecular weight was lower than the other copolymers. Similarly, PK9, incorporated 18.7 mole % of 1,5-pentanediol, had a medium molecular weight ($M_w/M_n=7,494/4,511$), which is higher than PK10 but lower than PK8. The $^1\text{H-NMR}$ spectrum and GPC spectrum of PK9 and PK10 are shown in Figure 2.4 and Figure 2.5 respectively, confirming their chemical structure and molecular weight.

Table 2.2 Compositions and molecular weights of polyketal copolymers and PCADK synthesized from DEP/DMP mixtures

Polymer ID	CDM/1,5-Pentanediol Ratio		M_w/M_n	Yield
	Start	Final		
PK8	80/20	82.99/17.01	12,136/6,338	30 %
PK9	70/30	81.30/18.70	7,494/4,511	20 %
PK10	60/40	69.45/30.55	6,408/2,974	10 %
PCADKi	100/0	100/0	6,720/3,369	55 %

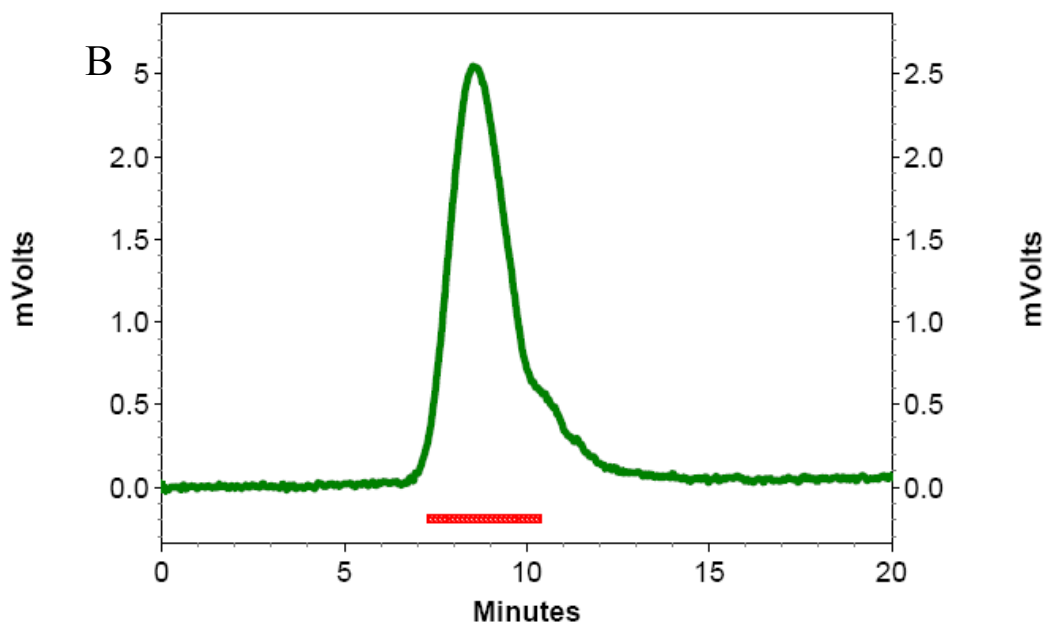
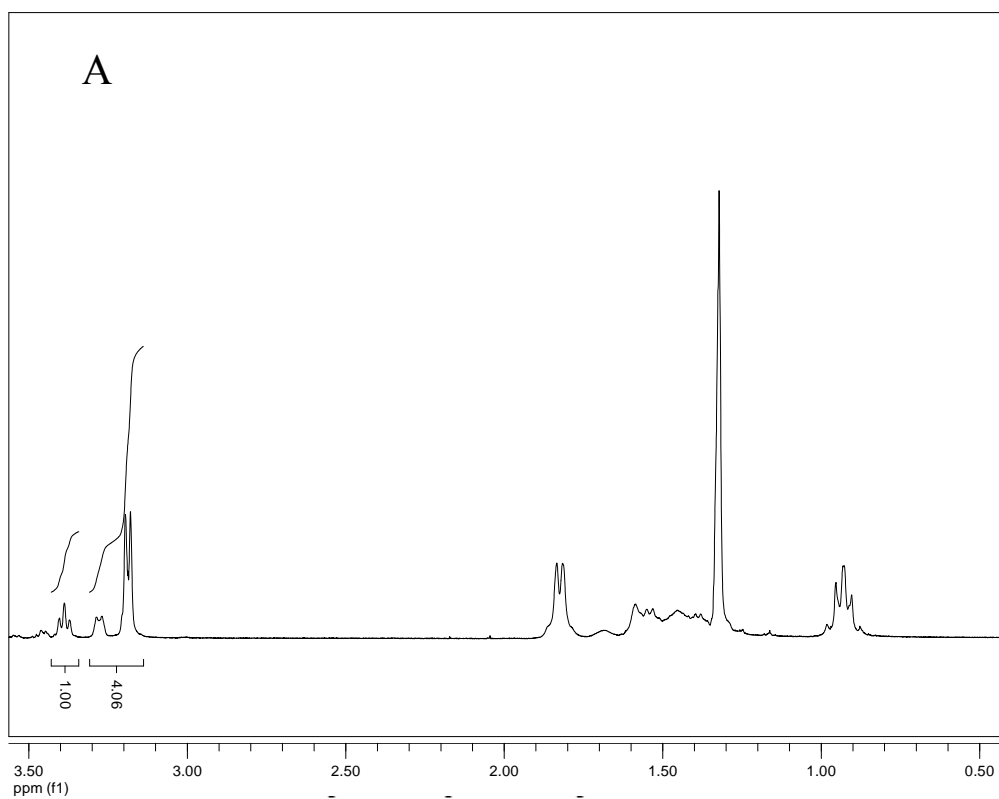


Figure 2.4 (A) ^1H -NMR and (B) GPC spectra of PK9

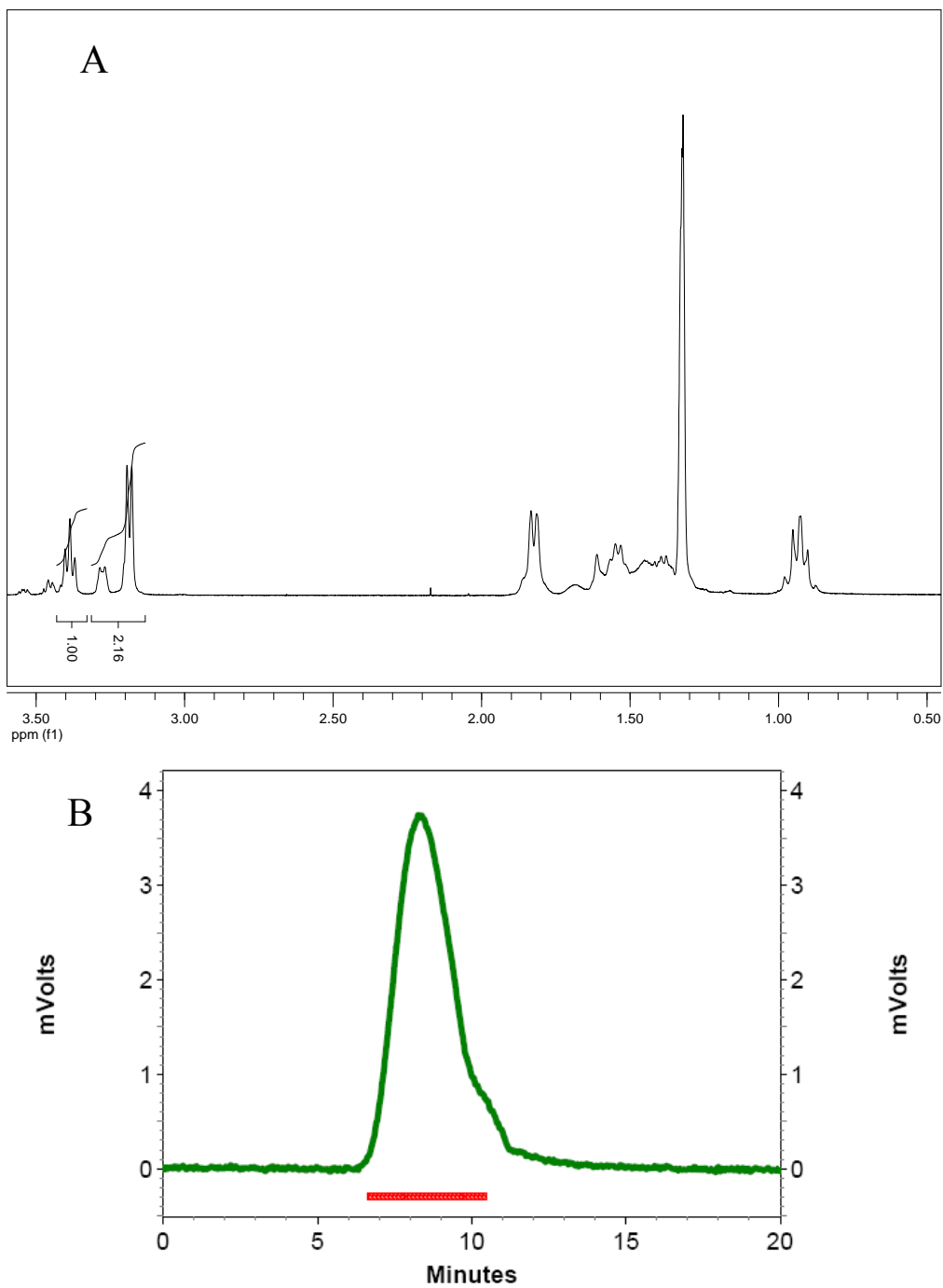


Figure 2.5 (A) $^1\text{H-NMR}$ and (B) GPC spectra of PK10

We also used the same technique and condition to synthesize PCADKe, however, the reaction became very viscous after we added the additional DMP, consequently

forming a solid bulk PCADK and halted the polymerization. The resulting PCADKi (insoluble PCADK) polymer had very low solubility in both THF and DCM at room temperature. To avoid damage of the GPC column, we centrifuged and filtered the PCADKi-THF solution to remove the insoluble part of PCADKi, and only measured the soluble part of PCADKi. The results showed that the PCADKi's molecular weight was only slightly higher than the original PCADK synthetic method.

Optimization of PCADKe

PCADKe was synthesized at a multi-gram scale with yield of 53 % by using a modified DEP/DMP method. To decrease the viscosity of the reaction and enhance the mixing efficiency, we either added an extra volume of toluene or continuously added small amount of benzene to the reaction. The optimized results were shown in Table 2.3

Table 2.3 Optimization of PCADKe

PCADKe sample	Starting Solvent	Additional Solvent	Catalyst	Mw/Mn
1*	20 mL of Benzene	0	PTSA	4764/3103*
2		3 mL of toluene	PTSA	6833/3583
3		1 mL of benzene per hour, for 48 hour	PTSA	10191/4968
4			PPTSA	7205/3841

All polymerizations were conducted at 95 °C for 48 hours and the molecular weight of PCADKe were measured by GPC.

* the reaction was stopped at 24 hours due to formation of insoluble PCADKi.

The results showed that only continuously added small amount of benzene can generate high molecular weight PCADKe. Although the toluene is not evaporated under these conditions, an extra volume of toluene also diluted the concentration of the reactants and therefore the molecular weight of PCADKe only increases slightly. Thus, the modified DEP/DMP methods described below were conducted by continuously adding small amount of benzene.

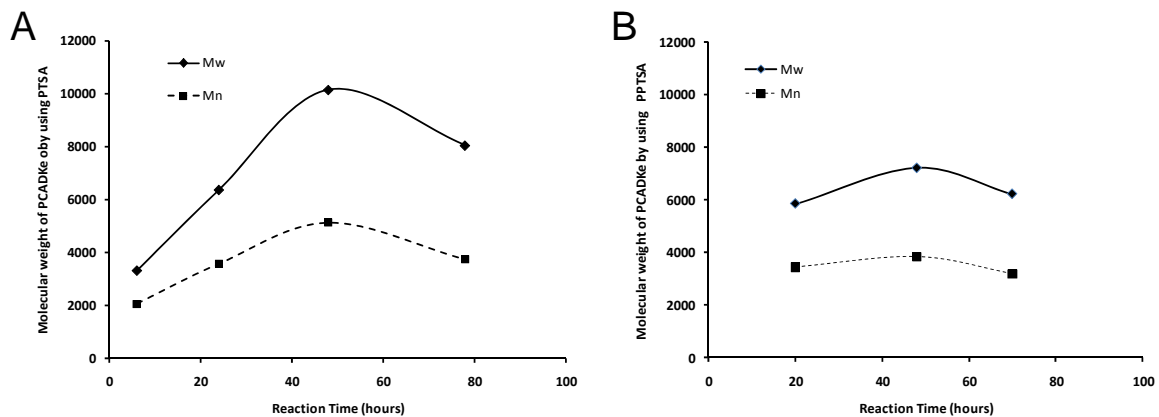


Figure 2.6 Optimization of reaction temperature for PCADKe using (A) PTSA, (B) PPTSA as catalyst

To optimize the reaction temperature, the reactions were conducted at the various reaction time (6, 24, 48, and 72 hour), and the results were shown in Figure 2.6 (A). We also tried to use different catalyst pyridinium *p*-toluenesulfonate (PPTSA) to avoid the degradation due to acid hydrolysis. However, PPTSA is also less efficient than PTSA, thus the molecular weight of PCADKe generated by PPTSA is lower than PCADKe generated by PTSA (Figure 2.6 (B)).

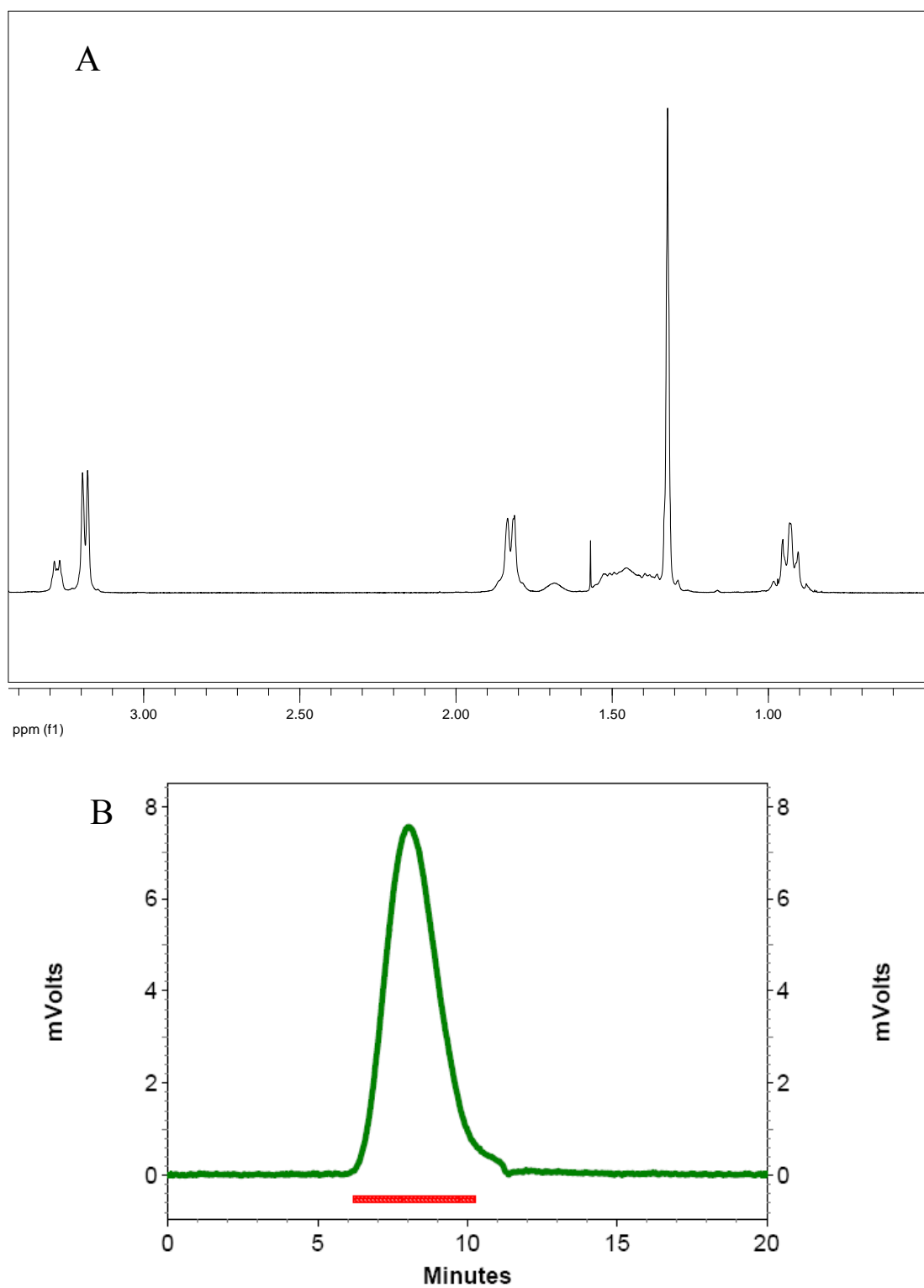


Figure 2.7 (A) $^1\text{H-NMR}$ and (B) GPC spectra of PCADKe

The $^1\text{H-NMR}$ spectrum and GPC spectrum of PCADKe is shown in Figure 2.7, confirming its chemical structure and molecular weight.

Characterization and performance of high molecular weight polyketals

Hydrolysis of PK3, PK8 and PK10 at pH5 and pH7.4

The hydrolysis of PK3, PK8 and PK10 were measured by ^1H NMR in buffered water at the pH values of 5.0 and 7.4 at 37°C to determine their behavior in the acidic environment of phagolysosomes and in the blood. Figure 2.6 demonstrates that all polyketal copolymers undergo acid hydrolysis. The hydrolysis half-lives of PK 3, PK8 and PK10 at pH 5.0 are 6 days, 3 days and 2 days respectively.

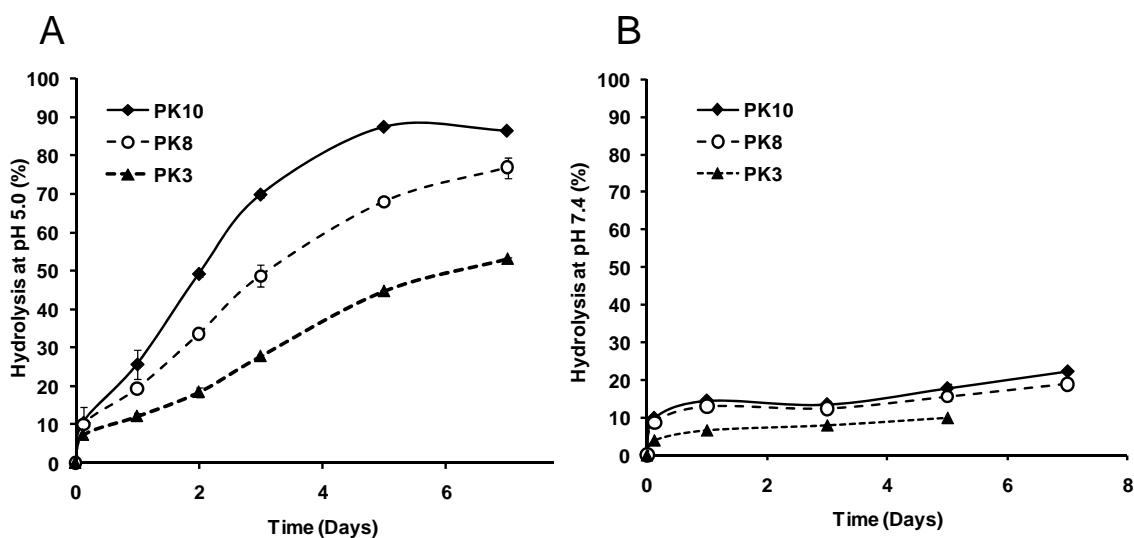


Figure 2.8 Hydrolysis of PK3, PK8 and PK10 at (A) pH 5.0 and (B) pH 7.4 environment
Enhanced loading of anti-inflammatory drug AOPHA-Me with high molecular weight PCADKe

Although the high molecular weight polyketals are originally developed for preparation of calpain inhibitor-loaded microparticles, we also explore their potential application in delivery the other therapeutic agents. An anti-inflammatory drug AOPHA-Me was encapsulated into two different molecular weights of PCADK microparticles, and compared their encapsulation efficiency. The encapsulation efficiency of AOPHA-

Me into PKMs was calculated to be 3 ± 1 % (n=4) and the loading of AOPHA-Me into PKMs was 3 ± 1 μg AOPHA-Me per 1 mg of particles. By using lower Mw PCADK, the loading of AOPHA-Me into PKMs was 0.7 ± 0.6 μg AOPHA-Me per 1 mg of particles (n=7). The morphology of AOPHA-Me PKMs prepared from two different molecular weight PCADKe were shown in Figure 2.9

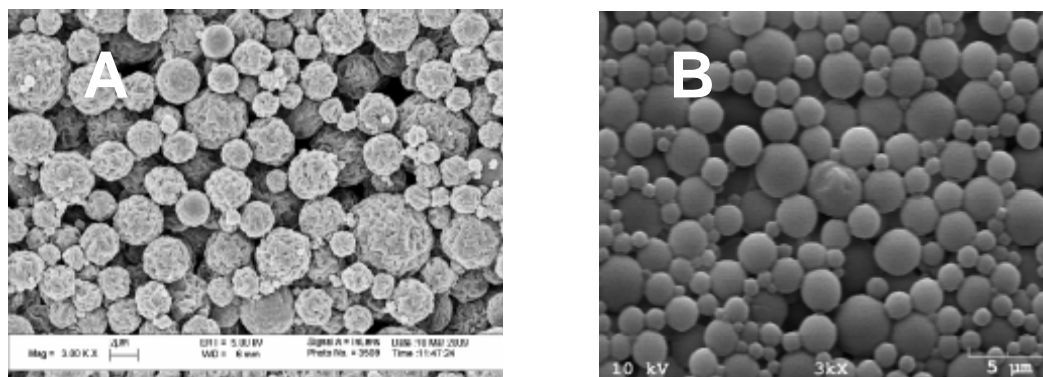


Figure 2.9 SEM images of AOPHA-Me PKMs prepared from (A) high molecular weight PCADK (Mw=9,623), (B) medium molecular weight PCADK (Mw=6,317).

Nanoparticles formulated from high molecular weight PCADKe are stable

Formulation of PCADKe nanoparticles

We demonstrated that both high and low Mw PCADK can form nanoparticles after sonication, however only nanoparticles made from high Mw PCADK remain intact during centrifugation step (Figure 2.10 (A)) while the nanoparticles made from low molecular weight collapsed in the same condition (Figure 2.10 (B)). The size of the high molecular weight PKMs is 377.9 ± 19.5 nm (by DLS) and the size of the low molecular weight PKMs is not available due to deformation. We also tried to prepare nanoparticles with PK8, which have similar molecular weight as high Mw PCADK, however, the PK8 nanoparticles also collapsed during centrifugation as low Mw PCADK nanoparticles (data not shown).

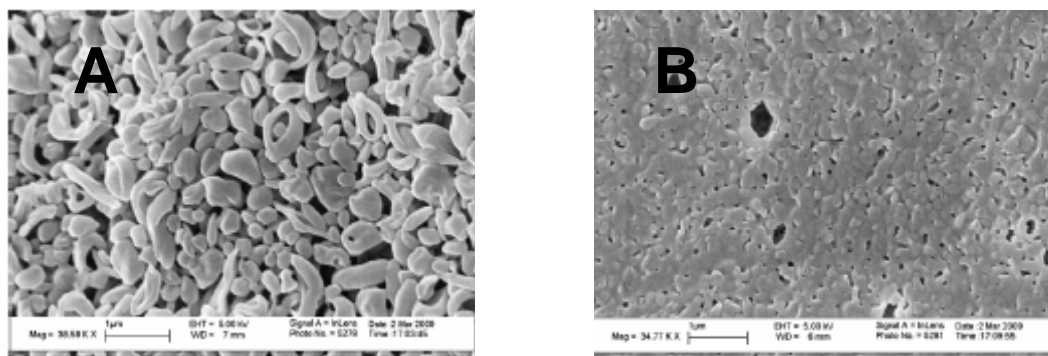


Figure 2.10 SEM images of PCADKe nanoparticles prepared from (A) High molecular weight PCADKe ($M_w/M_n = 12,234/6,623$) and (B) low molecular weight PCADK ($M_w/M_n = 2,849/1,981$)

Thermal analysis of polyketal polymers

Thermal analyses of the polyketal polymers were carried out on a differential scanning calorimeter (DSC) and results were shown in Figure 2.11 and Table 2.4. In general, the high molecular weight PCADKe has higher melting temperature (T_m) and glass transition temperature (T_g) than the low molecular weight PCADK and, the PCADK has higher T_m than PCADK copolymers.

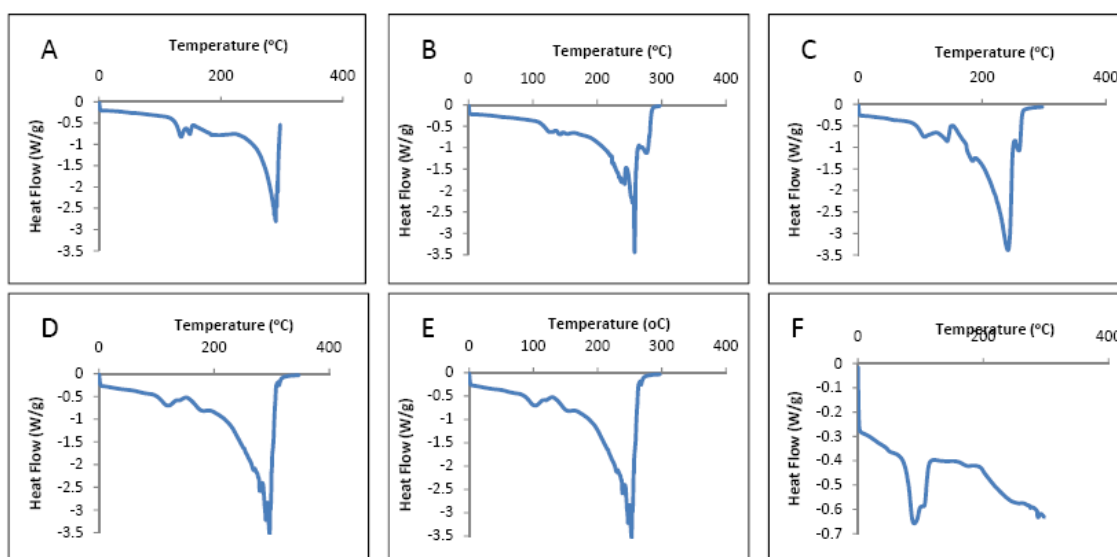
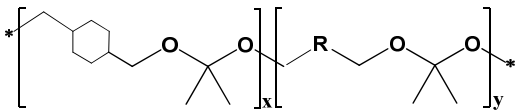


Figure 2.11 DSC of polyketals. (A) High molecular weight PCADK, (B) Medium molecular weight PCADK, (C) Low molecular weight PCADK, (D) PK3, (E) PK8, (F) PK10.

Table 2.4 The DSC results of polyketal polymers.

Repeating Unit Formula					
Sample ID	CDM (x %)	1,5-Pentanediol (y %)	Mw/Mn	Tm (°C)	Tg (°C)
High Mw PCADKe	100	0	12,234/6,623	288	133
Medium Mw PCADK	100	0	5,407/3,265	257	115
Low Mw PCADK	100	0	2,849/1,981	241	106
PK3	87	13	4,503/2,593	248	105
PK8	83	17	11,548/5,651	252	101
PK10	70	30	6,448/3,609	98	48

Enhance the *in vitro* uptake of fl-siRNA PKNs in HUVEC cells

Fluorescein-labeled siRNA (fl-siRNA) was encapsulated within the PCADKe nanoparticles with an encapsulation efficiency of 35.6 %. The SEM images showed that the morphology of the fl-siRNA PCADKe nanoparticles (fl-siRNA PKNs) and the size is $168.8 \pm 74.7 \mu\text{m}$ (Figure 2.12 A). The uptake of fl-siRNA nanoparticles was then measured by flow cytometry and compared against HUVECs incubated with fl-siRNA complexed with 1,2-Dioleoyl-3-Trimethylammonium-Propane (DOTAP, a cationic lipid) (DOTAP-fl-siRNA complexes) and free fl-siRNA. Figure 2.12 (B) demonstrates that the fl-siRNA PKNs were 2-3 orders of magnitude more effective at delivering fl-siRNA into HUVECs than DOTAP-fl-siRNA complexes and free-fl-siRNA. Figure 2.12 (C) and (D) showed that mean fluorescent intensity increased in the HUVECs after delivery of fl-siRNA PKNs.

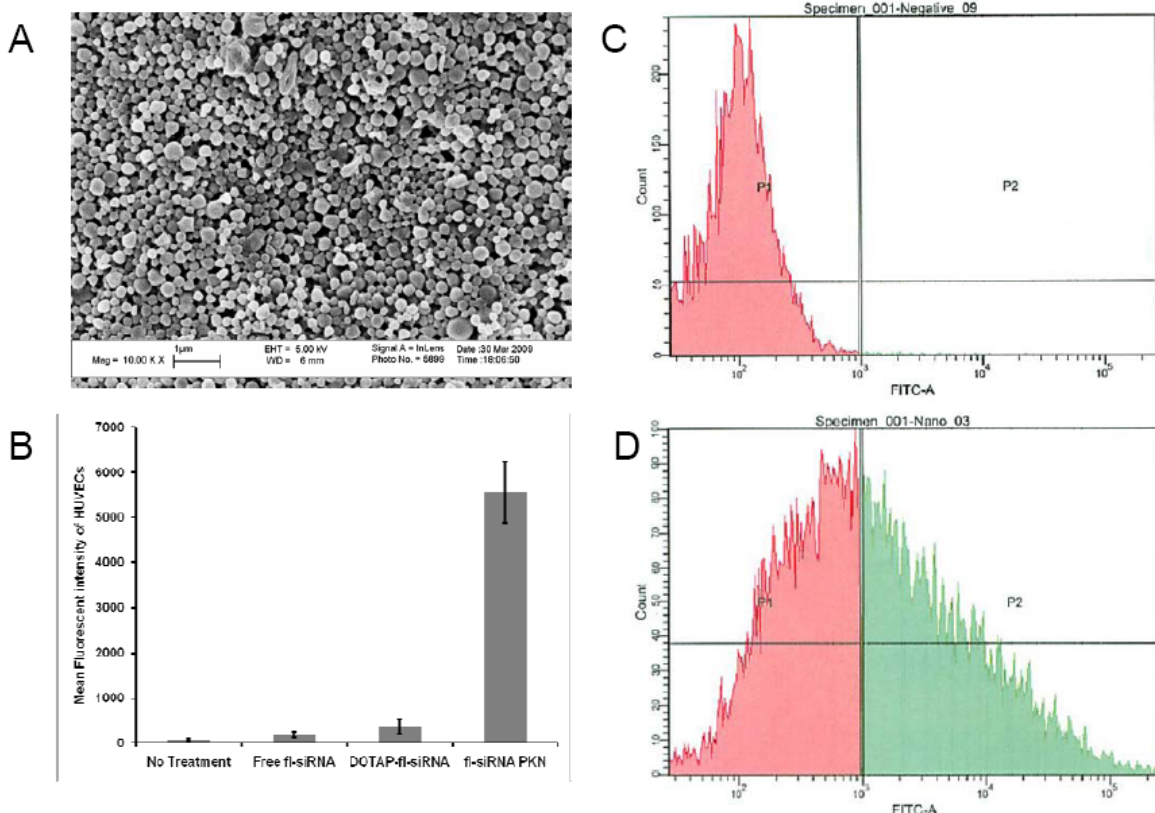


Figure 2.12 Uptake of fl-siRNA PKN in HUVEC cells. (A) A SEM image of fl-siRNA PKNs. (B) Mean fluorescent intensity of HUVECs after treated with free fl-siRNA, DOTAP-fl-siRNA complex and fl-siRNA PKNs. (C) HUVECs, (D) HUVECs after uptaking of fl-siRNA PKNs.

***In vitro* release of hydrophobic dyes from PCADKe microparticles**

Formulation and characterization of dye encapsulated PCADKe microparticles

Various formulations and sizes of PKMs were prepared and their *in vitro* release rates were characterized and optimized. First, we showed that the speed of homogenization during an oil/water single-emulsion process can affect the size of microparticles. The sizes and morphologies of Nile Red polyketal microparticles (NR-PKMs) are shown in Figure 2.13.

However, the fluorescent intensity of the Nile Red in aqueous environment was too low to be detected by using fluorescence spectrometry. Same problem occurred when

we prepare the coumarin-6 polyketal microparticles. Among these hydrophobic dyes, only DiI showed detectable fluorescent intensity. To maximize the fluorescent signal of DiI, we found that 0.1 % sodium dodecyl sulfate (SDS) solution can amplify the DiI fluorescent intensity up to 93 times (Figure 2.14).

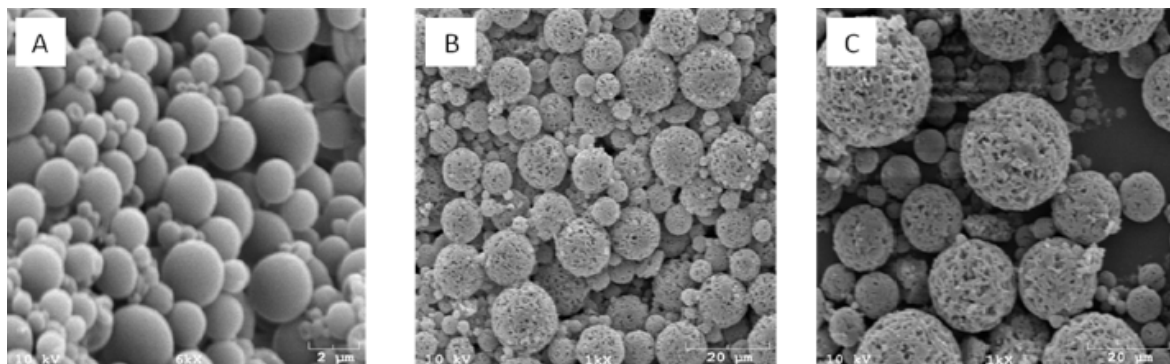


Figure 2.13 SEM images of Nile Red PCADKe microparticles prepared at different homogenization speeds (A) 24,000 rpm, the particle size ranges from 1 to 2 μm (6,000X magnification) , (B)17,500 rpm, the particle size ranges from 1 to 5 μm (1,000X magnification), and (C) 9,500 rpm, the particle size ranges from 2 to 10 μm (1,000X magnification).

DiI-PKMs with various particle size distributions were prepared by changing the speed of homogenization during an oil/water single-emulsion process. The morphology and sizes of the DiI-PKMs were shown in Figure 2.15. The encapsulation efficiency of the DiI in the DiI-PKMs ranges from 67.8 to 83.1 %. The *in vitro* release data of DiI PKMs showed that approximately 16 % of free DiI released in the 35 day period for the small particles ($1.96 \pm 0.64 \mu\text{m}$) and 5 % for the larger particles ($2.90 \pm 1.17 \mu\text{m}$ and $5.49 \pm 3.21 \mu\text{m}$). In general, the smaller particles ($1.96 \pm 0.64 \mu\text{m}$) have faster release rates of the hydrophobic dye than the larger particles (Figure 2.16).

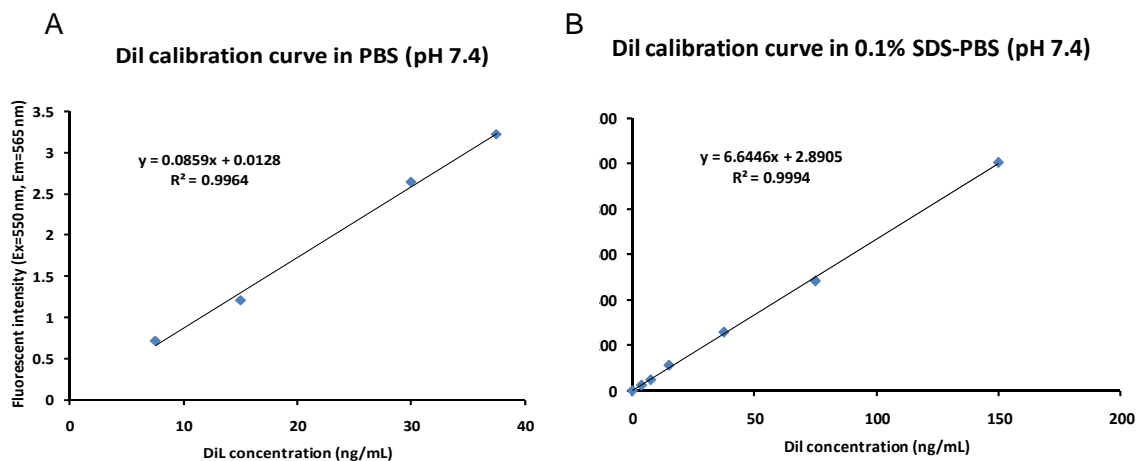


Figure 2.14 Calibration curve of DiI in (A) PBS (pH 7.4), (B) 0.1 % SDS in PBS (pH 7.4). The results showed that 0.1 % SDS increase the fluorescent intensity of DiI up to 92 times ($\lambda_{ex} = 550 \text{ nm}$, $\lambda_{em} = 565 \text{ nm}$).

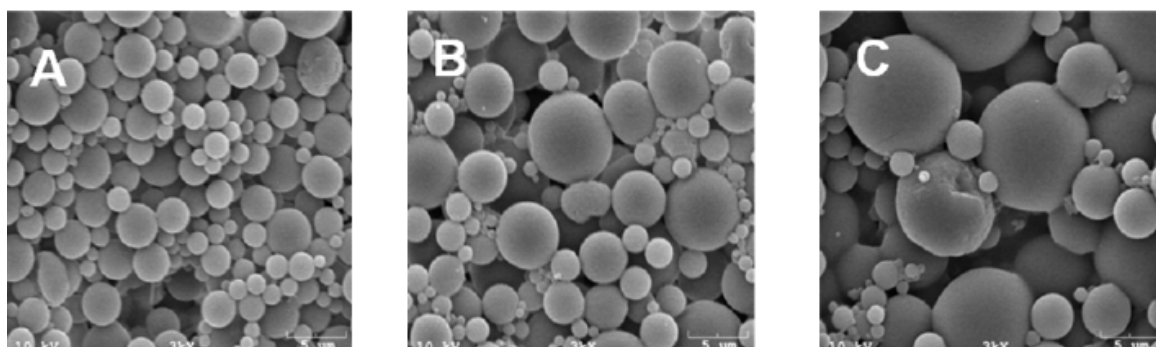


Figure 2.15 SEM images of DiI-encapsulated PCADKe microparticles prepared at different homogenization speeds (A) 21,500 rpm, the particle size is $1.96 \pm 0.64 \mu\text{m}$ (encapsulation efficiency: 67.79 %), (B) 13,500 rpm, the particle size is $2.90 \pm 1.17 \mu\text{m}$ (encapsulation efficiency: 82.87 %), and (C) 9,500 rpm, the particle size is $5.49 \pm 3.21 \mu\text{m}$ (encapsulation efficiency: 82.16 %).

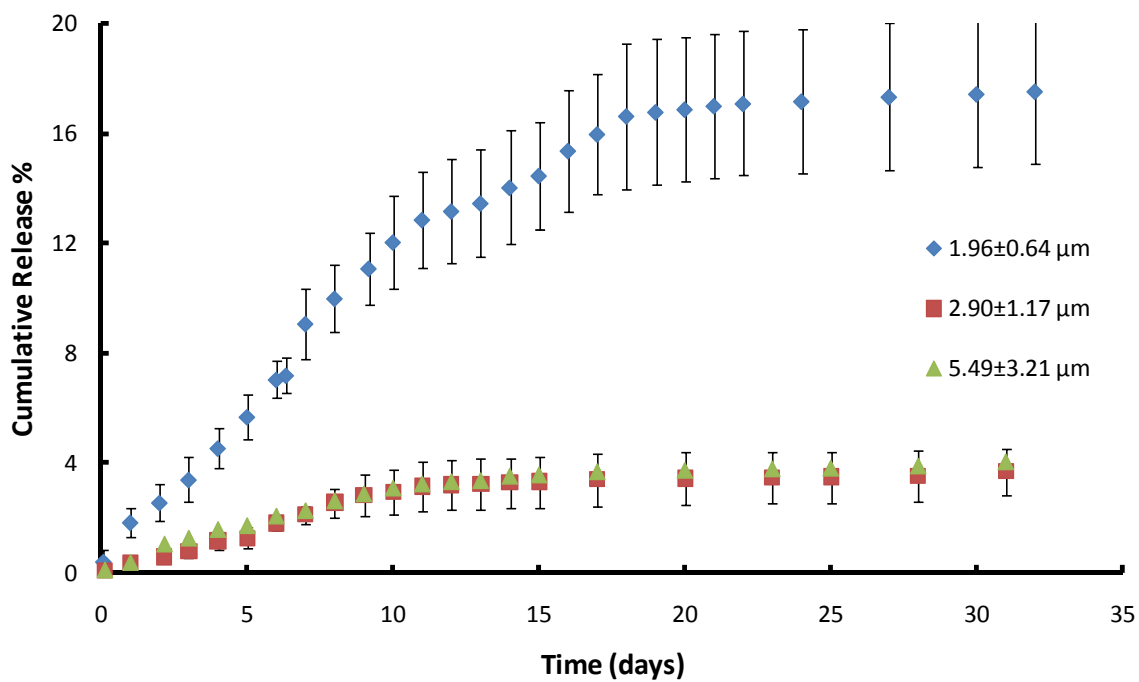


Figure 2.16 Effects of particle size on the *in vitro* release of DiI from polyketal microparticles: $1.96 \pm 0.64 \mu\text{m}$ (◆), $2.90 \pm 1.17 \mu\text{m}$ (■) and $5.49 \pm 3.21 \mu\text{m}$ (▲), $n=5$ for each time point. Polyketal microparticles have drug contents of 0.68 % (◆), 0.83 % (■) and 0.82 % (▲).

2.4 Discussion

New synthetic methodology can increase the molecular weight of polyketal

In this study, we used an alternative ketal, 2,2-diethoxypropane (DEP), which has a boiling point of 117 °C, for this acetal-exchange reaction to alleviate the removal of the reactants. However, in our first few experiments, we could only slightly increase the molecular weight of PK3 by using the DEP method. Thus, we speculate that there was still some DEP being evaporated with benzene and ethanol. To compensate the loss of DEP, we added additional ketals (DEP or DMP) at 2 hours after the reaction starts. The results showed a dramatic increase in molecular weight by adding additional DMP but not DEP.

In this acetal exchange reaction, we used re-crystallized *p*-toluenesulfonic acid (PTSA) to increase the efficiency of the catalyst. We found that the molecular weight increased with minimal amount of the PTSA in the reaction, however, when the PTSA amount is lower than 1.5 mg, it only formed viscous liquid polymer which has low molecular weight. When we increased the amount of PTSA in the reaction, the molecular weight of polyketals became lower. This might be due to the extra amount of PTSA might accelerate the acid hydrolysis of polyketal.

As described before, high temperature is needed to remove the byproducts methanol and ethanol, but it also removed the DMP and small amount of DEP, and resulted in low molecular weight. To find the optimal reaction temperature for polymerization, the reactions were set at various temperatures (90, 95, 100 and 110 °C). No solid polymers were formed below 90 °C. The results suggest that the PK8 has high

molecular weight when the reaction was conducted at 95 °C (Figure 2.2). The reaction carried at higher or lower temperature than the optimization temperature generated low molecular weight due to either imbalance of reactants or incomplete removal of the byproduct.

New synthetic methodology can generate solid polyketals with rapid hydrolysis kinetics

Yang *et al.* showed that the hydrolysis kinetics of PCADK copolymers scaled with the amount of 1,5-pentanediol incorporated in their backbone, suggesting that the hydrolysis of polyketals is governed by their hydrophilicity (Yang, Bhide et al. 2008). Among the PCADK copolymers they synthesized using DMP method, PK3, a copolymer that incorporated 13 % 1,5-pentanediol and 87 % 1,4-cyclohexanedimethanol, had a shortest hydrolysis half-life of 2 days at pH 4.5. By using this DEP/DMP mixture technique, we have developed new polyketal copolymers which can incorporate higher 1,5-pentanediol ratios within the copolymers than PK3, thus the new polyketal copolymers should have fast hydrolysis kinetics than PK3.

To investigate the hydrolysis properties of these new PCADK copolymers, we compared PK8 and PK10 with PK3, a polyketal polymer currently used for treating acute liver failure. The hydrolysis kinetics of PK3, PK8 and PK10 were measured at the pH values of 5.0 and 7.4 to determine their behavior in the acidic environment of phagolysosomes and in the blood. Figure 2.8 demonstrates that all the polyketal copolymers undergo acid-catalyzed hydrolysis, and that their hydrolysis kinetics scale with the amount of 1,5-pentanediol incorporated into the copolymer. For example, PK8, a

copolymer that incorporates 17 mole % 1,5-pentanediol and 83 mole % 1,4-cyclohexanedimethanol, had a hydrolysis half-life of 3 days at pH 5.0. Similarly, PK10, another PCADK-derived copolymer synthesized from DEP/DMP method, incorporating 30 mole % of 1,5-pentanediol, had a hydrolysis half-life of only 2 days at pH 5, which is faster than PK3, which had a hydrolysis half-life of 6 days. And also, we expect microparticles formulated from PK8 and PK10 are suitable for treating acute inflammatory diseases due to their fast hydrolysis properties.

In general, the DEP/DMP technique did not cause any complications in the polymer synthesis, and could generate higher molecular weight polymers than the traditional method. More importantly, all the polyketal copolymers synthesized were solid, and therefore have a great potential for formulation into microparticles.

Modified DEP/DMP method is needed to generate high molecular weight PCADKe

From Table 2.2, we found that the molecular weights and yields of PCADK copolymers were proportional to the amount of 1,4-cyclohexanedimethanol incorporated within the polyketal copolymers. Thus, it is expected that using the same technique, we should generate high molecular PCADKe polymer. However, the same trend was not observed in the synthesis of PCADK. When we used the DEP/DMP method to synthesize PCADK, the reaction became very viscous after we added the additional DMP, consequently forming a solid bulk PCADK and halted the polymerization. The resulting PCADKi (insoluble PCADK) polymer had very low solubility in both THF and DCM at room temperature. The GPC results showed that the PCADKi's molecular weight ($M_w = 6,720$) was only slightly higher than the PCADK ($M_w = 5,345$) synthesized

by DMP method. The insolubility of PCADKi also caused problems for the fabrication of PCADK microparticle. High temperature was needed to dissolve the PCADKi, and it might denature the drugs and subsequently decrease their bioactivity.

We believe the low solubility of PCADKi is due to the increases of viscosity during the polymer synthesis. The relationship between molecular weight and viscosity is well documented. The viscosity of polymer increases in proportional to an increase in molecular weight. At higher molecular weight, the polymer become very viscous and difficult to mix (Rogers, Long et al. 2003). To decrease the viscosity of the reaction and enhance the mixing efficiency, we either added an extra volume of toluene or continuously added small amount of benzene to the reaction mixture. The results showed that only continuously added small amount of benzene can generate high molecular weight PCADKe. Although the toluene is not evaporated in this condition, the extra volume of toluene also diluted the concentration of the reactants and only slightly increased the molecular weight.

Figure 2.6 shows that the Mw of PCADKe changes with reaction time when the reactions were conducted at 95 °C. For the reaction using PTSA as a catalyst, the molecular weight increased with increasing reaction time to reach the maximum of 12,000 Da at 48 hour, but decreased after that time point. We observed the same trend for the reaction using PPTSA as catalyst except the highest Mw is around 9,000 Dalton and decreased less after 48 hour. This might be due to the moisture entering to the reaction while we added the benzene via the pressure equalizing funnel and cause the hydrolysis of polyketals. Although the acidity of the PPTSA is milder than PTSA, the

efficiency of the PPTSA is lower than PTSA and resulted in low molecular weight PCADKe.

High molecular weight PCADKe can enhance the encapsulation efficiency of drug

One of the benefits of using high molecular weight polymers for drug delivery is to enhance the encapsulation efficiency and reduce the initial burst effect due to denser structure of the microparticles prepared from high molecular weight polymers (Jalil and Nixon 1990; Jaraswekin, Prakongpan et al. 2007).

Although the high molecular weight polyketals are originally developed for preparation of calpain inhibitor-loaded microparticles, we also explore their drug delivery applications in the other therapeutics. In collaboration with Dr. May's group, the high molecular weight PCADKe was used to encapsulate AOPHA-Me, an anti-inflammatory drug for arthritis (Bauer, Sunman et al. 2007). In this experiment, AOPHA-Me was encapsulated into two different molecular weights of PCADKe microparticles, and their encapsulation efficiency were compared. The encapsulation efficiency of AOPHA-Me into PKMs was calculated to be 3 ± 1 % (n=4) and the loading amount of AOPHA-Me into PKMs was 3 ± 1 μ g AOPHA-Me per 1 mg of particles. Using lower Mw PCADK, the loading amount of AOPHA-Me into PKMs was 0.7 ± 0.6 μ g AOPHA-Me per 1 mg of particles (n=7). The resulted microparticles formulated from high molecular weight PCADKe enhanced drug loading up to four times. The increase of drug loading in polyketal microparticles agreed with the other studies that high molecular weight can improve the drug loading efficiency.

AOPHA-Me-PKMs prepared from high molecular weight PCADKe were injected to the rats with adjuvant induced polyarthritis. The preliminary results showed that *in vivo* anti-inflammatory activity of AOPHA-ME-PKMs in adjuvant-induced polyarthritis in rats. The paws of the positive control animals were severe swelling and paw volume increased, however no paw swelling were observed in the animals treated with AOPHA-Me-PKMs (Data not shown).

Molecular weight and 1,5-pentanediol incorporated ratio affect the T_m of polyketal

Thermal analyses of the polyketal polymers were carried out on a differential scanning calorimeter (DSC) and results were shown in Table 2.4. In general, the high molecular weight PCADKe has a higher melting temperature (T_m) than low molecular weight PCADK polymer, and the PCADKe has higher T_m than PCADK copolymers. For example, the T_m of high Mw PCADKe is 288 °C which is 45 °C higher than the T_m of low Mw PCADK. This explains why nanoparticles formulated from high Mw PCADKe could withstand the centrifuge force and low Mw PCADK failed, since the T_m is closely correlated with the mechanical property of polymer.

The portion of non-flexible structure unit of polyketal also affects the T_m. In polyketal copolymers, the T_m decreases with increasing molar ratios of 1,5-pentanediol incorporated. For example, PK3, a copolymer that incorporates 13 mole % 1,5-pentanediol and 87 mole % 1,4-cyclohexanedimethanol, had a T_m of 248 °C. Similarly, PK10, a PCADK-derived copolymer synthesized from DEP/DMP method, incorporating 30 mole % of 1,5-pentanediol, had a T_m of 98 °C, which is 150 °C lower than PK3. The

only exception is the PK8 which incorporates 17 mole % 1,5-pentanediol and 87 mole % 1,4-cyclohexanedimethanol, had a T_m of 252 °C due to its high molecular weight.

It has been known that high molecular weight polymers have higher melting temperature (T_m) than low molecular weight polymer (Gopalan and Mandelkern 1967; Luo, Jones et al. 2002). And there are close correlation between T_m and the polymer properties: Polymers with high T_m present high tensile strength and high thermal resistance (Luo, Jones et al. 2002; Fradet and Tessier 2003). We demonstrated that both high and low Mw PCADK can form nanoparticles after sonication, however only the nanoparticles made from high Mw PCADKe remain intact during centrifugation step (Figure 2.10 A) while the nanoparticles made from low molecular weight collapsed in the same condition (Figure 2.10 B). We also tried to prepare nanoparticles with PK8, which have similar molecular weight as high Mw PCADKe, however, the PK8 nanoparticles also collapsed during centrifugation as low Mw PCADK nanoparticles. Both results suggest T_m is an important factor for the mechanic properties of polyketal polymers.

High molecular weight PCADKe can fabricate nanoparticles that can be delivered to the endothelium cells

Although the high molecular weight polyketals are originally developed for preparation of calpain inhibitor-loaded microparticles, we also found the other useful applications of these high molecular weight polyketals. In our experiment, we showed that the high molecular weight polyketal can provide the structural stability needed for fabrication of nanoparticles (Figure 2.10). Studies have shown that nanoparticles can enhance the drug delivery to the endothelium cells or other non-phagocytic cells (Davda

and Labhasetwar 2002; Thorek and Tsourkas 2008). Since polyketal are biocompatible, nanoparticles formulated from polyketal could be used to target therapeutics to endothelium to achieve sustained therapeutic effect.

Current applications of polyketal microparticles mainly focused on delivery of therapeutic agents to the Kupffer cells due to their size limitations. Yang et al. demonstrated that delivery of superoxide dismutase (SOD) encapsulated polyketal microparticles (SOD-PKMs) can significantly reduce the TNF- α level in the serum of mice which were suffered from acute liver failure, however, only moderately reduce the Alanine aminotransferase (ALT) level, an index for liver injury (Stephen Yang, manuscript in preparation). The result suggested delivery of SOD-PKMs cannot completely remove the extracellular superoxide that could cause hepatocyte necrosis and liver injury. Therefore, developing a nanoparticle delivery system that can target to the hepatocyte might benefit the acute liver failure therapy.

In this experiment, we have characterized the uptake of polyketal nanoparticles by Human umbilical vein endothelial cells (HUVECs) in cell culture. Figure 2.12 (B) demonstrates that the fl-siRNA PKNs were 2-3 orders of magnitude more effective at delivering fl-siRNA into HUVECs than DOTAP-fl-siRNA complexes and free-fl-siRNA. The result suggested that polyketal nanoparticles can enhance the uptake in the endothelium cells and have the potential to delivery therapeutics to hepatocytes.

Polyketal microparticles can release hydrophobic dye in a sustained manner

The goal of my research is to formulate a polyketal microparticle delivery system which can sustain release of calpain inhibitors to the spinal cord. Since AK295 is not

commercially available and the quantity of AK295 is limited, we have to utilize the other commercially available hydrophobic molecules to optimize the encapsulation and *in vitro* release kinetics. Three different hydrophobic dyes (Nile Red, DiI and coumarin-6) were chosen as model compounds for the calpain inhibitors because they have similar hydrophobic profiles as calpain inhibitors and should have similar release kinetics (Figure 2.1)

Among these hydrophobic dyes, Nile Red has the closest logP value (3.103 ± 1.187) to AK295 (2.327 ± 0.813) and MDL-28170 (4.156 ± 0.75), and the release profile of Nile Red should be similar to AK295. However, Nile Red only shows strong fluorescent intensity in the lipid rich environment, we were not able to detect the fluorescent signal in the pH7.4 phosphate buffer saline by using fluorescence spectrometry. Although coumarin-6 showed strong fluorescent intensity in saline, however, the release rate of coumarin-6 is always low due to its hydrophobicity ($\log P = 6.064 \pm 0.75$). Hu *et al.* showed that only 5 % of coumarin 6 was released from coumarin-6-labeled PEG-PLA nanoparticles and have to be analyzed using HPLC (Hu, Li et al. 2009). Since PCADKe is also very hydrophobic, the interaction between PCADKe and coumarin-6 decrease the release of coumarin-6 and we also cannot detect the coumarin-6 in the buffer by using fluorescence spectrometry.

DiI have been used as neuronal fluorescent tracers for CNS delivery (Krenz and Weaver 1998; Shibata-Iwasaki, Dekimoto et al. 2007; Liu, Li et al. 2008). Although it doesn't have logP value, it has been generally considered as lipidphilic or hydrophobic dye. When excited at 550 nm, DiI has two emission wavelengths at 565 nm, and 593 nm respectively. At same concentration, the fluorescent intensity at 593 nm is two times

higher than the intensity at 565 nm. However, when the DiI solution mixed with equal volume of 0.2 % SDS, the fluorescent intensity at 565 nm increased 92 times while the intensity in the 593 nm only increased 16 times. At this condition, the fluorescent intensity at 565 nm is three times stronger than the intensity at 593 nm, therefore we measured DiI concentration at 565 nm instead of 593 nm. At 565 nm, we were able to detect a small amount of DiI present in the buffer and allow us to study the *in vitro* release of this hydrophobic dye.

The size of microsphere is an important factor that affects the release rate of hydrophobic drugs (Dawes, Fratila-Apachitei et al. 2009). In general, smaller microparticle release drug faster due to an increased surface area to volume ratio. They also tend to have lower encapsulation efficiency due to the loss of encapsulated drug in the washing steps. Budhian *et al.* also showed that increasing the particle size can reduce the initial burst effect and extend the period of release within nanoparticle formulations (Budhian, Siegel et al. 2008). In our experiment, we observed the similar size effects when we compare the encapsulation efficiency and *in vitro* release of DiI of the smaller DiI-PKMs (1.9 μm) with the other larger DiI-PKMs. However, when size of the DiI-PKMs is larger than 3 μm , the size effect on encapsulation efficiency and *in vitro* release kinetics become less apparent. From our *in vitro* release study, we observed that all sizes of DiI-PKMs exhibited different levels of incomplete release of DiI. The small microparticles can achieve higher cumulative release than larger particles because of their fast diffusion rate due to the short diffusion pathway.

In summary, we showed that we can increase the molecular weight of polyketals by using a DEP/DMP method. One of the high molecular weight polyketals, PCADKe,

had lowest hydrolysis rate of the polyketals, thus microparticles formulated from PCADKe have the potential for sustained delivery of hydrophobic compounds at pH 7.4. The release kinetics of polyketal microparticles (PKMs) were optimized by using a fluorescent dye, DiI as a model compound for calpain inhibitors, due to a similar hydrophobicity between DiI and calpain inhibitors (AK295 and MDL-28170), and can be measured by fluorescence spectrometry. We demonstrated that microparticles based on high molecular weight polyketals can provide sustained release of DiI for at least one month. The formulation procedures developed in this chapter were used to prepare the calpain inhibitors-encapsulated microparticles in the next chapter.

CHAPTER 3

PCADK_e MICROPARTICLES AS A SUSTAINED RELEASE SYSTEM FOR HYDROPHOBIC CALPAIN INHIBITORS

3.1 Introduction

In this chapter, we discuss Specific Aim 2, which is to develop polyketal microparticles which have a release half-life of 1 month *in vitro* for calpain inhibitors. To reach this goal, we encapsulated calpain inhibitors in polyketal microparticles and evaluated their *in vitro* release kinetics and bioactivity.

It is known that calpain activation is an important mechanism of motor neuron degeneration in ALS (Fischer, Culver et al. 2004), and therapeutic strategies that can inhibit calpain activity in the CNS have great clinical potential. As we described in chapter 1, calpain inhibitors have been demonstrated to be neuroprotective in animal models of neurological injury, and should have great potential to treat ALS; however delivery problems have hindered their clinical success. For example, AK295 is a hydrophobic calpain inhibitor which shows great drug properties but has low efficacy *in vivo*, due to the CNS barriers (Saatman, Murai et al. 1996). Another potent calpain inhibitor, MDL-28170, can penetrate the blood brain barrier and had shown promising neuroprotective effects in the animal models of focal ischemic brain damage and Parkinson's disease (Dong, Tan et al. 2006; Ai, Liu et al. 2007; Samantaray, Ray et al. 2008). However, like AK295, MDL-28170 also exhibits a dose-dependent neuroprotective effect (Markgraf, Velayo et al. 1998). In order to maintain the concentration needed for therapeutic effects in the spinal cord, it required multiple injection of MDL-28170 within 48 hours (Ai, Liu et al. 2007). In the treatment of ALS, a

larger delivery (volume/dose) may be needed and complications such as, infection, catheter obstruction, and discomfort can arise in patients when using this delivery method. The other drawback of the current AK295 and MDL-28170 delivery system is that both drugs need to be dissolved in acidic solutions (pH 5.6) or organic solvent before injections (Saatman, Murai et al. 1996), which might cause some unwanted inflammatory effects. Therefore, there is a great need to improve delivery systems for calpain inhibitors.

In the Specific Aim 1, we demonstrated that microparticles based on high molecular weight polyketals can sustain the release of DiI, a hydrophobic dye for at least one month. In this aim, PKMs which contain the calpain inhibitor (AK295 or MDL-28170) were fabricated, using formulation procedures developed in Aim 1. The size of AK-PKMs and MDL-PKMs were characterized by scanning electron microscopy (SEM). The encapsulation efficiency of AK295 in AK-PKMs was measured by liquid chromatography-mass spectrometry (LC-MS). The encapsulation efficiency and *in vitro* release profile of MDL-28170 in MDL-PKMs was measured by reverse phase high performance liquid chromatography (HPLC). The inhibitory activity of AK295 and MDL-28170 released from the microparticles were measured by a modified *in vitro* calpain assay.

3.2 Experimental Method

Preparation of AK295 PCADKe microparticles (AK-PKMs)

Briefly, 5 mg of AK295 and 50 mg of PCADKe were dissolved in 500 μ L of a single-phase solvent (1:3 N,N-dimethylformamide : dichloromethane). This solution was combined with 5 mL of 5 % poly(vinyl alcohol) (PVA) Tris buffer solution (pH=9.0) and the mixture was homogenized at 17,500 rpm for 1 minute. The resulting oil-in-water emulsion was added to 20 mL of 1 % PVA Tris buffer solution (pH=9.0) and stirred for 4 hours, evaporating the dichloromethane, forming particles. The resulting particles were washed three times in deionized water (with centrifugation at 10,000 rpm) to remove dimethylformamide (DMF) and PVA, and lyophilized. Various pHs and concentrations of the PVA buffer were used to optimize the AK295 encapsulation.

Characterizations of AK-PKMs

The size of the AK-PKMs was characterized by scanning electron microscopy (SEM). Encapsulation efficiency of the AK295 in PCADKe microparticles was determined by liquid chromatography-mass spectrometry (LC-MS). Briefly, 1 mg of AK295 PKMs were dissolved in 360 μ L of sample solution (70:30:0.1 water: acetonitrile: trifluoroacetic acid) before analysis. The mass transition for quantitation was set for the best sensitivity at m/z 505.18 to m/z 443.2 for AK295. Various concentrations of AK295, and internal standard (Zlak-3001, Zlak-3002 and Zlak-3005) were used to establish a calibration curve. The calculated coefficient of correlation was 0.9998 for an analytical range from 0.1 to 5.0 μ M.

Preparation of MDL-PKMs

Briefly, 5 mg of MDL-28170 and 50 mg PCADKe were dissolved in 500 μ L of dichloromethane. This solution was combined with 5 mL of 5 % poly(vinyl alcohol)(PVA) Tris buffer solution (pH 9.0) and the mixture was homogenized at 17,500 rpm for 1 minute. The resulting oil-in-water emulsion was added to 20 mL of 1 % PVA Tris buffer solution (pH 9.0) and stirred for 4 hours, evaporating dichloromethane and forming particles. The resulting particles were washed three times in deionized water (with centrifugation at 10,000 rpm) to remove PVA, and lyophilized. The MDL-28170 encapsulation efficiency was optimized by formulating MDL-PKMs with various PCADKe with different molecular weights. The morphology and size of MDL-PKMs were characterized by scanning electron microscopy (SEM).

Characterization of MDL-PKMs by HPLC

The encapsulation efficiency and *in vitro* release profile of MDL-PKMs were measured by reverse phase high performance liquid chromatography (HPLC).

Encapsulation efficiency

Briefly, 2-4 mg of MDL-PKMs were dissolved in 1 mL of 50 % acetonitrile, 0.1 % trifluoroacetic acid (TFA) solution. The resulting solution was then injected into a Shimadzu HPLC with an Apollo C18 Column (250 mm x 4.6 mm, 5 μ m) using a linear gradient elution of water/acetonitrile from 80/20 to 20/80 containing 0.1 % TFA, using a mobile phase at 1.5 mL/min with a PDA detector set at 215 nm. A standard curve of MDL-28170 was generated from 0.053 mg/mL to 0.00053 mg/mL to fit a least square linear regression. Blank PKMs were also analyzed as a control.

In vitro release profile of MDL-28170

Briefly, a 10 mg sample of MDL-PKMs (containing 650 µg of MDL-28170) (n=4) were added to a 2 mL microcentrifuge tube and suspended with 1200 µL of PBS (pH 7.4). The microcentrifuge tubes were shaken at 120 rpm, 37°C. At different time intervals (1, 3, 6, 12, 24 hours, 3, 7, 14, 28, and 60 days), the particle suspensions were centrifuged at 10,000 rpm for 15 min. An 1100 µL volume of the supernatant was pipetted out and transferred to another microcentrifuge tube. This supernatant was then recentrifuged at 10,000 rpm for 15 min to minimize the particles present in the solution. A 1000 µL volume of the supernatant was pipetted out and the same volume of fresh buffer was added to the tube.

The MDL-28170 released into the supernatant was then injected into a Shimadzu HPLC with an Apollo C18 Column (250 mm x 4.6 mm, 5 µm) using a linear gradient elution of water/acetonitrile from 80/20 to 20/80 containing 0.1 % TFA, using mobile phase at 1.5 mL/min with a PDA detector set at 215 nm. A standard curve of MDL-28170 was generated from 0.053 mg/mL to 0.00053 mg/mL to fit a least square linear regression. At the last time point (60 days) the remaining particles were hydrolyzed and the amount of unreleased MDL-28170 in the particles were measured and used to calculate the percentage of MDL-28170 released at each time point. The supernatant collected from blank PKMs were also analyzed as control.

***In vitro* activity assay of AK295- and MDL-28170-PKMs**

Establish a method for measuring the inhibitory activity of AK295 and MDL-28170

The inhibition of calpain activity in response to AK295 or MDL-28170 was used to evaluate the bioactivity of the AK295- or MDL-28170-PKMs. The calpain activity was measured by using the modified calpain assay methods described by Korukonda *et al.* and Mallya *et al.* (Mallya, Meyer et al. 1998; Korukonda, Guan et al. 2006). Briefly, 2 mg samples of AK295 or MDL-28170 were dissolved with 1 mL of DMSO. This stock solution was then diluted to various concentrations of AK295 or MDL-28170 to prepare standard curves of AK295 and MDL-28170. The fluorogenic substrate Suc-Leu-Tyr-AMC for calpain I was obtained from Bachem. Calpain I from porcine erythrocytes was purchased from Calbiochem. The fluorescence was monitored using a SpectraMaxMINI microplate reader (Molecular Devices).

Calpain assays were performed in a calpain assay buffer which consists of 50 mM Tris HCl, 50 mM NaCl, 1 mM EDTA, 1 mM EGTA, 0.1 % CHAPS, pH 7.5, 10 mM DTT, 5 mM CaCl₂ and 0.2 μM substrate (Suc-Leu-Tyr-AMC). A 10 μL aliquot of DMSO (control) or inhibitor solution in DMSO was added to 200 μL of calpain assay buffer. The reaction was initiated by adding a 2 μL aliquot of Calpain I (with a final concentration of 10 nM) to the well. The reaction was monitored by quantifying the release of 7-amino-4-methylcoumarin (AMC) ($\lambda_{\text{ex}} = 360 \text{ nm}$, $\lambda_{\text{em}} = 465 \text{ nm}$). Different concentrations of AK295 and MDL-28170 were used as the calibration standard and the calibration curves were plotted against the relative-fluorescence-units (RFU) increased amounts for different concentrations of calpain inhibitors.

Measure the bioactivity of AK295 and MDL-28170 within the PCADKe microparticles

To extract the AK295 or MDL-28170 from the PCADKe microparticles, the inhibitor encapsulated microparticles (10 mg) were dissolved in 200 μ L of DCM in a 4 mL vial. After the DCM was evaporated, 1 mL of DMSO was added into the vial to extract the inhibitors. The DMSO-drug solution was analyzed by HPLC (MDL-28170 only) to determine the extraction efficiency. A standard curve of MDL-28170 was generated with various concentrations of MDL-28170/DMSO solution.

After determining the extraction efficiency, the AK295/DMSO or MDL-28170/DMSO solutions were diluted to 2 to 20 times with DMSO. A 10 μ L of diluted AK295/DMSO or MDL-28170/DMSO solution was added to 200 μ L of calpain assay buffer. The reaction was initiated by adding a 2 μ L aliquot of Calpain I (with a final concentration of 10 nM) to the well. The reaction was monitored by the release of 7-amino-4-methylcoumarin ($\lambda_{\text{ex}} = 360$ nm, $\lambda_{\text{em}} = 465$ nm). The inhibitory activities of AK295 or MDL-28170 within the PCADKe microparticles were calculated from the AK295/DMSO or MDL-28170/DMSO dilutions which fall into the correct range of the calibration curve. Blank PKMs were used as a negative control in this experiment.

Measure the bioactivity of AK295 and MDL-28170 released from microparticles

A 20 mg sample of AK295 PKMs (containing 40 μ g of AK295) or MDL-28170 PKMs (containing 1200 μ g of MDL-28170) were added to a 2 mL centrifuge tube and suspended with 1200 μ L of buffer containing 50 mM Tris-HCl (pH7.4), 50 mM NaCl, 1 mM EDTA, 1 mM EGTA, and 0.1 % CHAPS). The microcentrifuge tubes were shaken at 120 rpm, 37°C. At various time intervals (3, 7, 14, 28 and 60 days), the particle

suspension were centrifuged at 10,000 rpm for 15 min. An 1100 μL volume of the supernatant was pipetted out and transferred to another micricentrifuge tube. This supernatant was then recentrifuged at 10,000 rpm for 15 min to minimize the particles present in the solution. A 1000 μL volume of the supernatant was pipetted out and the same volume of fresh buffer was added to the tube. The resulting supernatants were then stored in a 4 $^{\circ}\text{C}$ refrigerator until the time of testing. For the calpain activity assay, DMSO was added to the supernatants to form 5 % DMSO drug containing assay solutions. A 210 μL of drug containing assay solution was added to the 96 well plates. The reaction was initiated by adding a 2 μL aliquot of Calpain I (with a final concentration of 10 nM) to the well. The reaction was monitored by the release of 7-amino-4-methylcoumarin ($\lambda_{\text{ex}} = 360 \text{ nm}$, $\lambda_{\text{em}} = 465 \text{ nm}$). The inhibitory activities of AK295 or MDL-28170 within the PCADKe microparticles were calculated from the AK295/DMSO or MDL-28170/DMSO dilutions which fall into the correct range of the calibration curve. Blank PKMs were used as a negative control in this experiment.

3.3 Results

Formulation of AK295-loaded PCADKe microparticles

The calpain inhibitor AK295 was encapsulated into microparticles using a single oil-in-water emulsion, solvent evaporation method. Encapsulation efficiency of the AK295 in PCADKe microparticles was determined by liquid chromatography-mass spectrometry (LC-MS). As shown in Figure 3.1, both free AK295 (A) and AK295-PCADKe particles (B) showed a strong intensity of the AK295 ion fragments at m/z 505.18 to m/z 443.2.

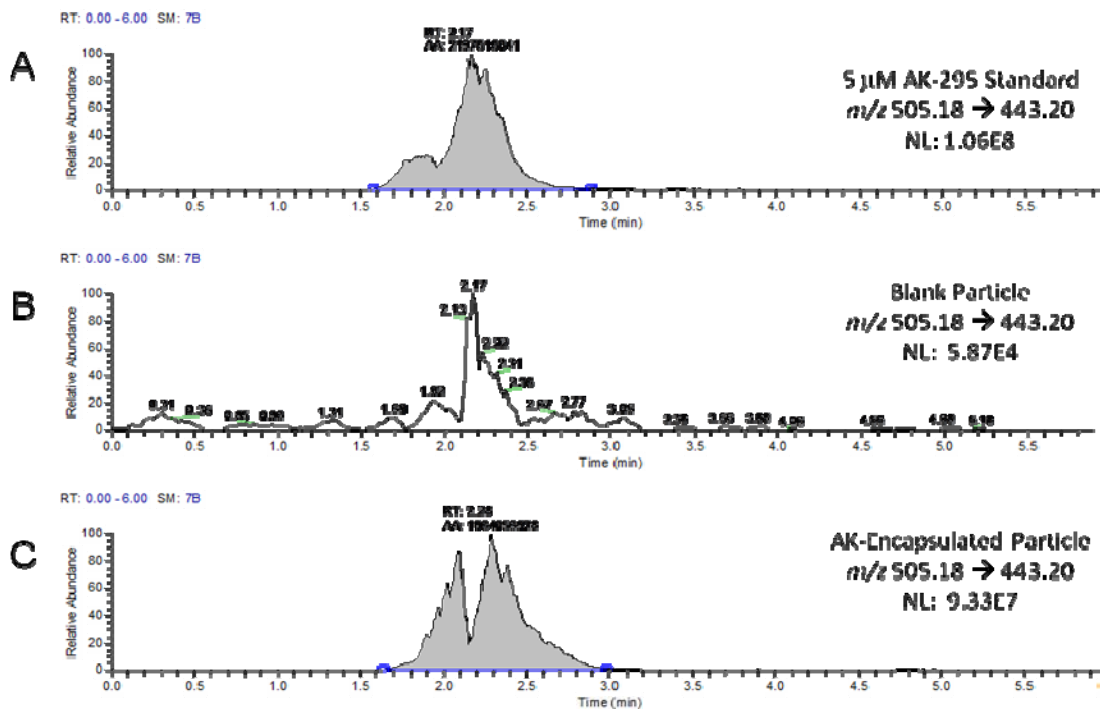


Figure 3.1 Representative chromatogram of (A) AK295 standard solution, (B) blank PCADKe microparticles, and (C) AK295-encapsulated PCADKe particles from LC-MS. (Courtesy from Christina Hampton from Dr. Fernandez's Lab.)

In contrast, the intensity of the same fragment in the blank PCADKe microparticles was about 200 times lower than the free AK295 and AK295-encapsulated

PCADKe microparticles. This indicates that LC-MS technique is suitable for measuring the amount of AK295 encapsulated in the PCADKe particles.

Table 3.1 Encapsulation efficiency, and particle sizes of various AK295 encapsulated polyketal microparticles

Sample ID	w/ DMF	Homogenized speed (rpm)	PVA buffers	E.E.* (%)	Particle Size (nm)
AK-PKM1	Yes	13,500	5.0 % PVA in Tris-NaCl	5.08	5542 ± 1837
AK-PKM2	Yes	21,500	5.0 % PVA in Tris-NaCl	0.64	1064 ± 156
AK-PKM3	No	21,500	5.0 % PVA in Trisl	2.67	2344 ± 448
AK-PKM4	No	21,500	1.0 % PVA in Trisl	1.03	2173 ± 662
AK-PKM5	No	21,500	0.4 % PVA in Trisl	0.82	5750 ± 1445
AK-PKM6	No	21,500	5.0 % PVA in Tris-NaCl	1.85	1676 ± 366
AK-PKM7	No	21,500	1.0 % PVA in Tris-NaCl	17.7	4895 ± 2379
AK-PKM8	No	21,500	0.4 % PVA in Tris-NaCl	2.69	3886 ± 998

*Encapsulation Efficiency

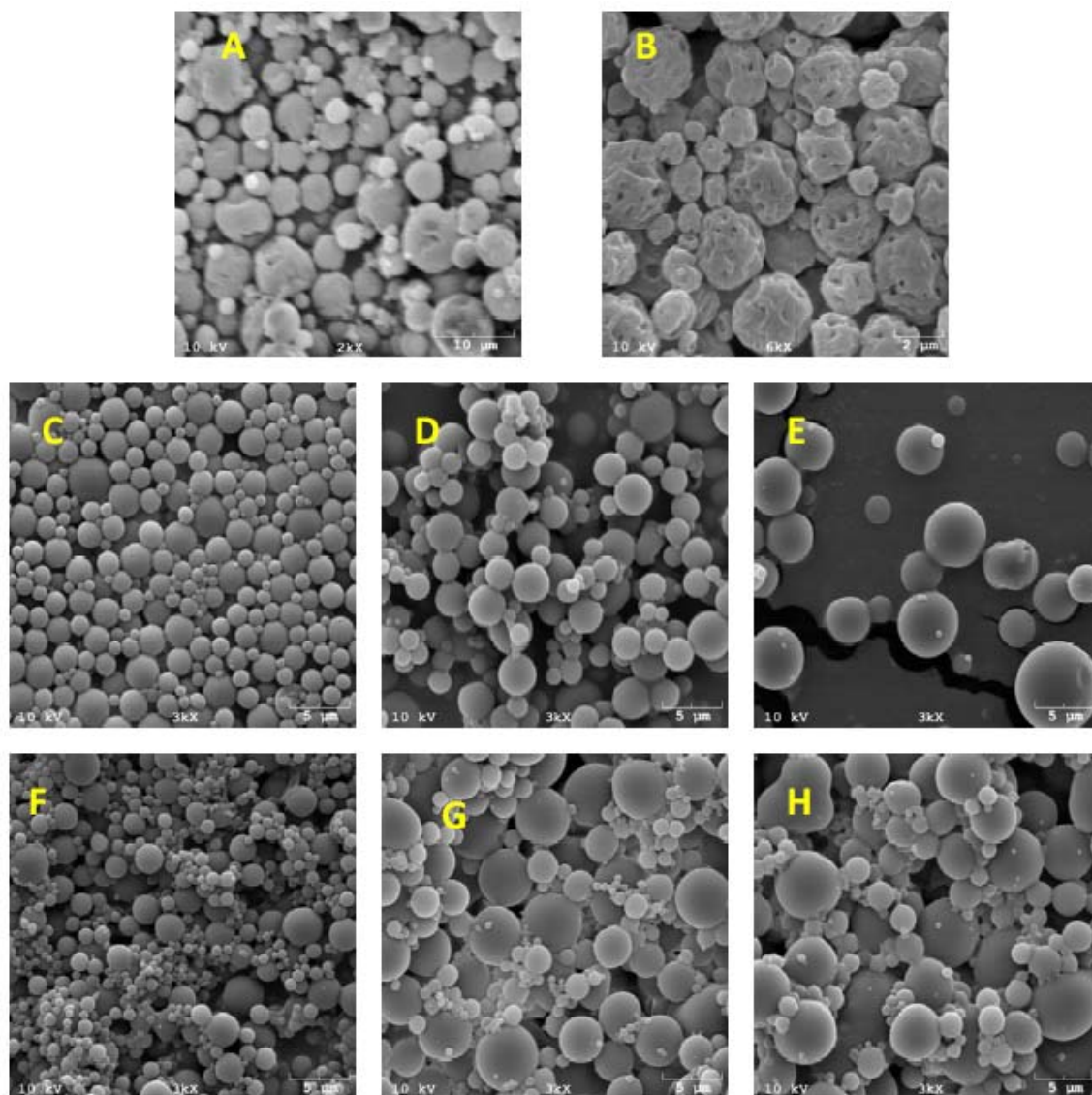


Figure 3.2 SEM images of AK-PKMs. (A) AK-PKM1, (B) AK-PKM2, (C) AK-PKM3, (D) AK-PKM 4, (E) AK-PKM5, (F) AK-PKM6, (G) AK-PKM7 and (H) AK-PKM8

Characterizations of MDL-28170 PKMs

The calpain inhibitor MDL-28170 was encapsulated into microparticles using a single oil-in-water emulsion, solvent evaporation method. Encapsulation efficiency of the MDL-28170 in PCADKe microparticles was determined by reverse phase HPLC. As shown in Figure 3.3, both MDL-28170-PKMs (A) and free MDL-28170 (B) showed a strong peak around 15 min. In contrast, the intensity of the same fragment in the blank PCADKe microparticles was about 1,000 times lower than the free MDL-28170 and MDL-PKMs. This indicates that reverse HPLC technique is suitable for measuring the amount of MDL-28170 encapsulated in the PCADKe microparticles.

MDL-PKMs were prepared from three different molecular weights of PCADKe to maximize the MDL-28170 encapsulation efficiency. The morphology and sizes of these MDL-PKMs were characterized by SEM and DLS. Figure 3.4 shows the SEM images of MDL-28170-loaded PCADKe microparticles and demonstrate that their size ranges from 1 to 2 μm . The MDL-28170 encapsulation efficiency varies between 43.5 to 76.8 %. The results of encapsulation efficiency and particles size of MDL-PKMs were shown in Table 3.2. In general, the encapsulation efficiency and particles size of MDL-PKMs increased as the molecular weight of PCADKe increases under the same procedure.

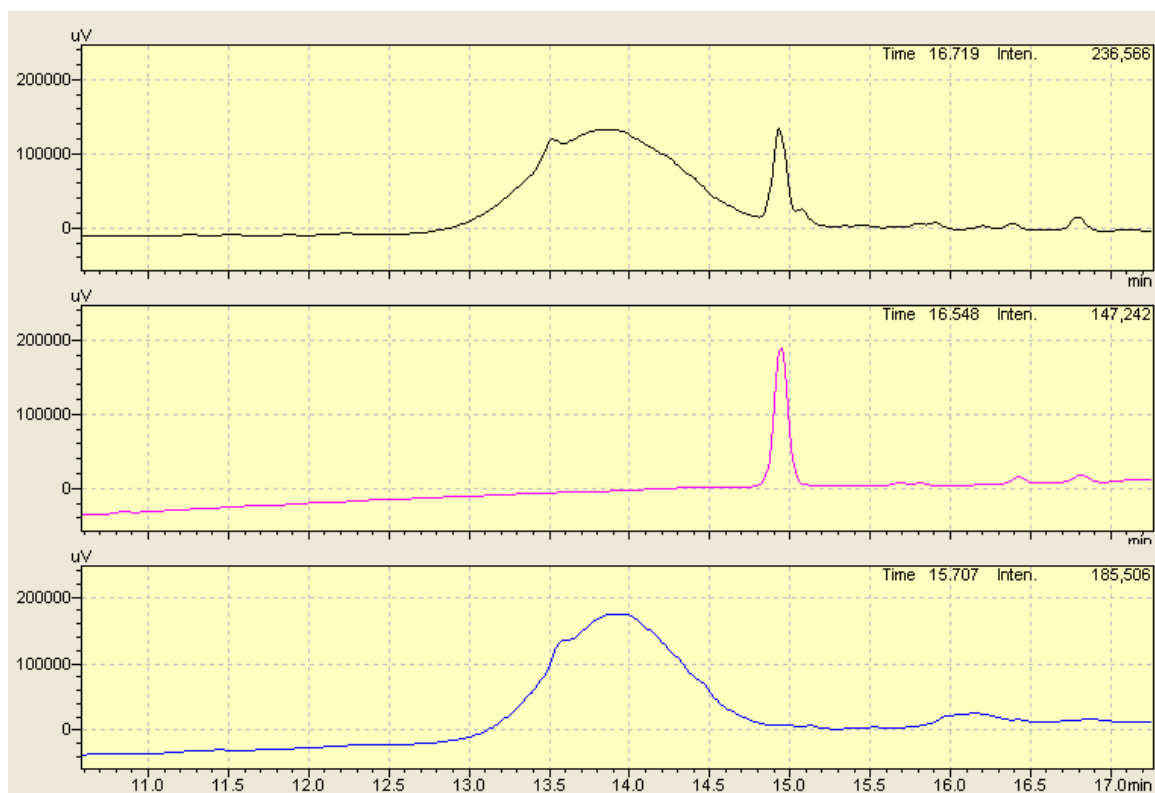


Figure 3.3 Representative chromatogram of (A) MDL-28170-encapsulated PCADKE particles (B) MDL-28170 standard solution, and (C) blank PCADK microparticles from reverse phase HPLC.

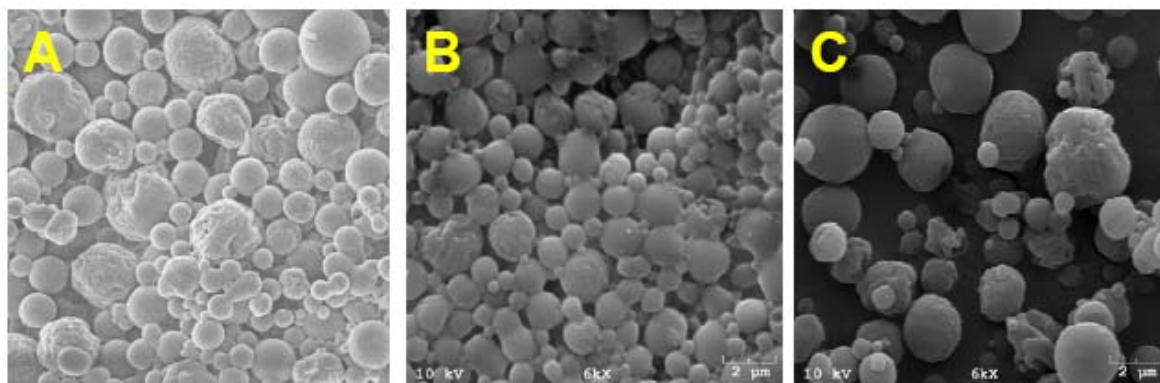


Figure 3.4 SEM images of (A) MDL-PKM1, (B) MDL-PKM2, and (C) MDL-PKM3

Table 3.2 Encapsulation efficiency and particle size of MDL-PKMs

MDL-PKMs	Molecular weight (Mw) of PCADKe (Da)	Encapsulation Efficiency (%)	Particle size (μm)
1	6,317	43.5	1.23 ± 0.36
2	9,623	56.3	1.05 ± 0.19
3	12,234	76.8*	2.02 ± 0.64

* The encapsulation efficiency of MDL-28170 in the PCADKe microparticles was determined by reverse phase HPLC at 215 nm.

Encapsulation efficiency (%) = (amount of MDL-28170 loaded in microparticles) / (initial amount of MDL-28170 used to make microparticles) x 100

** Particle size was determined by dynamic light scattering (DLS)

***In vitro* release profile of MDL-28170 from MDL-PKMs**

In order to determine whether or not MDL-PKMs have suitable properties for sustained delivery of MDL-PKMs in a physiological environment, we investigated the *in vitro* release kinetics of MDL-PKMs in pH 7.4 phosphate buffer saline by using high performance liquid chromatography (HPLC). The release profile of MDL-28170 from PCADKe microparticles is shown in Figure 3.5. We observed a burst release within the first 3 days (16 %). Approximately 50 % of the MDL-28170 was released in the first 30 days and slowly released until Day 55. The morphology of the MDL-PKMs changed after drug release. At Day 55, the large MDL-PKMs still retain their size, however, they become porous when compare to the MDL-PKMs day 1. We also observed that most of the small MDL-PKMs completely lose their structure and become amorphous hydrolyzed polymer (Figure 3.6)

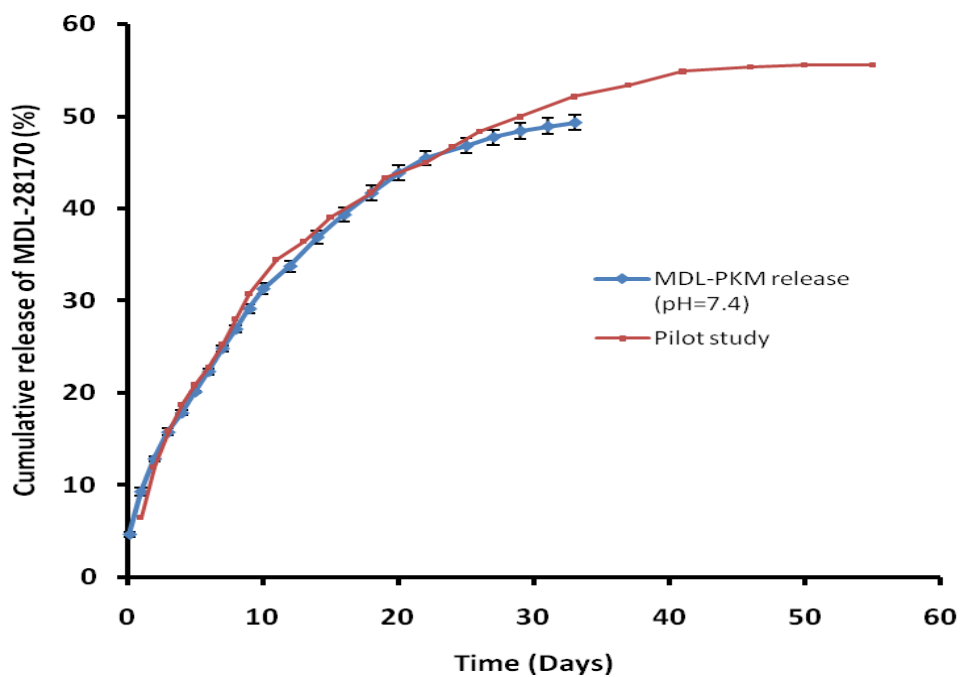


Figure 3.5 Release kinetics of MDL-28170 encapsulated in PCADKe microparticles (n=4 for each time point)

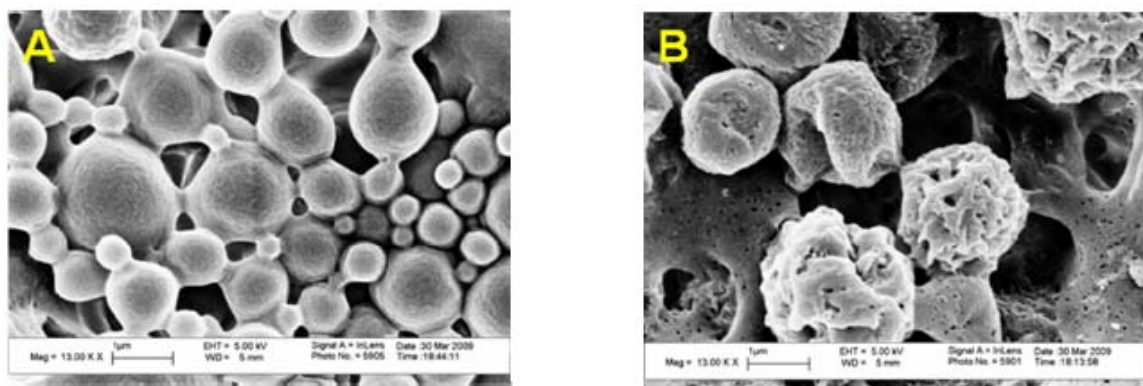


Figure 3.6 SEM images of MDL-PKMs at (A) Day 0, and (B) Day 60 in PBS (pH 7.4)

Measure the bioactivity of AK-PKMs and MDL-PKMs

The inhibition of calpain activity in response to AK295 or MDL-28170 was used to evaluate the bioactivity of the AK-PKMs or MDL-PKMs. The calpain activity was measured by using the modified calpain assay methods described by Korukonda *et al.* and Mallya *et al.* (Mallya, Meyer et al. 1998; Korukonda, Guan et al. 2006). The calpain activity was measured by monitoring the release of 7-amino-4-methylcoumarin ($\lambda_{\text{ex}} = 360$ nm, $\lambda_{\text{em}} = 465$ nm). Different concentrations of AK295 and MDL-28170 were used as the calibration standard and the calibration curves were plotted against the RFU increased amounts for different concentrations of calpain inhibitors. The calibration curve for AK295 is shown in Figure 3.7 and the calibration curve for MDL-28170 is shown in Figure 3.8. From these calibration curves, the calpain inhibitory activity of the AK-PKMs and MDL-PKMs was calculated. The inhibitory activity of encapsulated calpain inhibitors was determined by dividing the concentration of active calpain inhibitor of the microparticles with the total amount of calpain inhibitors encapsulated within the microparticles. The inhibitory activity of the calpain inhibitors from AK-PKMs and MDL-PKMs were summarized in Table 3.3. The released buffers from AK-PKMs and MDL-PKMs showed inhibitory activity even after 1 month.

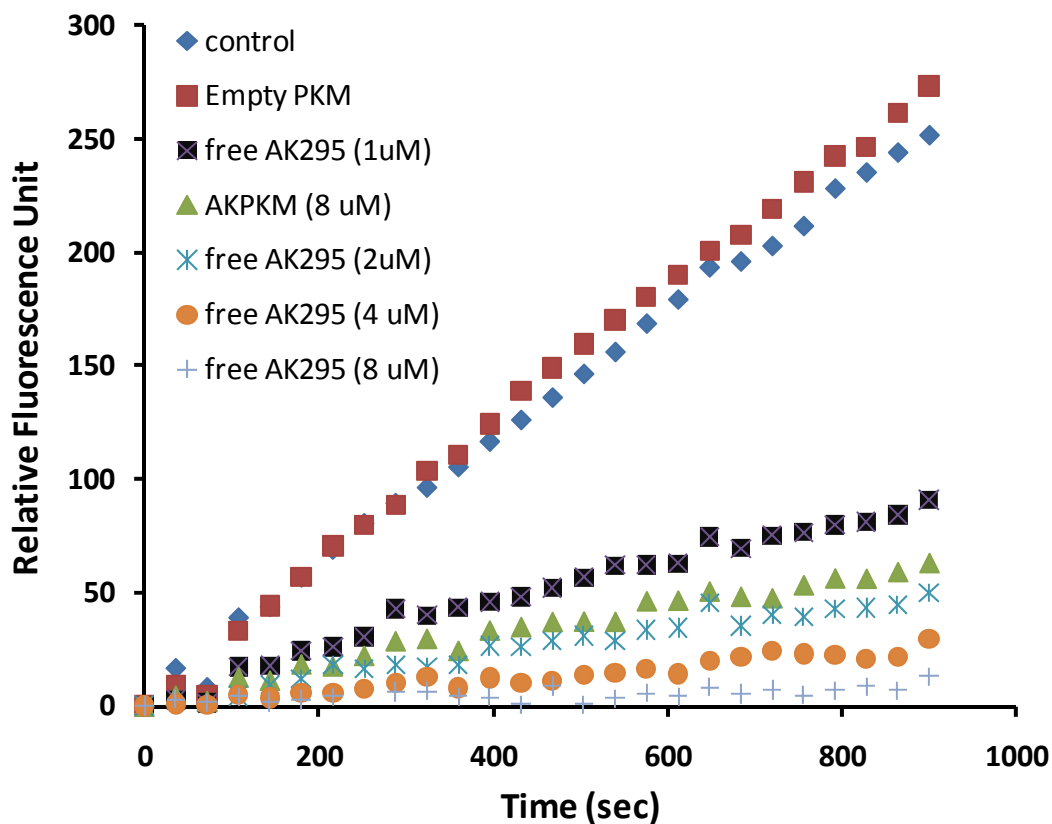


Figure 3.7 Inhibitory activities of AK295 were determined by establishing a calibration curve. The inhibitory effect of AK295 was determined by measuring the fluorescent intensity of AMC released from calpain substrate ($\lambda_{\text{ex}} = 360 \text{ nm}$, $\lambda_{\text{em}} = 465 \text{ nm}$)

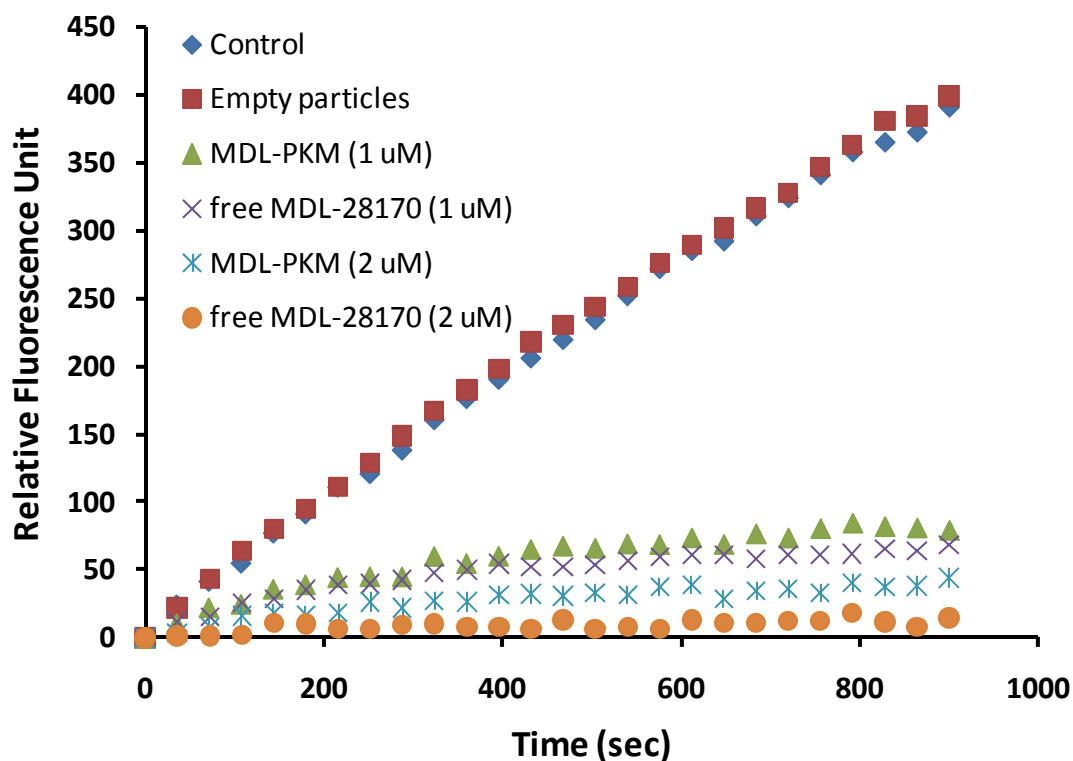


Figure 3.8 Inhibitory activities of MDL-28170 were determined by establishing a calibration curve. The inhibitory effect of MDL-28170 was determined by measuring the fluorescent intensity of AMC released from calpain substrate ($\lambda_{\text{ex}} = 360 \text{ nm}$, $\lambda_{\text{em}} = 465 \text{ nm}$)

Table 3.3 Calpain inhibitors loading, encapsulation efficiency and inhibitory activity in PCADKe microparticles from AK295-PKMs and MDL-28170-PKMs.

	AK295-PKMs	MDL-28170-PKMs
Encapsulation Efficiency	2.69 %	56.3 %
Calpain inhibitor loading by weight	0.25 μg AK295 per mg of AK-PKMs	5.12 μg MDL-28170 per mg of MDL-PKMs
Calpain inhibitor activity	19.58 \pm 3.41 %	72.75 \pm 9.58 %
Active Calpain inhibitors loading by weight	48.96 ng of active AK295 per mg of AK-PKMs	3725 ng of active MDL-28170 per mg of MDL-PKMs

3.4 Discussion

Because of the ongoing nature of ALS, sustained delivery of calpain inhibitor to the motor neurons is needed to enhance the therapeutic effects. Both AK295 and MDL-28170 showed a dose-dependent neuroprotective effect (Markgraf, Velayo et al. 1998). To achieve the desired therapeutic effect, it requires delivery of sufficient amount of active calpain inhibitor to the spinal cord. Therefore, it is important to establish a method to quantify the calpain concentration in the calpain encapsulated polyketal microparticles. Because AK295 and PCADKe show a severe overlapping between their absorption spectra, we have tried to separate them by reverse phase HPLC. AK295 showed a broad peak from 4.0 to 5.8 min and a sharp peak at 6 min (Figure 3.9 A) and PCADKe microparticle had a sharp peak from 5.2 to 5.6 min (Figure 3.9 B), thus we should be able to differentiate the AK295 and PCADKe microparticles. However, the peak of PCADKe microparticles is seven times higher than the peak of AK295 at 6 min, it is very difficult to quantify the AK295 by HPLC when the AK295 concentration is low (Figure 3.9 C). In collaboration with Dr. Fernandez's lab at Georgia Tech, we were able to quantify the encapsulation efficiency of AK295 by using LC-MS. The results showed that LC-MS can detect AK295 at very low amount (pg), and is suitable for quantification of AK295 in the AK-PKMs. The results showed that the encapsulation efficiency of AK-PKM1 was 5.08 %, however, AK-PKM1 is not suitable for intraspinal cord injection due to their size. In our preliminary study, we injected various sizes of Nile Red microparticles to the wild type animals. We found the delivery efficiency drastically decreased when the Nile Red microparticles was larger than 3 μm . However, the encapsulation efficiency decreased to 0.6 % as the particle size dropped to 1-2 μm . Several parameters including

with or without DMF in organic phase, PVA concentration of 0.2 to 5 % as stabilizer, and the salt in PVA solution were examined to optimize the formulations (Table 3.1 and Figure 3.2).

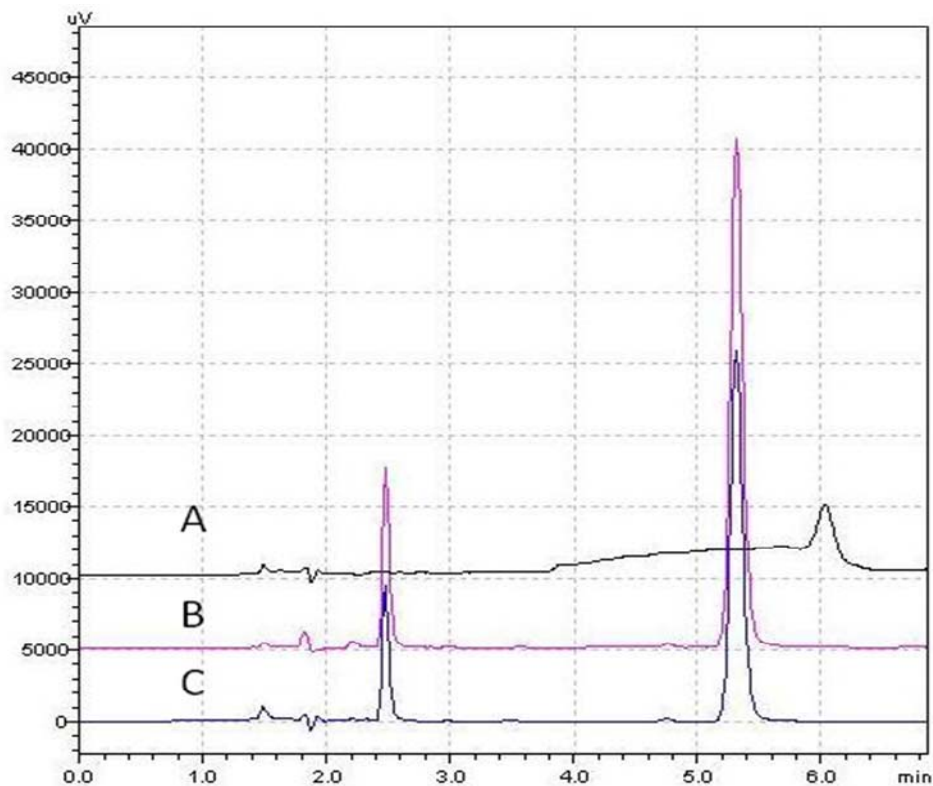


Figure 3.9 Representative chromatogram of (A) AK295, (B) Blank PCADKe microparticles and (C) AK295-encapsulated PCADKe microparticles from reverse phase HPLC.

Generally, porous microparticles, which were prepared from DMF-DCM solution, have lower AK295 encapsulation efficiency than non-porous microparticles in same size range. The removal of the DMF during particle preparation created porous structures in AK-PKMs. This porous structure allowed the water to enter into the center of the particle and increase the loss of AK295 during the washing steps.

Several studies have shown that decrease in the concentration of surfactant can increase the encapsulation efficiency (Esmaeili, Atyabi et al. 2008; Guo and Chu 2008), however, it also increases the particle size. In our experiment, we observed the similar effect on the size of AK-PKMs, however, the effect of surfactant on encapsulation efficiency was not clear. In general, AK295 encapsulation efficiency is higher as the particles size increase, and the particle size distribution of AK-PKMs is narrower when they were prepared from the Tris buffer without NaCl.

Due to the low encapsulation efficiency of AK295, we decided to encapsulate another calpain inhibitor MDL-28170 as an alternative therapeutic agent because it has lower K_i value (8 nM) than AK295 (41 nM) and can be quantified by reverse phase HPLC (Figure 3.3). The MDL-28170 encapsulation efficiency in PCADKe microparticles ranges from 43.5 to 76.8 %, which is 16 to 29 times higher than AK295. The high encapsulation efficiency mainly due to its hydrophobicity ($\log P = 4.156 \pm 0.705$).

We also observed that microparticles prepared from high molecular weight polyketals resulted in higher encapsulation efficiency of MDL-28170 and larger particle size (Table 3.2). Ziberman *et al.* showed that as the molecular weight of PLGA increases, the viscosity of the organic phase also increases and subsequently increases the sizes of microparticles (Zilberman and Grinberg 2008). As we described in Chapter 1, the encapsulation efficiency is higher in the larger particle. This might explain the increase of encapsulation efficiency in the polyketal microparticle formulated from high molecular weight PCADKe.

The *in vitro* release profile of MDL-PKMs at pH 7.4 PBS was shown in Figure 3.5. We observed a burst release within the first 3 days (16 %). Approximately 50 % of MDL-28170 released in the first 30 days and slowly released until Day 55. The *in vitro* release profile of MDL-28170 is similar to the other release profile of hydrophobic compound from polymeric microparticles which undergo bulk erosion.

To investigate whether polyketal microparticles undergo bulk erosion, we also performed an experiment to investigate the degradation of the polyketal microparticles by observing their morphology changes using SEM. The SEM pictures showed that the size of the MDL-PKMs ranges from 0.5 to 1.5 μm at Day 0 (Figure 3.6 A). After releasing drug into PBS for 60 days, the size of larger MDL-PKMs (ranges from 1 to 1.5 μm) remained unchanged however, the structure of MDL-PKMs become porous. In the mean time, small MDL-PKMs (under 1 μm) collapsed and became amorphous hydrolyzed polymer (Figure 3.6 B). We hypothesized that MDL-PKMs undergoes bulk erosion mechanism, because we didn't observe significant change in the size of MDL-PKMs after incubation with PBS for 60 days. The bulk erosion mechanism might undergo the following scenarios. Upon contact with PBS water diffused into MDL-PKM and the MDL-28170 diffused out of MDL-PKMs due to the concentration gradient. In the same time, the polyketal was hydrolyzed and cleaved into short chains. The porous structure of MDL-PKMs was created by the removal of MDL-28170 and hydrolyzed polyketal. For the smaller MDL-PKMs (under 1 μm), water can rapidly diffuse to the center of the particle due to the short distance between surface and center of the small microparticles. And subsequent hydrolysis in the particles leads to collapse of the microparticles. Our hypothesis was supported by the research done by von Burkersroda *et al* (von

Burkersroda, Schedl et al. 2002). In their study, polyketals will undergo bulk erosion when the polymer devices are smaller than 400 μm .

The goal of my thesis is to deliver therapeutic levels of calpain inhibitors into the spinal cord, therefore it is important to verify the activity of these calpain inhibitors. In order to estimate accurate amount of active drug delivered into the animals, it is essential to establish a reliable method to measure the calpain activity within the particles. The HPLC results showed that 95 % of the MDL-28170 was extracted from MDL-28170 PKM by this extraction method. Since AK295 is less hydrophobic than MDL-28170, we expect the same or higher extraction efficiency (> 95 %) for AK295.

The activity of AK295 and MDL-28170 encapsulated in PKMs was shown in Table 3.3. The results showed that 73 % of the encapsulated MDL-28170 maintained activity, while only 20 % of the AK295 remains active after formulation of the microparticles. Combining the results of activity assay with previous encapsulation efficiency data; the amount of active MDL-28170 in PCADKe microparticles is 75 times higher than the amount of active AK295 in the PCADKe microparticles. However, AK295 might have a higher retention time in the spinal cord due to its poor BBB permeability. Therefore both AK295 and MDL-28170 should have potential to success in the *in vivo* ALS model.

CHAPTER 4

***IN VIVO* EVALUATION OF CALPAIN INHIBITORS- ENCAPSULATED PCADKe MICROPARTICLES**

4.1 Introduction

In Specific Aim 3, the objective was to evaluate the *in vivo* performance of drug containing PCADKe microparticles in the spinal cord. The high molecular weight PCADKe microparticles are designed to deliver calpain inhibitors (AK295 and MDL-28170) to the L1-L2 lumbar cord of rat, where the calpain inhibitors will inhibit the calpain activation and slow down the progress of motor neuron death.

Our working hypothesis was that calpain inhibitors-encapsulated polyketal microparticles will deliver therapeutic levels of calpain inhibitor to the spinal cord and extend the period of calpain inhibitors release to two months after an intraspinal cord injection.

Two calpain inhibitors, AK295 and MDL-28170 were used in this study to increase the potential for success. AK295 is a hydrophobic calpain inhibitor, which shows great drug properties but has low efficacy *in vivo*, due to the presence of the highly impermeable blood brain barrier (BBB) and blood spinal cord barrier (BSCB). Another potent calpain inhibitor, MDL-28170, can penetrate blood brain barrier and had promising neuroprotective effects in the animal models of focal ischemic brain damage and Parkinson's disease. However, like AK295, MDL-28170 also exhibits a dose-dependent neuroprotective effect. In order to maintain the concentration needed for therapeutic effects in the spinal cord, it requires high dose. In the treatment of ALS, a

larger delivery (volume/dose) may be needed and complications can arise from the delivery method used such as, infection, catheter obstruction, and discomfort to the patient when using this delivery method to treat humans.

To test our hypothesis, we first investigated the fate of the microparticles after an spinal cord injection by studying the distribution of the dye-encapsulated PKMs in Sprague Dawley rats. Then we evaluated the efficacy of calpain inhibitor-encapsulated PKMs by evaluation of behavior studies and survival of SOD1^{G93A} rats, a genetic rat model for ALS (Howland, Liu et al. 2002; Matsumoto, Okada et al. 2006).

The dye encapsulated PKMs (Nile Red PKMs, DiI-PKMs and coumarin-6 PKMs) formulated in Aim 1 were used to study the fate of the polyketal microparticles after intraspinal cord injection. The distribution of the microparticles was measured by fluorescence microscopy. The AK-PKMs and MDL-PKMs formulated in Aim 2 were used to investigate the *in vivo* activity of calpain inhibitors in the spinal cord tissue. In this specific aim, either AK-PKMs (n = 8), MDL-PKMs (n = 8), or PBS (n = 6) was injected into the lumbar enlargement, L1-L2, of SOD1^{G93A} rats. For each SOD1^{G93A} rats, 5 μ L of either 50 mg/mL AK-PKMs, 50 mg/mL MDL-PKMs, or PBS was injected into both hemispheres of the spinal cord at 70 days, which precedes symptom onset. Disease progression was monitored by weekly assessment of weight loss, grip strength, rotarod performance, and ALS motor score. The survival curve of ALS animals was generated with a Kaplan-Meier method.

These experiments were conducted in collaboration with Dr. Boulis's laboratory in Emory. Dr. Michele Kleim, Dr. Bethwel Raore, Dr. Colin Franz, Ms. Jing Ma, Ms.

Christina Krudy and Mr. Brenten Heeke made significant contributions to the *in vivo* experiments present in this Chapter.

4.2 Experimental Methods

Animal models

Experiments were performed on two strains of rat. Sprague Dawley wild-type rats were purchased from Charles River Laboratories (Whilmington, WA). The SOD1^{G93A} rats, which were transgenically engineered to express the human Cu⁺²/Zn⁺² superoxide dismutase 1 gene with a glycine to alanine base pair mutation at its 93rd codon. The founders for the SOD1ALS^{G93A} colony were obtained from Taconic Farms (Germantown, NY) and bred locally. Four week from the breeding date, the SOD1^{G93A} litters were genotyped. This process was used to generate a homologous population by exclusion of animals with abnormally high or low SOD1 copy numbers. Genotyping was performed by PCR as previously described (Howland, Liu et al. 2002). All procedures were approved by the Institutional Animal Care and Use Committee of Emory University.

Determine the fate of PKMs after intraspinal cord injection

Three hydrophobic fluorescence dyes (Nile Red, DiI and coumarin-6) were encapsulated in PCADK in order to study the fate of PKMs after intraspinal cord injection. The NR-PKMs with three different size distributions (1-2 μm , 1-5 μm , and 2-10 μm) and other dye encapsulated PKMs were prepared by a single emulsion technique as described in chapter 2. The sizes of the dye encapsulated PKMs were determined by SEM and DLS.

Intraspinal cord injection

The intraspinal cord injection procedure is modified from the method described by Franz *et al.* (Franz, Federici *et al.* 2009). Briefly, 120 μL of phosphate buffer saline (pH 7.4) was added to a 500 μL microcentrifuge tube containing 6 mg of NR-PKMs. The mixture was sonicated and vortexed to form a NR-PKM suspension (50 mg/mL). 10 μL of this NR-PKM solution was directly injected into L1-L2 lumbar spinal cord of adult Sprague Dawley rats (n=2) to study the fate of PKMs after intra-spinal cord injection. In order to achieve direct access to the spinal cord, the paraspinous muscles were elevated from the lamina and spinous processes, and then a T13 laminectomy were performed (note: the T13 vertebrate corresponds to the L1-4 spinal cord segments). A volume of 5 μL of NR-PKMs (50 mg/mL) was injected bilaterally at both sites of L1-L2 or a total injection volume of 10 μL per rat. In order to perform the injection a micropipette pulled to an approximately 100 μm diameter were mounted on a nanoject oocyte injector apparatus (Drummond Scientific). The pipette then were positioned over the dorsal root entry zone and advanced into the parenchyma using a micromanipulator. NR-PKMs were slowly infused with 50 nL boluses spread over 20 minutes. To minimize the reflux of the NR-PKMs, the pipette was left in place for at least 1 minute following the last injection of each site. The animals were euthanized at day 1, day3, day 14 and 1 month after NR-PKMs injection.

Coumarin-6-PKMs (1-2 μm) and DiI-PKMs (1-2 μm) were injected to the Sprague Dawley rats via the same procedure as NR-PKMs, except we only injected the dye encapsulated PKMs with a single particle size distribution. Since DiI-PKMs had strong signals under the both optical and fluorescent microscopes, we included more

animals in this group. The animals receiving DiI-PKMs were sacrificed at 3 hours, day 7 and day 14.

Histology

At the time of sacrifice, spinal cords were fixed in phosphate buffer saline containing 4 % paraformaldehyde overnight. The spinal cords were dissected and placed in 30 % sucrose solution overnight and preserved in optimized cutting temperature compound (OCT) for cryosectioning. The spinal cords were coronally sectioned into 30 μm samples and mounted on positive charged plus slides and stored in a $-20\text{ }^{\circ}\text{C}$ freezer until fluorescent microscopy. The frozen sections were analyzed by fluorescence microscopy to determine the locations and distribution of the dye-encapsulated PKMs.

***In vivo* performance of calpain inhibitor encapsulated microparticles**

To investigate the *in vivo* performance of the calpain inhibitor encapsulated PKMs, AK-PKMs or MDL-PKMs were directly injected into L1-L2 lumbar spinal cord of SOD1^{G93A} rats. Three experimental groups: a) AK295-PKMs (n=8); b) MDL-28170-PKMs (n=8) and c) phosphate buffered saline (n=5) were used in this study. Drug (and vehicle) effects on behavior, survival and motor neuron counts were evaluated. All tests and surgery were done in a double-blind fashion.

Intraspinal cord injection

AK295-PKMs (n = 8), MDL-28170-PKMs (n = 8), or PBS (n = 5) was injected into the lumbar enlargement, L1-L2, of SOD1^{G93A} rats, a genetic rat model for ALS. For

each rat, 5 μ L of 50 mg/mL AK295-PKM or 50 mg/mL MDL-28170-PKM, or PBS was injected into both hemispheres of the spinal cord at 70 days, which precedes symptom onset.

Behavior study

No earlier than one week prior to intraspinal cord injection surgery, baseline behavior measurements were performed to assess motor function. Following surgery, rat underwent behavior testing 1-2 times per week until reaching experimental end-stage. Disease progression was monitored by weekly assessment of grip strength, rotarod performance, ALS motor score (Howland, Liu et al. 2002; Matsumoto, Okada et al. 2006) and Basso, Beattie, Bresnahan Locomotor Rating Scale (BBB scale) (Howland, Liu et al. 2002; Matsumoto, Okada et al. 2006). The grip strength measurements were made with a Chatillon Digital Force Gauge DFIS-2 (Ametek Inc.), and the best of 5 trials was recorded. An Eonomex accelerating rotarod (Columbus Instruments, Columbus, OH) was used to analyze motor coordination and balance. The test was performed beginning at 5 rpm and increasing by 0.1 rpm/s until the rat fell off. Latency to fall was recorded for each trial.

Body weight

Animals were weighed weekly from the week of intraspinal cord injection surgery till the end stage of the SOD1^{G93A} rat with an electronic scale.

Survival Study

ALS was allowed to progress until the animal showed signs of morbidity (ALS motor score 0, the rat was unable to right itself from either side), at which point interventional euthanasia was administered. Time of death was determined to be the following date. The survival curve was statistically analyzed with Kaplan-Meier method.

Motor neuron analysis

At the time of sacrifice, spinal cords were fixed in phosphate buffer saline containing 4 % paraformaldehyde overnight. The spinal cords were dissected and placed in 30 % sucrose solution overnight and preserved in optimized cutting temperature compound (OCT) for cryosectioning. The spinal cords were coronally sectioned into 30 μm samples and mounted on positive charged plus slides and stored in a $-70\text{ }^{\circ}\text{C}$ freezer. The quantification of the motor neuron density and size was performed on a 30 μm thick sections of L1-L2 spinal cord with Nissl stain.

Nissl staining was used for the detection of Nissl body in the cytoplasm of neurons, and can be used to identify the basic neuronal structure in spinal cord tissue. Briefly, the spinal cord frozen sections were rehydrated by placing the slides through 100 % and 95 % alcohol to distilled water to reduce the background fat staining. The slides then were stained in crystal violet solution (Fisher, USA) for 20-30 minutes. The slides were rinsed quickly in distilled water. The slides were dehydrated through 95 % and 100 % for 5 minutes. The slides then again were placed in 100 % alcohol and checked microscopically for the best result. The slides were placed in Histo-Clear® solutions for 5

minutes to remove the extra crystal violet, and mounted with permaslip mounting medium and liquid (Alban Scientific Inc, St Lous, MO).

The ventral horns of each sample were captured using a Nikon Eclipse E400 microscope and Nikon DS-Fi1 CCD camera. The area of ventral horn neurons was measured with NIS Elements Imaging BR, SP3 Hotfix 4 (Build 473) image analysis software (Nikon Instruments Inc). Nissl positive cells were considered to be motor neurons if their soma was greater than $300 \mu\text{m}^2$ in area.

4.3 Results

Distribution of hydrophobic dye-loaded PCADKe microparticles in the spinal cord

To evaluate the fate of PCADKe microparticles after intraspinal cord injection, NR-PKMs, DiI-PKMs and coumarin-6-PKMs were injected to ventral horn of L1-L2 spinal cord of Sprague Dawley rats. In our first experiment, we found only small NR-PKMs (1-2 μm) could easily pass the needle tip of nanoinjector. The animals that received NR-PKMs were euthanized at day 1, day 3, day 14 and 1 month after intraspinal cord injection. However, the fluorescent of the NR-PKMs or released Nile Red were not detected in the spinal cord.

The fluorescent images of DiI-PKMs and coumarin-6-PKMs were taken from the spinal cord of rat at L1-L2. As shown in Figure 4.1 A, DiI-PKMs and coumarin-6-PKMs showed strong signals in the spinal cord of rat, and both particles were confined in the injection area three hours after implantation.

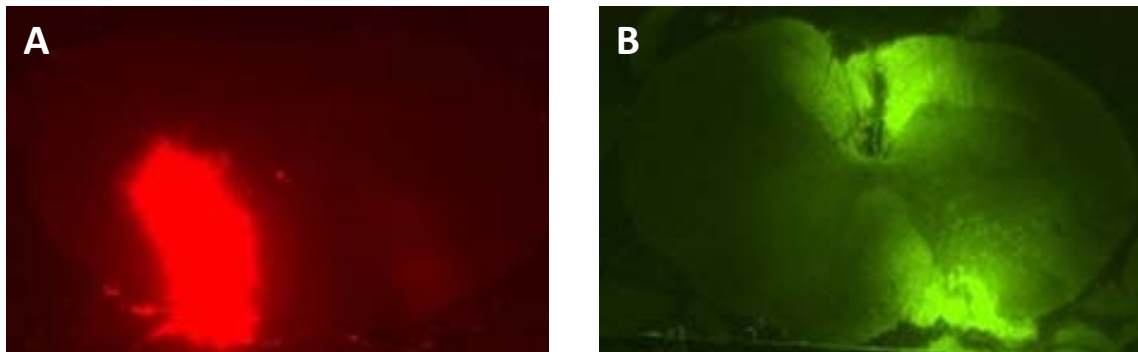


Figure 4.1 Distribution of the (A) DiI-PKMs, (B) coumarin-6-PKMs in the spinal cord.

We took another image of the distribution of the DiI-PKMs in the spinal cord at Day 7. As shown in Figure 4.2, merged images of DAPI and DiI-PKMs revealed that

most of the DiI-PKMs stayed in ventral horn of L1-L2 spinal cord of rat and did not get cleared from the spinal cord.

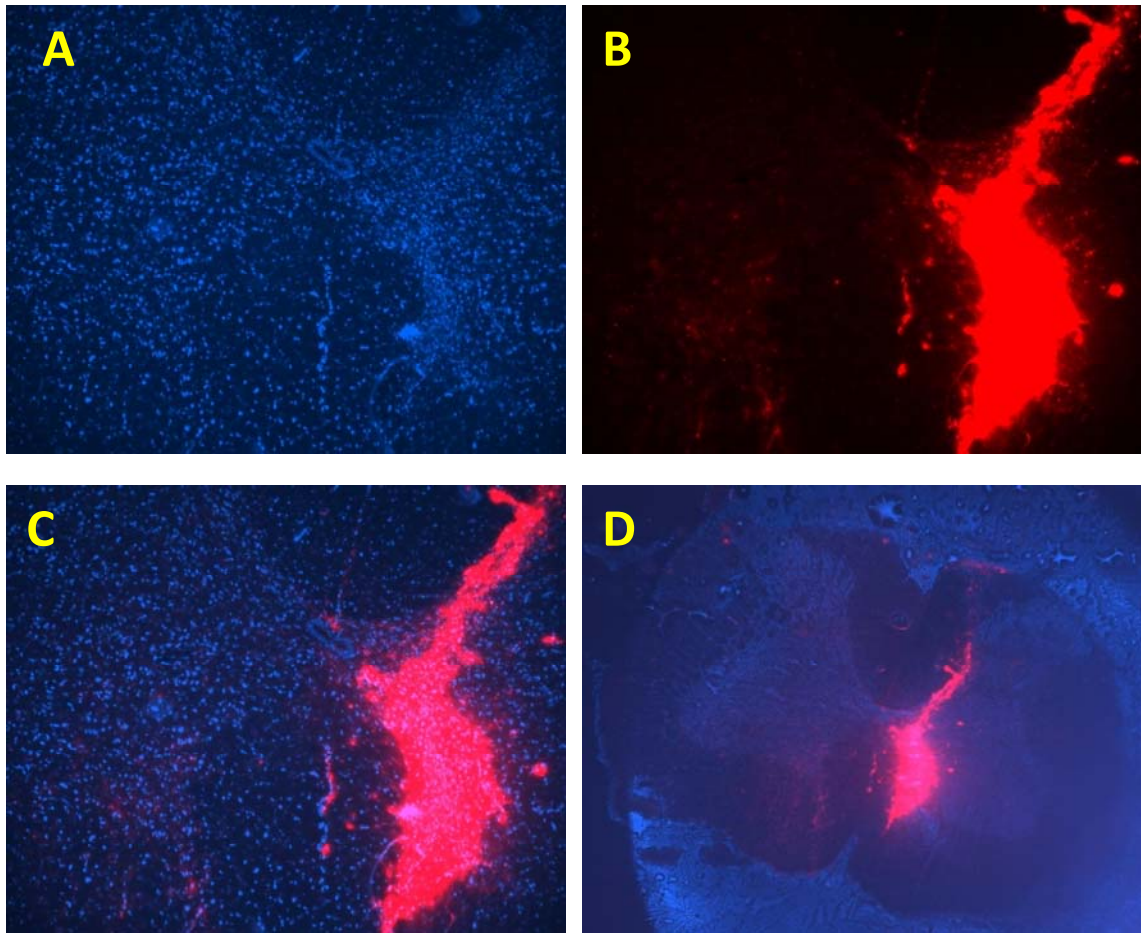


Figure 4.2 Distribution of DiI loaded PCADKe microparticles in the spinal cord. (A) the nuclei were stained with DAPI to visualize the structure of spinal cord section (B) DiI-PKMs distribution in the L1-L2 spinal cord, (c) merged images of DAPI and DiI-PKMs (10 X) (D) merged images of DAPI and DiI-PKMs (2 X)

Behavior studies of ALS rats

We started the behavior studies with three experimental groups consisting of 8 rats each: a) AK-PKMs; b) MDL-PKMs and c) saline control. However, three animals were removed from the control group. One control animal died during surgery and the

other two control animals were excluded due to its light weight or for not showing progression of ALS.

ALS motor score

ALS motor scale proposed by Matsumoto *et al.* (Matsumoto, Okada et al. 2006) was used to determine the stage of ALS of SOD1^{G93A} rats in our experiment. In their paper, the rats with different progression of ALS were divided into six groups by giving them scores between 0 and 5. The detail testing procedure for the ALS motor score is described in their paper (Matsumoto, Okada et al. 2006). Briefly, a rat without any observable function deficits were given a score of 5 (normal) and a rat with any observable function deficits was given a score of 4 (onset of ALS). And a rat cannot right itself within 30 sec was given a score of 0 (end point).

For our *in vivo* experiment, all animals in all groups started with a motor score of 5. Each month represents 3 weeks of measurements. At baseline (BL), we have a total of 21 rats (AK-PKMs, n=8; MDL-PKMs, n=8; and saline control, n=5). Time plots of ALS motor scores show all the animals began to onset the disease around 91 to 112 days, and show no differences in the progression of muscle weakness in animals of AK-PKMs and MDL-PKMs compared to the animals that received saline (Figure 4.3 A).

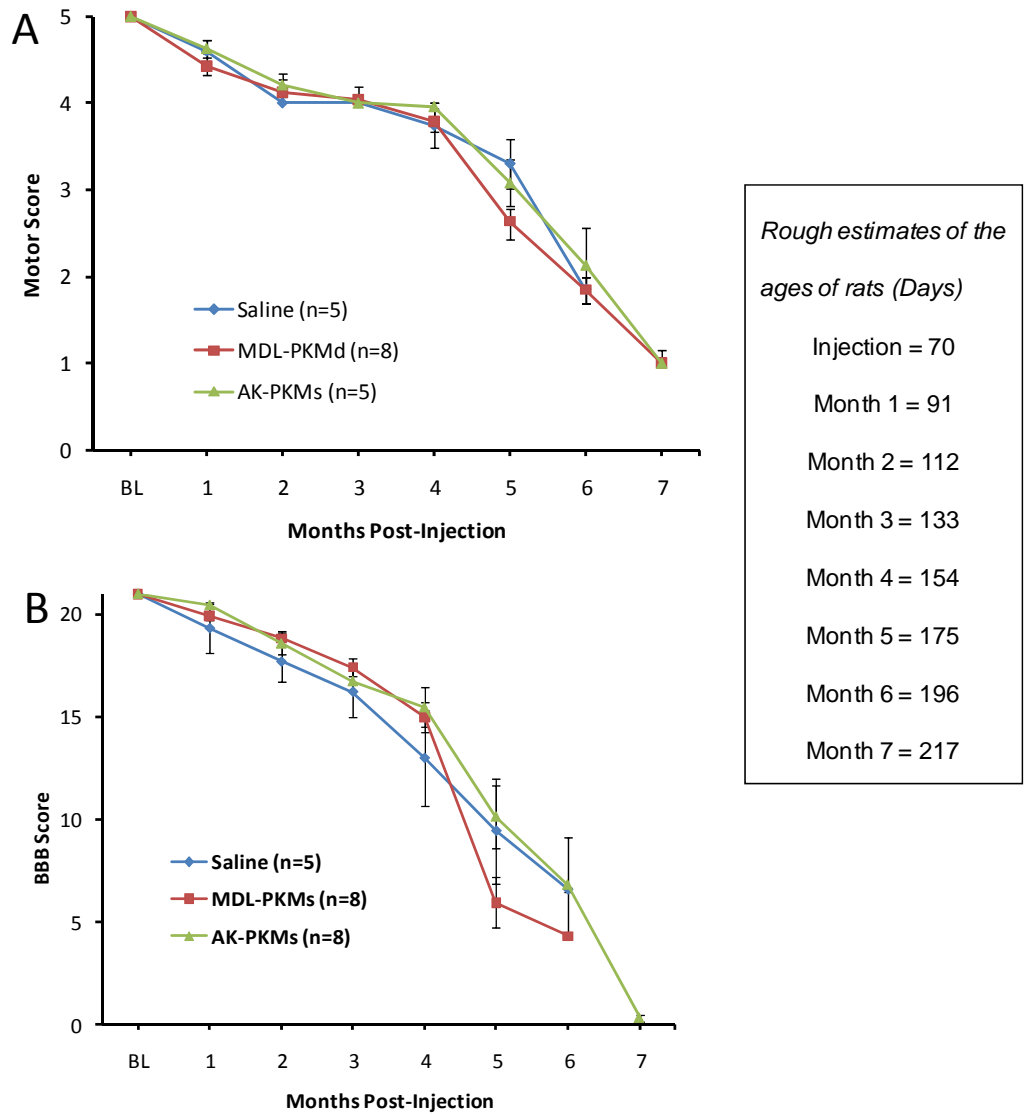


Figure 4.3 Comparison of disease progression by (A) ALS motor score (B) BBB score.

Basso, Beattie, Bresnahan locomotor rating

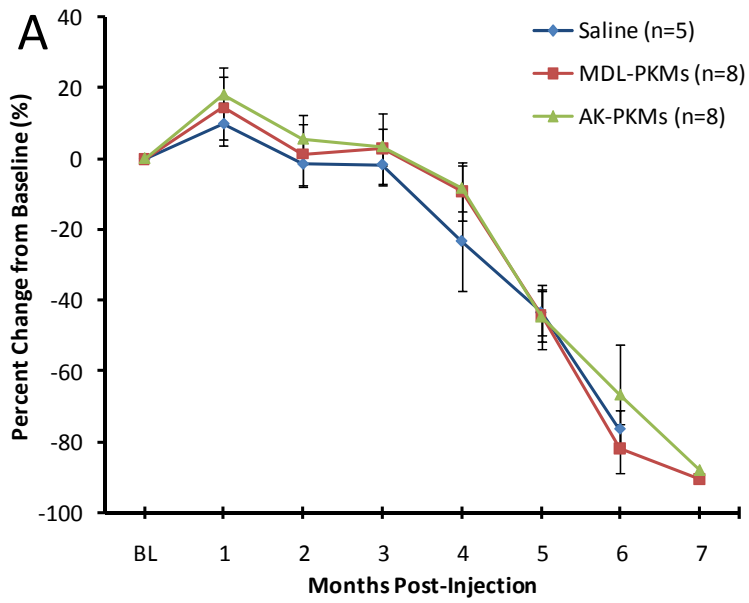
The Basso, Beattie, Bresnahan Locomotor Rating Scale (BBB scale) has become a golden standard for assessing hindlimb motor function after spinal cord injury (SCI) in rat (Basso, Beattie et al. 1995; Magnuson, Trinder et al. 1999). In recent years, BBB

scale also has been used to estimate the locomotor function of ALS rat model (Suzuki, Tork et al. 2007).

To compare the locomotor function of ALS rats between each experimental group, we evaluated these ALS rats by following the guideline of 21-point BBB scale proposed by Basso *et al.* (Basso, Beattie et al. 1995; Basso, Beattie et al. 1996). If a rat displayed no signs of movement was given a score of 0 (end point). And the rat with normal locomotion was given a score of 21 (normal). Time plots of BBB open field scores show no differences in the progression of muscle weakness in animals of AK-PKMs and MDL-PKMs compared to the animals that received saline (Figure 4.4 B).

Hindlimb grip strength and rotarod treadmill performance

The results of the hindlimb grip strength and rotarod treadmill performance were shown in Figure 4.4. We observed the average grip strength of both AK-PKMs and MDL-PKMs treated animal are slightly higher than the control animal in the first four months post injection, however, there is no statistical differences between each group. We observed the same trend in the rotarod treadmill performance test, but again, it is difficult to reach statistical significance between each group.



Rough estimates of the ages of rats (Days)

Injection = 70

Month 1 = 91

Month 2 = 112

Month 3 = 133

Month 4 = 154

Month 5 = 175

Month 6 = 196

Month 7 = 217

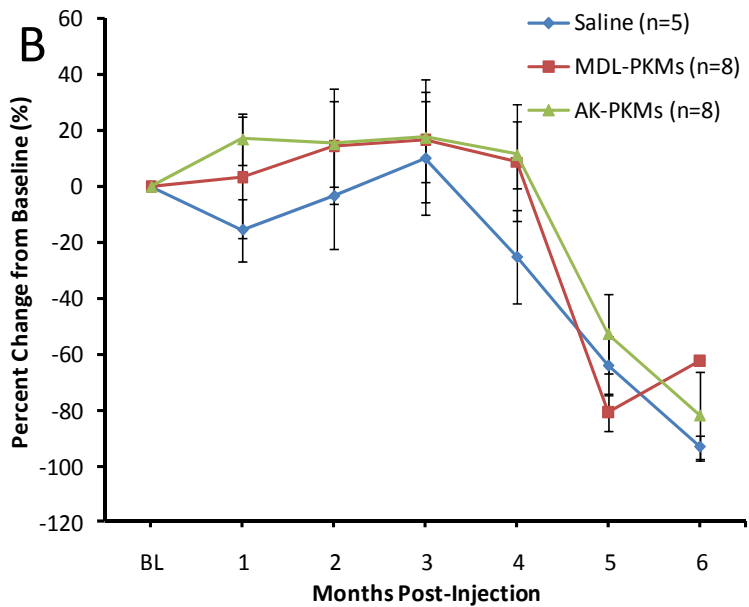


Figure 4.4 (A) Hindlimb grip strength and (B) Rotarod treadmill performance

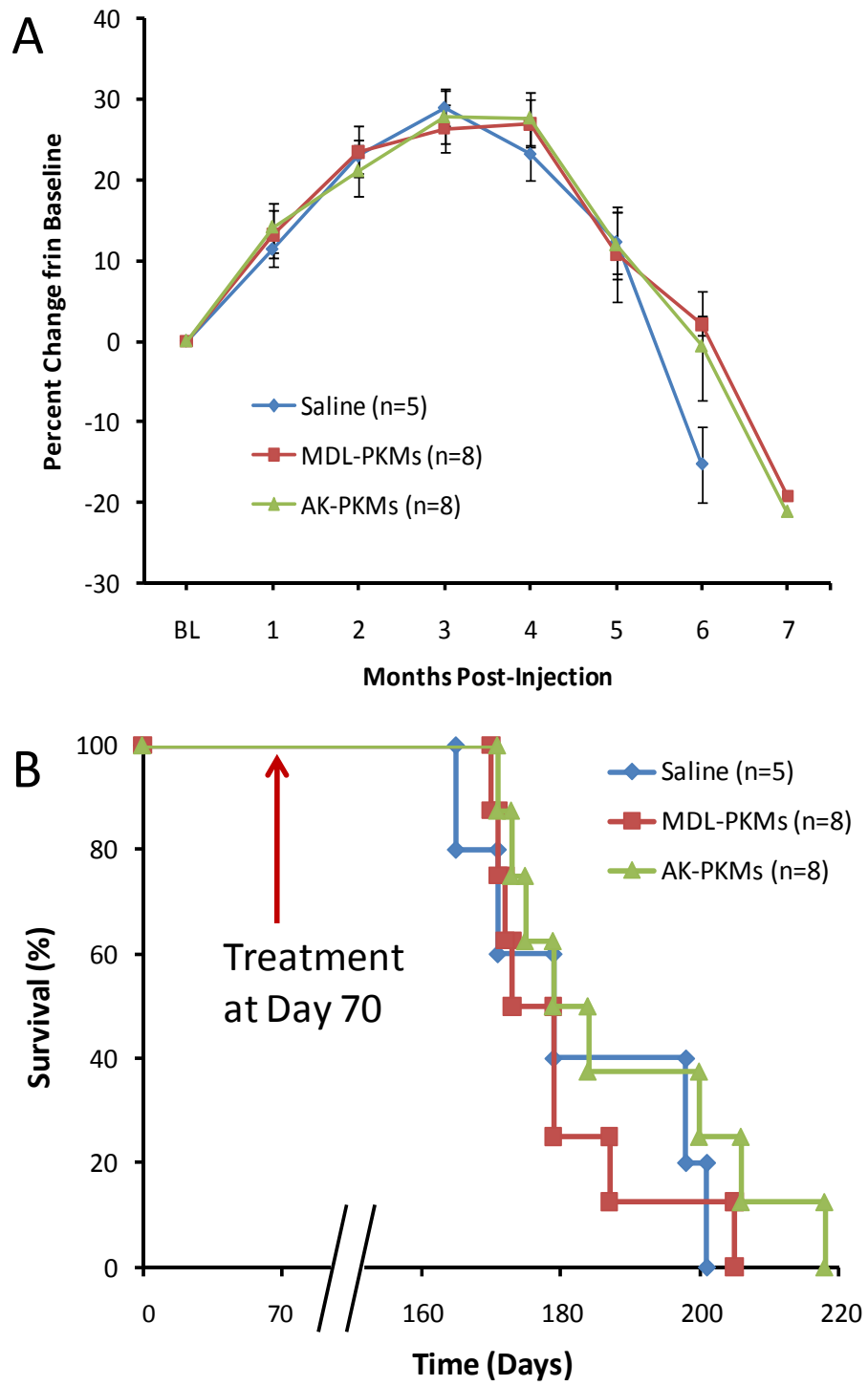


Figure 4.5 (A) Weight loss (B) Survival study

Weight Loss

Weight loss of ALS rat also can be used to monitor the progression of ALS. Masutomo et al showed that the peak of weight loss can be used as an index of “pre-symptomatic” disease onset, which is approximately 13 days prior to the symptomatic onset. The results of weight loss of each experimental group are shown in Figure 4.5 A. The bodyweights of ALS rat peaked between month 3 and 4 (between day 133 and 154). In our experiment, the peak of the weight was very close to the disease onset, which is at an ALS score of 4.0 (Figure 4.3 A). We observed no statistical differences between each experimental group.

Survival Studies

The therapeutic effects of AK-PKMs and MDL-PKMs treatment were determined by comparing the respective survival times in response to treatment type. Kaplan-Meier survival curves were generated for each experimental group. As shown in Figure 4.5 B, no significant differences were observed in all the groups. The mean survival (\pm SE) was not increased by AK-PKMs (188.25 d \pm 17.52) or MDL-PKMs (179.5 d \pm 4.16) delivery to ALS rats relative to saline injected control (182.8d \pm 16.07).

Motor neuron assay

Both AK295 and MDL-28170 are potent calpain inhibitors and have shown promising neuroprotective effects in the animal models of focal ischemic brain damage. However, the effect of calpain inhibitor therapy has not been studied in SOD1^{G93A} rat model. To study the effect of calpain inhibitors on the protection of motor neurons, we

investigated the efficacy of the AK295 and MDL-28170 by injecting the AK-PKMs and MDL-PKMs into the L1-L2 ventral horn in SOD1^{G93A} rat. After the rats were sacrificed at endpoint, the spinal cords were sectioned and stained with Nissl staining agents to visualize the (Figure 4.6). Nissl positive cells were considered to be motor neurons if their soma was greater than 300 μm^2 in area. The motor neuron density and soma area were analyzed and the results were shown in Figure 4.7. The mean (\pm SE) cell density of motor neurons counted in ventral horns of AK-PKMs treated group was 19.27 ± 8.03 (n=2). This was more motor neuron than the MDL-PKM treated group (4.79, n=1) and saline control group (11.08 ± 2.51 , n=3). The results showed that animals that received AK-PKMs have higher motor neuron density than the saline control and MDL-PKMs treated animals, however more animal numbers are required to get statistically differences. We also calculated the mean area of motor neuron, but found no differences between any of the treatment groups.

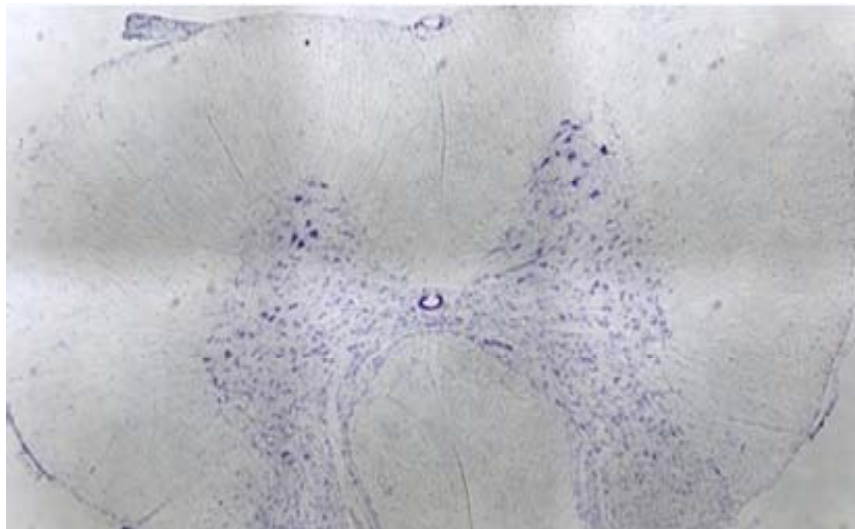


Figure 4.6 Nissl stain of spinal cord

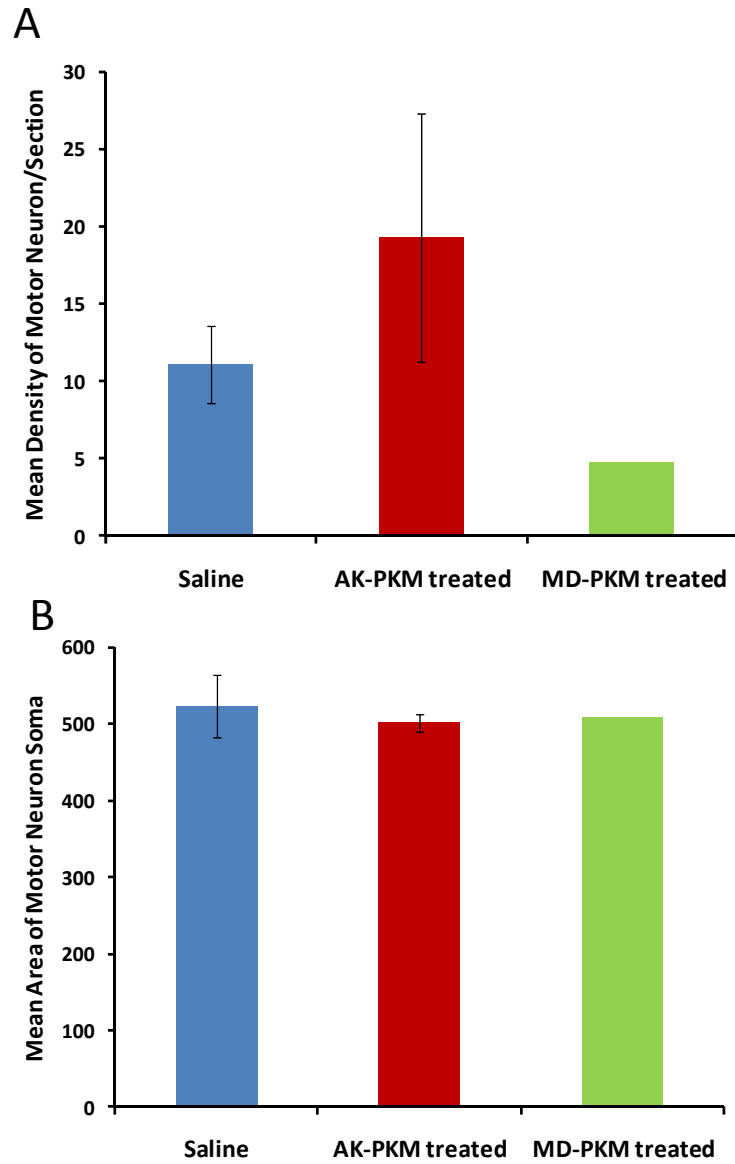


Figure 4.7 (A) motor neuron density and (B) motor neuron soma area in the spinal cord at L1-L2

4.4 Discussion

This is the first study to examine the efficacy of calpain inhibitor therapy in the SOD1^{G93A} rats by intraspinal injection of calpain inhibitor-loaded microparticles. It is known that calpain activation is an important mechanism of motor neuron degeneration in ALS (Fischer, Culver et al. 2004), and therapeutic strategies that can inhibit calpain activity in the CNS have great clinical potential. As we described in chapter 1, calpain inhibitors have been demonstrated to be neuroprotective in animal models of neurological injury, and should have great potential to treat ALS; however delivery problems have hindered their clinical success. Because of the ongoing nature of ALS, sustained delivery of calpain inhibitor to the motor neurons is needed to enhance the therapeutic effects. In previous chapter, we have confirmed that MDL-PKMs can continuously release MDL-28170 for 55 days *in vitro*. In this study, we delivered the AK-PKMs and MDL-PKMs to the spinal cord of SOD1^{G93A} rats via intraspinal cord injection. The microparticles serve as a depot for AK295 and MDL-28170, and continuously release these them to inhibit the abnormal calpain function in the motor neurons. The *in vivo* efficacy of AK-PKMs and MDL-PKMs were tested by evaluating the behavior, survival study of SOD1^{G93A} rats and their histology at the end stage. We observed that AK-PKMs can enhance the performance of behavior study in the early stage. Animals treated the AK-PKMs have longer survival time and higher motor neuron density than those treated with MD-PKMs or saline control.

Intraspinal cord delivery of microparticles

Our objective in this study was to demonstrate that PCADKe microparticles could be injected into the spinal cord and serve as a delivery system for calpain inhibitor, which can protect motor neurons and stop the progression of ALS.

The initial experiments were conducted using dye-encapsulated microparticles to optimize the injection technique and study the fate of the microparticles after intraspinal cord injection. These results suggest only particles smaller than 1-2 μm can be delivered to the spinal cord by using a nanoinjector system. As discussed in chapter 2 and 3, the size of the microparticles plays a major role in the encapsulation efficiency and release profile. More dyes or calpain inhibitors can be loaded into a larger particle since less amount of dye or calpain inhibitors are washed out or diffused out. The other advantage of using larger particles as delivery vehicles is that they are not cleared easily *in vivo* when compared to smaller particle formulations. Despite these advantages, microparticles which sizes are larger than 2 μm cannot be use in our intraspinal injection experiment. This is because when delivered by the nanoinjector system, these large particles suffered from sedimentation and clogged the needle tip resulting in low delivery efficiency of the particles.

NR-PKMs, DiI-PKMs and coumarin-6-PKMs were used to evaluate the fate of PCADKe microparticles after intraspinal cord injection; however, only DiI-PKMs and coumarin-6-PKMs can be detected by fluorescent microscopy. This might be due to the nature of the Nile Red since Nile Red only showed strong fluorescence in the lipid rich environment. Although we didn't observe the fluorescent signals from the Nile Red microparticles 3 hour after injection, we expect the released Nile Red might show

fluorescence when they diffuse out and contacted with cell membrane. However, we still did not observe any fluorescent signal from the spinal sections obtained on day 3, day 7, day 14 and 1 month.

Unlike NR-PKMs, DiI- and coumarin-6-PKMs showed a strong fluorescent signal in the spinal cord sections near the ventral horn, and this suggested we can deliver the microparticles to our targeted area using this intraspinal cord technique. Since the DiI-PKMs showed stronger fluorescent intensity than coumarin-6-PKMs and their *in vitro* release profile also been studied as described in Chapter 2. DiI have been used as neuronal fluorescent tracers for CNS delivery (Krenz and Weaver 1998; Shibata-Iwasaki, Dekimoto et al. 2007; Liu, Li et al. 2008). Therefore, DiI-PKMs were chosen to study the fate of the PCADKe microparticles after intraspinal cord injection. The result showed that most of the DiI-encapsulated polyketal microparticles (DiI-PKMs) remained at the injection site after seven days which suggest that polyketal microparticles (1-2 μm) are not easily cleared in the neutral physiological environment and can have potential to continuously release drug from the injection sites in the spinal cord.

AK-PKMs showed a trend toward improvement

The efficacy of calpain inhibitor-encapsulated PKMs were studied by evaluation the behavior and survival of SOD1^{G93A} rats. We observed the trend toward improvements in grip strength and rotarod performance in the first two months from the AK-PKMs treated group, however, there was no statistical differences between calpain inhibitor treated group with saline control. The motor neuron assay showed that animals that received AK-PKMs have higher motor neuron density than the saline control and MDL-

PKMs treated animals. This result can explain the improvement of AK-PKMs treated group in the behavior study might contribute to the increase of motor neuron density in the spinal cord, however more animal numbers are required to get statistically differences. We also calculated the mean area of motor neuron, but found no differences between any of the treatment groups. The same phenomenon was also observed in the other ALS treatment study using intraspinal cord delivery technique (Franz, Federici et al. 2009).

Several factors that may have accounted for the ineffective treatment such as, low calpain inhibitor dosage, diffusion problem of drugs and the timing for treatment were discussed to improve the future treatment.

Due to safety consideration, the maximum volume of intraspinal cord injection is 10 μL (5 μL , bilateral). To maximize the amount of particles can be delivered to the spinal cord, a high concentration of calpain inhibitor-loaded particles (50 mg/mL) were used in this study. The total amount of drug loaded particles can be delivered to the spinal cord is 0.5 mg per rat. The results of our *in vitro* experiment (Chapter 3, Table 3.3) suggest that 24.48 ng (0.0485 nmole) of active AK295 or 1862.5 ng (4.87nmole) of active MDL-28170 was injected into each animal.

The average weight of spinal cord is 560 mg, and the average length of the spinal cord is 10.5 cm. Assuming that calpain inhibitor can diffuse 5 mm away from the injection site (10 mm in one direction) and 50 % of the drug is release in the first 30 days (from MDL-28170 *in vitro* release data in Chapter 3), the amount of calpain inhibitors we delivered to the spinal cord generate a total concentration of 0.455 μM of AK295 and 45.55 μM of MDL-28170, and a daily concentration of 0.015 μM of AK295 and 1.522

μM of MDL-28170 in the first 30 day. Both total and daily concentration of AK295 delivered to the spinal cord is lower than its IC50 value (1-14 μM of AK295), this might explain why we only observed little improvement from AK-PKM treatment. The concentration of active MDL-28170 delivered to the spinal cord is 100 times higher than the concentration of active AK295, and both total and daily concentration of MDL-28170 delivered to the spinal cord is higher than its IC50 value (0.01-1 μM of MDL-28170). However, we didn't observe improvement from MDL-PKMs. This might due to its BBB permeability and short half-life in circulation.

Although current data doesn't show a significant improvement of ALS treatment, they suggest that AK295-PKM has potential for future ALS treatment. The future study should focus on improvement of AK295 delivery method, such as: enhancing the AK295 encapsulation efficiency within the polyketal microparticles and increasing the injection volume by intrathecal injection technique. One of the possible methods to improve the encapsulation efficiency is to use spray-drying technique to prepare AK-PKMs. The spray-drying technique has shown to enhance the encapsulation efficiency of both hydrophilic and hydrophobic drugs in microparticles (Mu, Teo et al. 2005; Straub, Chickering et al. 2005; Piao, Kim et al. 2007; Guerrero, Muniz et al. 2008) therefore should be useful to improve the loading efficiency of AK295 in polyketal microparticles. The other method to enhance the dosage of the AK295 in the spinal cord is to increase the volume/amount of AK-PKMs that can be delivered to the spinal cord. Currently the intraspinal cord injection technique is very invasive and only small volume (maximum at 10 μL) of solution can be delivered by this technique. Other less invasive injection

technique such as intrathecal delivery of AK-PKMs should be pursued in future improvement of AK-PKMs delivery.

The transgenic rat model of ALS offer several advantages over existing mouse model of ALS, which may be limited in studies of drug disposition due to their size. However, the rat ALS model also is more variable than the mice ALS model. A detailed discussion about the variability of rat ALS model was described by Matsumoto *et al.* (Matsumoto, Okada et al. 2006). Suzuki *et al.* also reported that the onset of disease varied according to colonies and gender of SOD1^{G93A} rat (Klein, Behrstock et al. 2005; Suzuki, Tork et al. 2007). Comparing our survival data with their data, our SOD1^{G93A} rat showed slow disease progression (Suzuki, Tork et al. 2007). The disease onset of our animal model was near 113 days, however, all the animals were treated around day 70. There is a 43 days difference between the treatment and disease onset. Our *in vitro* data suggested very small amounts of calpain inhibitor were released at that time point. This might be one of the possible reasons why we didn't observe differences between treatment groups with the control group. To solve this problem, we might need to treat the animal immediately after observation of disease onset. And this treatment plan might be applicable since the patient already has symptoms when they began treatment. However, this treatment plan requires a more precise evaluation of the disease onset and might cause difficulties in the surgery schedule.

In conclusion, we have demonstrated the development of a biodegradable microparticles delivery system for hydrophobic calpain inhibitors. Experiments using dye-encapsulated microparticles showed that polyketal microparticles (1-2 μm diameter) are not easily cleared in the neutral physiological environment and can have potential to

continuously release drug from the injection sites in the spinal cord. We also observed the trend of improvement in the first two months in the AK-PKMs treated group, however, there was no statistic differences between calpain inhibitor treated group with saline control. The low efficacy of AK295-loaded microparticles can be improved by enhancing the AK295 encapsulation efficiency and increase the amount of AK-PKM delivered via intrathecal injection. We expect the improvements of AK-PKMs formulation and delivery method will deliver more AK295 into the spinal cord and thus, may be a viable therapeutic strategy to treat ALS.

CHAPTER 5

CONCLUSIONS AND FUTURE DIRECTIONS

5.1 Conclusions

In completing these specific aims, we have developed biodegradable polymeric microparticles for the delivery of calpain inhibitors to treat ALS. Using a new synthetic methodology, we synthesized a series of high molecular weight polyketal polymers, which can enhance the encapsulation efficiency of drugs and improve the structural stability of polyketal microparticles. Based on one of the high molecular weight polyketals, PCADKe, we developed a polyketal microparticle delivery system which has a sustained release profile of a hydrophobic dye, DiI for one month, as a model delivery system for calpain inhibitors. We demonstrated that the size of the particles is an important factor that affected the release rate and encapsulation efficiency of hydrophobic drugs in polyketal microparticles. In general, smaller microparticles release drugs faster due to an increased surface area to volume ratio. Based on these findings, we developed a polyketal microparticle delivery system for the calpain inhibitors, AK295 and MDL-28170. The results of calpain assays showed that both AK-PKMs and MDL-PKMs maintained most of their inhibitory activities even after the robust emulsion process. The *in vitro* release profile of MDL-28170 in MDL-PKMs showed that 50 % of the drug was released in the first 30 days. We also demonstrated that polyketal microparticles could be safely delivered to the spinal cord by using dye-encapsulated microparticles. The results of the dye-encapsulated microparticle experiment showed that polyketal microparticles (1-2 μm) are not easily cleared in the neutral physiological environment and have potential to continuously release drugs from the injection sites.

The efficacy of calpain inhibitor-encapsulated PKMs were studied by evaluation of the behavior and survival of SOD1^{G93A} rats, a genetic rat model for ALS. We observed the a trend of improvements in grip strength, rotarod performance in the first two months for the AK-PKMs treated group, however, there was no statistical differences between calpain inhibitor treated groups with the saline control. In summary, the results that polyketal microparticles have considerable potential as a delivery system for calpain inhibitor, however, further improvements are needed to enhance their *in vivo* efficacy.

5.2 Future direction

The efficacy of the current AK-PKMs can be improved by increasing the encapsulation efficiency of AK295, and the time for starting treatment. We can also deliver other potential ALS therapeutics by using this polyketal microparticle delivery system.

Prepare AK-PKMs by using a spray drying technique

We have shown that AK-PKMs can improve the grip strength, rotarod performance in the first two months even at low dosage of AK295 (24.5 ng per rat). Currently, the encapsulation efficiency of AK295 is around 2 to 17 % in PCADKe microparticles. Thus methods that could improve the AK295 encapsulation efficiency might benefit ALS treatment. One of the possible methods to improve the encapsulation efficiency is to use the spray-drying technique to prepare the AK-PKMs. The spray-drying technique has been shown to enhance the encapsulation efficiency of both hydrophilic and hydrophobic drugs in microparticles (Mu, Teo et al. 2005; Straub,

Chickering et al. 2005; Piao, Kim et al. 2007; Guerrero, Muniz et al. 2008) and therefore should be useful to improve the loading efficiency of AK295 in polyketal microparticles. The major limitation of this spray-drying technique is that we have to use a large quantity of the AK295 (500 mg) in a single experiment.

Increase the amount of AK-PKMs delivered to the animals by using intrathecal injection technique

The other method to enhance the dosage of AK295 into the spinal cord is to increase the volume/amount of AK-PKMs that can be delivered to the spinal cord. Currently the intraspinal cord injection technique is very invasive and only small volumes (maximum 10 μ L) of solution can be delivered by this technique. Intrathecal injection allows larger injection volumes and allows for repeated dosing (Svensson, Sottile et al. 1991) since it is less invasive than intraspinal cord injection. In addition, intrathecal injection of therapeutics can provide a more diffuse therapy than intraspinal cord surgery since the therapeutics are delivered into the cerebral spinal fluid (CSF), which bathes the whole spinal cord (Butler, Hayes et al. 2005). The AK-PKMs or other therapeutic encapsulated polyketal microparticles, which are delivered by intrathecal injection, will serve as a depot for sustained release of AK295 and the other therapeutic agents to the spinal cord. Furthermore, intrathecal injections, aka spinal taps, are a simple outpatient procedure in the clinic, reducing the stress to ALS patients and rendering repeated administration feasible.

Start AK-PKMs treatment immediately after disease onset

A large variation in disease progression of ALS rats has been reported (Klein, Behrstock et al. 2005; Matsumoto, Okada et al. 2006; Suzuki, Tork et al. 2007). Variations caused by litter and gender might affect the evaluation of the drug efficacy. In order to minimize the variation effect and evaluate the efficacy of the drugs accurately, we need to treat the animal immediately after the observation of disease onset. This treatment plan might be applicable since ALS patient is symptomatic at the time of treatment. To achieve this, requires an accurate method to monitor the progression of ALS. Matsumoto *et al.* demonstrated that pre-symptomatic disease onset can be identified by monitoring the peak body weight (Matsumoto, Okada et al. 2006). The weight fluctuation in the animals is the main limitation for this method. Recently Thonhoff *et al.* report a new method to detect slight motor deficits in the early stages of ALS by using a Photobeam Activity System (PAS) and wire mesh ascending test (Thonhoff, Jordan et al. 2007). Combing these new evaluation methods with bodyweight measurement can potentially define the early signs of disease progression in ALS rats and allowing for treatment with AK-PKMs as soon as the disease onset is observed. However, this treatment plan requires increasing the workload in behavior study and might cause difficulties in the surgery schedule if too many animals showed disease onset in the same day.

Deliver other therapeutics using PCADKe microparticles for ALS treatment

1) Rolipram

Rolipram is an inhibitor of phosphodiesterase IV (PDE4; $IC_{50} = 0.8 \mu\text{M}$). Studies have shown that PDE4 is involved in the degradation of cAMP in motor neurons, thus delivery of Rolipram can increase the intracellular cAMP level and enhance the survival of motor neurons (Tomimatsu and Arakawa 2008). Rolipram also has anti-inflammatory properties because it can enhance the level of norepinephrine which can suppress TNF- α (Ross, Williams et al. 1997). Based on these properties, delivery of Rolipram might benefit ALS treatment. The animal study done by the ALS Therapy Development Institute suggested that Rolipram can slightly improve the mean survival time of male ALS mice (ALS TDI website). However, systemic delivery of Rolipram might cause dose limiting side effects (Rock, Benzaquen et al. 2009). Therefore, drug delivery systems that can provide sustained release of Rolipram in the spinal cord have great potential in treating ALS. Our preliminary studies showed that Rolipram can be encapsulated in PCADKe microparticles via single emulsion with a 2% encapsulation efficiency. Further optimization of the Rolipram PKMs might be needed to generate desirable therapeutic effects on an ALS rat model.

2) siRNA

siRNA based therapeutics have tremendous potential to improve the treatment of human diseases. Recently, several studies have been reported on the effect of siRNA on ALS therapy (Ralph, Radcliffe et al. 2005; Raoul, Abbas-Terki et al. 2005; Locatelli, Corti et al. 2007; Rizvanov, Mukhamedyarov et al. 2009), however delivering siRNA *in*

The hydrophobic ion pairing technique has been used to encapsulate siRNA in polyketal nano- and micro-particles. TNF- α siRNA polyketal microparticles were shown to enhance the suppression of TNF- α level in RAW264.7 cells. *In vivo* studies also confirmed that TNF- α siRNA polyketal microparticles were effective in reducing liver damage and systemic inflammation in a mouse model of acute liver failure, as evidenced by decrease the serum level of TNF- α and alanine aminotransferase (ALT) (Sungmun Lee, manuscript submitted). Based on these findings, we believe the use of polyketal microparticles for delivery siRNA *in vivo* will potentially benefit ALS treatment.

3) Riluzole

Riluzole (2-amino 6-trifluoromethoxybenzothiazole) is an excitatory amino acid antagonist which specifically blocks NMDA, glutamate receptor and glutamate transporters (Couratier, Sindou et al. 1994; Estevez, Stutzmann et al. 1995). Currently, riluzole (Rilutek[®]) is the only drug treatment for ALS approved by the Food and Drug Administration (FDA). Dose limiting side effects are related to off-target effects of the medication including systemic and brain related symptoms. Preliminary studies have demonstrated that intrathecal administration of riluzole did not cause neurotoxic effects (Sung, Lim et al. 2003). However, the proper dosage and immune response to intrathecal

riluzole has not been characterized. Besides riluzole has a dose-dependent neuroprotective effect on rat motor neurons. Therefore, drug delivery systems that can provide sustained release of riluzole in the spinal cord might enhance the treatment efficacy of riluzole. Our preliminary studies showed that riluzole can be encapsulated in PCADKe microparticles via a single emulsion solvent evaporation procedure. Further characterization and optimization of the riluzole-PKMs might be needed to generate a desirable therapeutic effect in ALS rats.

REFERENCES

- Ai, J., E. Liu, et al. (2007). "Calpain inhibitor MDL-28170 reduces the functional and structural deterioration of corpus callosum following fluid percussion injury." J Neurotrauma **24**(6): 960-78.
- Bartus, R. T. (1997). "The calpain hypothesis of neurodegeneration: evidence for common cytotoxic pathway." The Neuroscientist **3**(5): 314-327.
- Bartus, R. T., N. J. Hayward, et al. (1994). "Calpain inhibitor AK295 protects neurons from focal brain ischemia. Effects of postocclusion intra-arterial administration." Stroke **25**(11): 2265-70.
- Basso, D. M., M. S. Beattie, et al. (1995). "A sensitive and reliable locomotor rating scale for open field testing in rats." J Neurotrauma **12**(1): 1-21.
- Basso, D. M., M. S. Beattie, et al. (1996). "Graded histological and locomotor outcomes after spinal cord contusion using the NYU weight-drop device versus transection." Exp Neurol **139**(2): 244-56.
- Bauer, J. D., J. A. Sunman, et al. (2007). "Anti-inflammatory effects of 4-phenyl-3-butenic acid and 5-(acetylamino)-4-oxo-6-phenyl-2-hexenoic acid methyl ester, potential inhibitors of neuropeptide bioactivation." J Pharmacol Exp Ther **320**(3): 1171-7.
- Brem, H. and P. Gabikian (2001). "Biodegradable polymer implants to treat brain tumors." J Control Release **74**(1-3): 63-7.
- Brem, H., M. S. Mahaley, Jr., et al. (1991). "Interstitial chemotherapy with drug polymer implants for the treatment of recurrent gliomas." J Neurosurg **74**(3): 441-6.
- Bruijn, L. I., T. M. Miller, et al. (2004). "Unraveling the mechanisms involved in motor neuron degeneration in ALS." Annu Rev Neurosci **27**: 723-49.
- Budhian, A., S. J. Siegel, et al. (2008). "Controlling the in vitro release profiles for a system of haloperidol-loaded PLGA nanoparticles." Int J Pharm **346**(1-2): 151-9.
- Butler, M., C. S. Hayes, et al. (2005). "Spinal distribution and metabolism of 2'-O-(2-methoxyethyl)-modified oligonucleotides after intrathecal administration in rats." Neuroscience **131**(3): 705-15.
- Clavreul, A., L. Sindji, et al. (2006). "Effect of GDNF-releasing biodegradable microspheres on the function and the survival of intrastriatal fetal ventral mesencephalic cell grafts." Eur J Pharm Biopharm **63**(2): 221-8.
- Couratier, P., P. Sindou, et al. (1994). "Neuroprotective effects of riluzole in ALS CSF toxicity." Neuroreport **5**(8): 1012-4.

- Davda, J. and V. Labhasetwar (2002). "Characterization of nanoparticle uptake by endothelial cells." Int J Pharm **233**(1-2): 51-9.
- Dawes, G. J., L. E. Fratila-Apachitei, et al. (2009). "Size effect of PLGA spheres on drug loading efficiency and release profiles." J Mater Sci Mater Med **20**(5): 1089-94.
- Domb, A., M. Maniar, et al. (1991). "Drug delivery to the brain using polymers." Crit Rev Ther Drug Carrier Syst **8**(1): 1-17.
- Dong, Y., J. Tan, et al. (2006). "Calpain inhibitor MDL28170 modulates Abeta formation by inhibiting the formation of intermediate Abeta46 and protecting Abeta from degradation." FASEB J **20**(2): 331-3.
- Esmaeili, F., F. Atyabi, et al. (2008). "Preparation and characterization of estradiol-loaded PLGA nanoparticles using homogenization-solvent diffusion method." DARU **16**(4): 196-202.
- Estevez, A. G., J. M. Stutzmann, et al. (1995). "Protective effect of riluzole on excitatory amino acid-mediated neurotoxicity in motoneuron-enriched cultures." Eur J Pharmacol **280**(1): 47-53.
- Fischer, L. R., D. G. Culver, et al. (2004). "Amyotrophic lateral sclerosis is a distal axonopathy: evidence in mice and man." Exp Neurol **185**(2): 232-40.
- Fradet, A. and M. Tessier (2003). Polyester. Synthetic methods in step-growth polymerization. M. E. Rogers and T. E. Long. New Jersey, John Wiley & Sons, Inc.: 17-134.
- Franz, C. K., T. Federici, et al. (2009). "Intraspinal cord delivery of IGF-I mediated by adeno-associated virus 2 is neuroprotective in a rat model of familial ALS." Neurobiol Dis **33**(3): 473-81.
- Fu, K., D. W. Pack, et al. (2000). "Visual evidence of acidic environment within degrading poly(lactic-co-glycolic acid) (PLGA) microspheres." Pharm Res **17**(1): 100-6.
- Galvez, A. S., A. Diwan, et al. (2007). "Cardiomyocyte degeneration with calpain deficiency reveals a critical role in protein homeostasis." Circ Res **100**(7): 1071-8.
- Gill, S. S., N. K. Patel, et al. (2003). "Direct brain infusion of glial cell line-derived neurotrophic factor in Parkinson disease." Nat Med **9**(5): 589-95.
- Giovagnoli, S., P. Blasi, et al. (2004). "Biodegradable microspheres as carriers for native superoxide dismutase and catalase delivery." AAPS PharmSciTech **5**(4): e51.
- Goldstein, G. W. and A. L. Betz (1986). "The blood-brain barrier." Sci Am **255**(3): 74-83.

- Gopalan, M. and L. Mandelkern (1967). "The effect of crystallization temperature and molecular weight on the melting temperature of linear polyethylene." The Journal of Physical Chemistry **71**(12): 3833-3841.
- Guerrero, S., E. Muniz, et al. (2008). "Ketotifen-loaded microspheres prepared by spray-drying poly(D,L-lactide) and poly(D,L-lactide-co-glycolide) polymers: characterization and in vivo evaluation." J Pharm Sci **97**(8): 3153-69.
- Guo, K. and C. C. Chu (2008). "Biodegradable and injectable Paclitaxel-loaded poly(ester amide)s micropsheres: fabrication and characterization." Journal of biomedical materials research. Part B, Applied biomaterials **89b**(2): 491-500.
- Habgood, M. D., D. J. Begley, et al. (2000). "Determinants of passive drug entry into the central nervous system." Cell Mol Neurobiol **20**(2): 231-53.
- Harbeson, S. L., S. M. Abelleira, et al. (1994). "Stereospecific synthesis of peptidyl alpha-keto amides as inhibitors of calpain." J Med Chem **37**(18): 2918-29.
- Heffernan, M. J. and N. Murthy (2005). "Polyketal nanoparticles: a new pH-sensitive biodegradable drug delivery vehicle." Bioconjug Chem **16**(6): 1340-2.
- Howland, D. S., J. Liu, et al. (2002). "Focal loss of the glutamate transporter EAAT2 in a transgenic rat model of SOD1 mutant-mediated amyotrophic lateral sclerosis (ALS)." Proc Natl Acad Sci U S A **99**(3): 1604-9.
- Hu, K., J. Li, et al. (2009). "Lactoferrin-conjugated PEG-PLA nanoparticles with improved brain delivery: in vitro and in vivo evaluations." J Control Release **134**(1): 55-61.
- Huang, Y. and K. K. Wang (2001). "The calpain family and human disease." Trends Mol Med **7**(8): 355-62.
- Ishigaki, A., M. Aoki, et al. (2007). "Intrathecal delivery of hepatocyte growth factor from amyotrophic lateral sclerosis onset suppresses disease progression in rat amyotrophic lateral sclerosis model." J Neuropathol Exp Neurol **66**(11): 1037-44.
- Jalil, R. and J. R. Nixon (1990). "Microencapsulation using poly(DL-lactic acid). II: Effect of polymer molecular weight on the microcapsule properties." J Microencapsul **7**(2): 245-54.
- James, T., D. Matzelle, et al. (1998). "New inhibitors of calpain prevent degradation of cytoskeletal and myelin proteins in spinal cord in vitro." J Neurosci Res **51**(2): 218-22.
- Jaraswekin, S., S. Prakongpan, et al. (2007). "Effect of poly(lactide-co-glycolide) molecular weight on the release of dexamethasone sodium phosphate from microparticles." J Microencapsul **24**(2): 117-28.

- Kirik, D., B. Georgievska, et al. (2004). "Localized striatal delivery of GDNF as a treatment for Parkinson disease." Nat Neurosci **7**(2): 105-10.
- Klein, S. M., S. Behrstock, et al. (2005). "GDNF delivery using human neural progenitor cells in a rat model of ALS." Hum Gene Ther **16**(4): 509-21.
- Korukonda, R., N. Guan, et al. (2006). "Synthesis, calpain inhibitory activity, and cytotoxicity of P2-substituted proline and thiaproline peptidyl aldehydes and peptidyl alpha-ketoamides." J Med Chem **49**(17): 5282-90.
- Krenz, N. R. and L. C. Weaver (1998). "Sprouting of primary afferent fibers after spinal cord transection in the rat." Neuroscience **85**(2): 443-58.
- Kupina, N. C., R. Nath, et al. (2001). "The novel calpain inhibitor SJA6017 improves functional outcome after delayed administration in a mouse model of diffuse brain injury." J Neurotrauma **18**(11): 1229-40.
- Kusuhara, H. and Y. Sugiyama (2001). "Efflux transport systems for drugs at the blood-brain barrier and blood-cerebrospinal fluid barrier (Part 1)." Drug Discov Today **6**(3): 150-156.
- Kusuhara, H. and Y. Sugiyama (2001). "Efflux transport systems for drugs at the blood-brain barrier and blood-cerebrospinal fluid barrier (Part 2)." Drug Discov Today **6**(4): 206-212.
- Langer, R. and J. Folkman (1976). "Polymers for the sustained release of proteins and other macromolecules." Nature **263**(5580): 797-800.
- Lee, S., S. C. Yang, et al. (2007). "Polyketal microparticles: a new delivery vehicle for superoxide dismutase." Bioconjug Chem **18**(1): 4-7.
- Lesniak, M. S. and H. Brem (2004). "Targeted therapy for brain tumours." Nat Rev Drug Discov **3**(6): 499-508.
- Li, C. X., A. Parker, et al. (2006). "Delivery of RNA interference." Cell Cycle **5**(18): 2103-9.
- Li, Z., A. C. Ortega-Vilain, et al. (1996). "Novel peptidyl alpha-keto amide inhibitors of calpains and other cysteine proteases." J Med Chem **39**(20): 4089-98.
- Li, Z., G. S. Patil, et al. (1993). "Peptide alpha-keto ester, alpha-keto amide, and alpha-keto acid inhibitors of calpains and other cysteine proteases." J Med Chem **36**(22): 3472-80.
- Liu, Z., Y. Li, et al. (2008). "Evaluation of corticospinal axon loss by fluorescent dye tracing in mice with experimental autoimmune encephalomyelitis." J Neurosci Methods **167**(2): 191-7.

- Locatelli, F., S. Corti, et al. (2007). "Fas small interfering RNA reduces motoneuron death in amyotrophic lateral sclerosis mice." Ann Neurol **62**(1): 81-92.
- Lucas, S. M., N. J. Rothwell, et al. (2006). "The role of inflammation in CNS injury and disease." Br J Pharmacol **147 Suppl 1**: S232-40.
- Luo, J., V. W. Jones, et al. (2002). "Thermal activation of molecularly-wired gold nanoparticles on a substrate as catalyst." J Am Chem Soc **124**(47): 13988-9.
- Magnuson, D. S., T. C. Trinder, et al. (1999). "Comparing deficits following excitotoxic and contusion injuries in the thoracic and lumbar spinal cord of the adult rat." Exp Neurol **156**(1): 191-204.
- Mallya, S. K., S. Meyer, et al. (1998). "A sensitive, continuously recording fluorogenic assay for calpain." Biochem Biophys Res Commun **248**(2): 293-6.
- Markgraf, C. G., N. L. Velayo, et al. (1998). "Six-hour window of opportunity for calpain inhibition in focal cerebral ischemia in rats." Stroke **29**(1): 152-8.
- Matsumoto, A., Y. Okada, et al. (2006). "Disease progression of human SOD1 (G93A) transgenic ALS model rats." J Neurosci Res **83**(1): 119-33.
- Milligan, E. D., R. G. Soderquist, et al. (2006). "Intrathecal polymer-based interleukin-10 gene delivery for neuropathic pain." Neuron Glia Biol **2**(4): 293-308.
- Mu, L., M. M. Teo, et al. (2005). "Novel powder formulations for controlled delivery of poorly soluble anticancer drug: application and investigation of TPGS and PEG in spray-dried particulate system." J Control Release **103**(3): 565-75.
- Nakamura, R., K. Kamakura, et al. (1997). "Concentration-dependent changes in motor behavior produced by continuous intrathecal infusion of excitatory amino acids in the rat spinal cord." Brain Res Brain Res Protoc **1**(4): 385-90.
- Nirmalanathan, N. and L. Greensmith (2005). "Amyotrophic lateral sclerosis: recent advances and future therapies." Curr Opin Neurol **18**(6): 712-9.
- Panyam, J., D. Williams, et al. (2004). "Solid-state solubility influences encapsulation and release of hydrophobic drugs from PLGA/PLA nanoparticles." J Pharm Sci **93**(7): 1804-14.
- Pardridge, W. M. (1997). "Drug delivery to the brain." J Cereb Blood Flow Metab **17**(7): 713-31.
- Pardridge, W. M. (2002). "Drug and gene targeting to the brain with molecular Trojan horses." Nat Rev Drug Discov **1**(2): 131-9.
- Pardridge, W. M. (2003). "Blood-brain barrier drug targeting: the future of brain drug development." Mol Interv **3**(2): 90-105, 51.

- Piao, M. G., J. H. Kim, et al. (2007). "Enhanced oral bioavailability of piroxicam in rats by hyaluronate microspheres." Drug Dev Ind Pharm **33**(4): 485-91.
- Ralph, G. S., P. A. Radcliffe, et al. (2005). "Silencing mutant SOD1 using RNAi protects against neurodegeneration and extends survival in an ALS model." Nat Med **11**(4): 429-33.
- Raoul, C., T. Abbas-Terki, et al. (2005). "Lentiviral-mediated silencing of SOD1 through RNA interference retards disease onset and progression in a mouse model of ALS." Nat Med **11**(4): 423-8.
- Rautio, J. and P. J. Chikhale (2004). "Drug delivery systems for brain tumor therapy." Curr Pharm Des **10**(12): 1341-53.
- Ray, S. K. and N. L. Banik (2003). "Calpain and its involvement in the pathophysiology of CNS injuries and diseases: therapeutic potential of calpain inhibitors for prevention of neurodegeneration." Curr Drug Targets CNS Neurol Disord **2**(3): 173-89.
- Rizvanov, A. A., M. A. Mukhamedyarov, et al. (2009). "Retrogradely transported siRNA silences human mutant SOD1 in spinal cord motor neurons." Exp Brain Res **195**(1): 1-4.
- Rock, E. M., J. Benzaquen, et al. (2009). "Potential of the rat model of conditioned gaping to detect nausea produced by rolipram, a phosphodiesterase-4 (PDE4) inhibitor." Pharmacol Biochem Behav **91**(4): 537-41.
- Rogers, M. E., T. E. Long, et al. (2003). Introduction to synthetic methods in step-growth polymers. Synthetic methods in step-growth polymers. M. E. Rogers and T. E. Long. New Jersey, John Wiley & Sons: 1-16.
- Ross, S. E., R. O. Williams, et al. (1997). "Suppression of TNF-alpha expression, inhibition of Th1 activity, and amelioration of collagen-induced arthritis by rolipram." J Immunol **159**(12): 6253-9.
- Saatman, K. E., H. Murai, et al. (1996). "Calpain inhibitor AK295 attenuates motor and cognitive deficits following experimental brain injury in the rat." Proc Natl Acad Sci U S A **93**(8): 3428-33.
- Saltzman, W. (2001). Drug Delivery: Engineering principles for drug therapy. Oxford, UK, Oxford University.
- Samantaray, S., S. K. Ray, et al. (2008). "Calpain as a potential therapeutic target in Parkinson's disease." CNS Neurol Disord Drug Targets **7**(3): 305-12.
- Sejvar, J. J., R. C. Holman, et al. (2005). "Amyotrophic lateral sclerosis mortality in the United States, 1979-2001." Neuroepidemiology **25**(3): 144-52.

- Shenderova, A., T. G. Burke, et al. (1999). "The acidic microclimate in poly(lactide-co-glycolide) microspheres stabilizes camptothecins." Pharm Res **16**(2): 241-8.
- Shibata-Iwasaki, R., H. Dekimoto, et al. (2007). "Anterograde labeling of the corticospinal tract in jimpy mutant mice by Di I injection into the motor cortex." Arch Histol Cytol **70**(5): 297-301.
- Stille, J. K. (1981). "Step-Growth Polymerization." Journal of Chemical Education **58**(11): 862-866.
- Straub, J. A., D. E. Chickering, et al. (2005). "Intravenous hydrophobic drug delivery: a porous particle formulation of paclitaxel (AI-850)." Pharm Res **22**(3): 347-55.
- Sugiyama, S., Y. Yamashita, et al. (2007). "Safety and efficacy of convection-enhanced delivery of ACNU, a hydrophilic nitrosourea, in intracranial brain tumor models." J Neurooncol **82**(1): 41-7.
- Sung, B., G. Lim, et al. (2003). "Altered expression and uptake activity of spinal glutamate transporters after nerve injury contribute to the pathogenesis of neuropathic pain in rats." J Neurosci **23**(7): 2899-910.
- Suzuki, M., C. Tork, et al. (2007). "Sexual dimorphism in disease onset and progression of a rat model of ALS." Amyotroph Lateral Scler **8**(1): 20-5.
- Svensson, B. A., A. Sottile, et al. (1991). "Studies on the development of tolerance and potential spinal neurotoxicity after chronic intrathecal carbachol-antinociception in the rat." Acta Anaesthesiol Scand **35**(2): 141-7.
- Sy, J. C., G. Seshadri, et al. (2008). "Sustained release of a p38 inhibitor from non-inflammatory microspheres inhibits cardiac dysfunction." Nat Mater **7**(11): 863-8.
- Taluja, A., Y. S. Youn, et al. (2007). "Novel approach in microparticle PLGA delivery systems encapsulating proteins." Journal of Materials Chemistry **17**: 4002-4014.
- Tamber, H., P. Johansen, et al. (2005). "Formulation aspects of biodegradable polymeric microspheres for antigen delivery." Adv Drug Deliv Rev **57**(3): 357-76.
- Taylor, E. M. (2002). "The impact of efflux transporters in the brain on the development of drugs for CNS disorders." Clin Pharmacokinet **41**(2): 81-92.
- Tehrani, R., S. Andell-Jonsson, et al. (2002). "Improved recovery and delayed cytokine induction after closed head injury in mice with central overexpression of the secreted isoform of the interleukin-1 receptor antagonist." J Neurotrauma **19**(8): 939-51.
- Thonhoff, J. R., P. M. Jordan, et al. (2007). "Identification of early disease progression in an ALS rat model." Neurosci Lett **415**(3): 264-8.

- Thorek, D. L. and A. Tsourkas (2008). "Size, charge and concentration dependent uptake of iron oxide particles by non-phagocytic cells." Biomaterials **29**(26): 3583-90.
- Tobita, H. and Y. Ohtani (1991). "Control of molecular weight distribution in step-growth polymerization by an intermediate monomer feed method: effect of interchange reactions." Polymer **33**(10): 2194-2202.
- Tomimatsu, N. and Y. Arakawa (2008). "Survival-promoting activity of pituitary adenylate cyclase-activating polypeptide in the presence of phosphodiesterase inhibitors on rat motoneurons in culture: cAMP-protein kinase A-mediated survival." J Neurochem **107**(3): 628-35.
- Urushitani, M., S. A. Ezzi, et al. (2007). "Therapeutic effects of immunization with mutant superoxide dismutase in mice models of amyotrophic lateral sclerosis." Proc Natl Acad Sci U S A **104**(7): 2495-500.
- von Burkersroda, F., L. Schedl, et al. (2002). "Why degradable polymers undergo surface erosion or bulk erosion." Biomaterials **23**(21): 4221-31.
- Wang, K. K., S. F. Lerner, et al. (2006). "Neuroprotection targets after traumatic brain injury." Curr Opin Neurol **19**(6): 514-9.
- Weydt, P., S. Hong, et al. (2005). "Cannabinol delays symptom onset in SOD1 (G93A) transgenic mice without affecting survival." Amyotroph Lateral Scler Other Motor Neuron Disord **6**(3): 182-4.
- Yang, S. C., M. Bhide, et al. (2008). "Polyketal Copolymers: A New Acid-Sensitive Delivery Vehicle for Treating Acute Inflammatory Diseases." Bioconjug Chem.
- Yang, S. C., M. Bhide, et al. (2008). "Polyketal copolymers: a new acid-sensitive delivery vehicle for treating acute inflammatory diseases." Bioconjug Chem **19**(6): 1164-9.
- Yoshihara, T., S. Ishigaki, et al. (2002). "Differential expression of inflammation- and apoptosis-related genes in spinal cords of a mutant SOD1 transgenic mouse model of familial amyotrophic lateral sclerosis." J Neurochem **80**(1): 158-67.
- Zhao, H., J. Gagnon, et al. (2007). "Process and formulation variables in the preparation of injectable and biodegradable magnetic microspheres." Biomagn Res Technol **5**: 2.
- Zilberman, M. and O. Grinberg (2008). "HRP-loaded bioresorbable microspheres: effect of copolymer composition and molecular weight on microstructure and release profile." J Biomater Appl **22**(5): 391-407.